Physicochemical phenomena at the plasma - polymer interface

Wheale, Samantha Hilary

PHYSICOCHEMICAL PHENOMENA AT THE PLASMA - POLYMER INTERFACE

Ph.D. Thesis

Samantha Hilary Wheale

University of Durham

Department of Chemistry

1997

For My Parents

STATEMENT OF COPYRIGHT

DECLARATION

The work described in this thesis was carried out in the Department of Chemistry at the University of Durham between October 1994 and September 1997. It is the original work of the author except where otherwise acknowledged, and has not previously been submitted for a degree in this or any other university.

PUBLICATIONS

Work in this thesis will be submitted for publication as follows:-

Plasma Chemistry at Polymer Surfaces, S.H. Wheale and J.P.S. Badyal, in Interfacial Science, A 'Chemistry for the 21st Century' Monograph, Blackwell Science, 1997, Chapter 10.

Mass Spectrometry at the Plasma - Polymer Interface, S.H. Wheale, C.P. Barker and J.P.S. Badyal, J. Chem. Phys. submitted for publication.

Xenon Difluoride Plasma Fluorination of Polymer Surfaces, S.H. Wheale and J.P.S. Badyal, J. Chem. Phys. submitted for publication.

VUV / XeF_2 of Polyethylene and Polystyrene, S.H. Wheale and J.P.S. Badyal, J. Chem. Phys. submitted for publication

Other Publications by the Author:

Synergistic Oxidation at the Plasma/Polymer Interface, J. Hopkins, S.H. Wheale and J.P.S. Badyal, J. Phys. Chem. **100**, 14062 (1996).

Plasma Polymerization of 2-Iodothiophene, M.E. Ryan, A.M. Hynes, S.H. Wheale, J.P.S. Badyal, C. Hardacre and R.M. Ormerod, Chem. Mater. **8**, 916 (1996).

ACKNOWLEDGEMENTS

I would like to thank my supervisor Prof. J. P. S. Badyal for all of his help, advice, and encouragement during my Ph.D. Thanks to everyone in Lab 98, past and present, for making my time here thoroughly enjoyable, for all the advice, discussions and proof reading.

I would like to acknowledge the technical assistance of George, Kelvin and Barry in the electrical workshop, Gordon and Ray the glassblowers, and Jim and Neil in the mechanical workshop, without whom my Ph.D. would never have been completed.

Thanks also goes to my Mum and Dad for their love and support, and to Bill who kept me sane and had faith in me when I doubted myself. Thanks to Tracy for being there when I needed her, and to the netball girls for all the Friday nights out. Finally I would like to thank all my friends in Durham and around the country for the all their encouragement (especially Alison who made my phonebill escalate by becoming a cockney!).

ABSTRACT

Non-isothermal plasma modification of polymer surfaces is of scientific and technological interest, since it can be used to improve wettability, adhesion, etc. This thesis covers three main areas, firstly a study of the processes occurring at the plasma - polymer interface using a newly developed technique, secondly the fluorination of polymer surfaces using a novel transportable reagent and lastly the oxidation of rubber substrates.

The interaction of N_2, O_2, air and H_2 glow discharges with polyethylene surfaces has been studied using a newly developed mass spectrometric technique. The species permeating through to the reverse side of the polymer substrate can be detected and characterised. Compared to previously reported approaches, this method is capable of sampling reaction products within closer proximity to the plasma - polymer interface, thereby circumventing the complication of primary product species undergoing secondary processes within the bulk of the electrical discharge prior to detection. The nature of the feed gas is found to strongly influence the chemical reaction pathways occurring at the plasma - polymer interface.

Xenon difluoride (XeF_2) plasma treatment of a series of polymers containing different repeat units gives rise to surface fluorination. A comparison with CF_4 plasma modification shows that XeF_2 electrical discharges are more effective at fluorinating polymers. The extent of fluorine incorporation can be accounted for in terms of a structure-behaviour relationship derived from extended Huckel molecular orbital calculations. Exposure of polyethylene and polystyrene to xenon difluoride (XeF_2) in the presence of vacuum ultraviolet (VUV) irradiation also causes surface fluorination. The extent of reaction is found to depend upon the VUV absorption characteristics of the XeF_2 feed gas as well as those of the polymer substrate.

Low pressure glow discharge, dielectric barrier discharge and ozone treatments all oxidise additive-free rubber substrates. The oxidation susceptibility of the rubber substrates differed during all three treatments, and was found to be dependent upon the concentration of unsaturated carbons, saturated carbons and phenyl rings. The additives placed in rubbers to improve properties such as tear resistance influence their degree of oxidation.

CONTENTS

CHAPTER 1: PLASMA CHEMISTRY AT POLYMER SURFACES

CHAPTER 1

PLASMA CHEMISTRY AT POLYMER SURFACES

1.1 INTRODUCTION

Since the early 1970's there has been an enormous expansion in the use of plasmas (also known as glow and electrical discharges).[1] This technology is of vital importance to a number of the world's largest manufacturing industries, e.g. microelectronics, steel, aerospace, automotive, biomedical, toxic waste management, etc.[2] However, the behaviour of these electrical discharges is poorly understood at the molecular level due to the inherent complexity of this form of matter. In order to develop commercially viable industrial processes, an understanding of the fundamental processes is imperative.

Non-equilibrium plasma treatment of polymeric materials can be used to improve the surface properties, e.g. optical reflection, adhesion, friction coefficient, surface energy, permeability, biocompatibility, etc. This chapter presents a systematic overview of the current state of knowledge related to the interaction of non-isothermal plasmas with solid polymer surfaces and the techniques used to analyse the modified surfaces.

Chapters two and three describe how quadrupole mass spectrometry has been used to study interfacial diagnostics during plasma modification of polymer surfaces and how the problem of primary product species undergoing secondary processes within the bulk of the electrical discharge prior to detection has been overcome.

Chapter four investigates the use of xenon difluoride (XeF_2) plasma treatment to fluorinate polymer surfaces. Chapter five is concerned with the surface fluorination of polyethylene and polystyrene when they are exposed to xenon difluoride (XeF_2) in the presence of vacuum ultraviolet (VUV) irradiation. Chapter six is a study of the oxidation of various rubber substrates.

1.2 LOW PRESSURE NON-EQUILIBRIUM PLASMAS

The term "plasma" was first used in 1929 by Langmuir to describe ionised gases.[3] A plasma can be considered as a partially or fully ionised gaseous state of matter which contains atoms and/or molecules in ground and excited states, ions of either polarity, electrons, and electromagnetic radiation.[4] All of these species can be regarded as potential reactants.[5] It is normally regarded as being an electrically conducting medium; although there is no overall charge imbalance, local perturbations from neutrality can

occur. The number of ions and electrons must be approximately equal for it to be classed as a plasma. This quasi neutral gas comprising charged and neutral particles usually behaves in a collective manner.[6] This requirement is satisfied when the dimensions of the discharge volume is greater than the Debye length, λ_D. The λ_D is the distance over which a small potential can perturb a plasma and is given by.[7]

$$\lambda_D = (E_o kT / ne^2)^{1/2}$$

where E_o is the permittivity of free space, n the electron density, T the electron temperature, e the electron charge and k the Boltzmann constant.

1.2.1 Discharge Theory

Plasmas can be produced using a variety of means: electric fields, heating, laser radiation, and chemical processes. When a gas is subjected to an electric field, randomly occurring free electrons originating from cosmic rays or background radioactivity[8] become accelerated, and undergo elastic and inelastic collisions, the latter cause ionisation of the gas together with the formation of secondary electrons.[4] This process leads to a cascade effect and the production of ions, atoms, metastables, free radicals, and electromagnetic radiation.

1.2.1.1 Electron Energy

The energy distribution of electrons in a plasma is important as they are reponsible for the ionisation processes occurring in the plasma. The electrons in a plasma have a range of energies determined by the electron energy distribution function (EEDF). This is often in the form of the Maxwellian distribution[7] which assumes that $T_e = T_g$ (where T_e is the electron temperature and T_g the gas temperature), Figure 1.1. However, for non-equilibrium plasmas the Druyvesteyn distribution[7] is a better approximation as it makes the assumption that $T_e >> T_i$ (where T_i is the temperature of the ions). Figure 1.1.

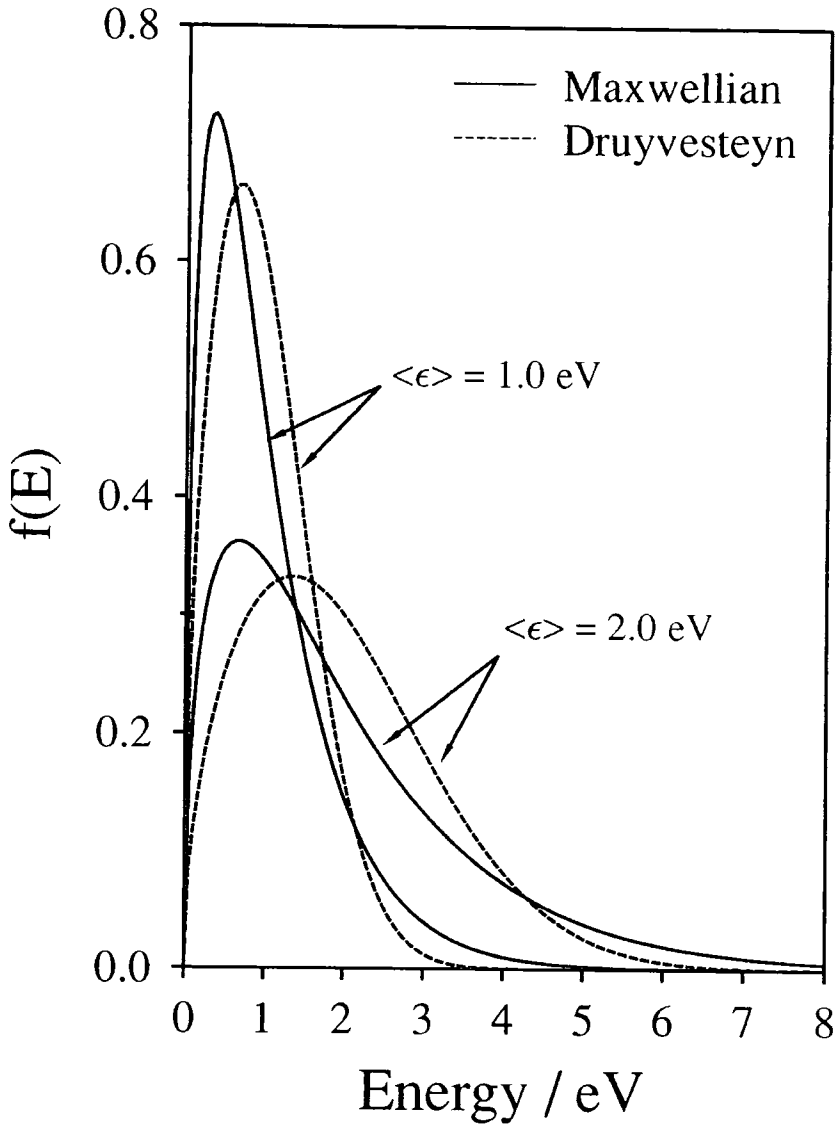

Figure 1.1: Maxwellian and Druyvesteyn energy distributions for electrons in a plasma.

1.2.1.2 Plasma Potential

The electrons within the plasma are more mobile than the ions and reach the borders of the plasma faster, resulting in the plasma becoming positively charged. However, as the positive charge increases it is harder for the electrons to leave and a steady state is achieved where the rate of loss of electrons equals the rate of loss of ions and the plasma thus retains neutrality. The average potential difference between the bulk of the gas and the chamber is known as the plasma potential and is several volts more positive than the most positive surface.[7,9]

1.2.1.3 Floating Potential

Similarly when an electrically floating surface is placed in a plasma the electrons reach the surface faster than the ions.[9] A steady state is again achieved, and due to the negative potential of the substrate with respect to the plasma, ion bombardment of the surface is possible.

1.2.1.4 Sheath

The electron density at the edge of the plasma in contact with the chamber wall differs from the bulk of the plasma. The name given to this region is the plasma sheath[7] and is visible as a dark space surrounding the plasma. The electron density here is lower than in the bulk and it has a much lower voltage. As the plasma has a uniform potential the voltage drop between the surface and plasma occurs mainly in the plasma sheath.

1.1.2 Equilibrium and Non-Equilibrium Plasmas

Plasmas can exist in three forms: complete thermodynamic equilibrium where the temperatures of all the species are equal (e.g. stars, explosions, etc.); local thermodynamic equilibrium where everything except the radiation temperature is equal (e.g. electric arcs, plasma jets, etc.); and non-equilibrium where the electron temperature (~ 10,000 K) far exceeds the temperature of the bulk gas (300 - 500 K, e.g. glow

discharges). Equilibrium plasmas are useful for inorganic chemical synthesis.[10] nuclear fusion,[4] metallurgy,[4] etc.

Non-equilibrium plasmas open up non-thermally activated reaction pathways. In the absence of external magnetic fields, their degree of ionisation is low (10^{-5} - 10^{-1}) so the gas consists of mainly neutrals at ambient temperature.[7,9] In this case, average electron energies can span 1 to 30 eV, however it is only the electrons contained within the high energy tail which are capable of causing ionisation.[11] Non-equilibrium plasmas provide low temperature processing environments under which thermodynamically unfavoured reactions are able to proceed. Such cold plasmas have found application in low temperature materials processing: e.g. amorphous silicon deposition,[12] plasma polymerisation,[13] etching,[14] restoration of archaeological artefacts,[15] polymer surface modification,[16] etc.

1.2.3 Generation of Low Pressure Non-Equilibrium Plasmas

Non-equilibrium plasmas can be generated at atmospheric and low (10^{-4} - 10 mbar) pressures. In the case of low pressure electrical discharges, there are three main components to a plasma processing system:

(i) Source of Electrical Power: Electrical power frequencies spanning the DC to microwave range are used at power levels ranging from 1 to 5000 W.

(ii) Coupling Mechanism: The electrical power source can be resistively, capacitively or inductively coupled to the gas under investigation. A matching network is usually necessary to ensure that there is efficient power dissipation.

(iii) Plasma Environment: The reactor geometry and other variables such as type of gas, pressure, flow rate, power level, processing time, must all be taken into consideration. Normally, the chamber is evacuated to a pressure well below its operating pressure, and then feed gas is introduced followed by ignition of the electrical discharge.

Variation of the electrical discharge parameters (e.g. gas flow rate, gas pressure, reactor geometry, substrate temperature, frequency/intensity of power, etc.) can have a direct influence upon the plasma characteristics (i.e. electron density, electron energy distribution, gas density, residence time, etc.).

1.3 FUNDAMENTAL PROCESSES

A variety of different reaction pathways are potentially viable at the surface of a polymer substrate immersed in a non-polymer forming electrical discharge, Figure 1.2.

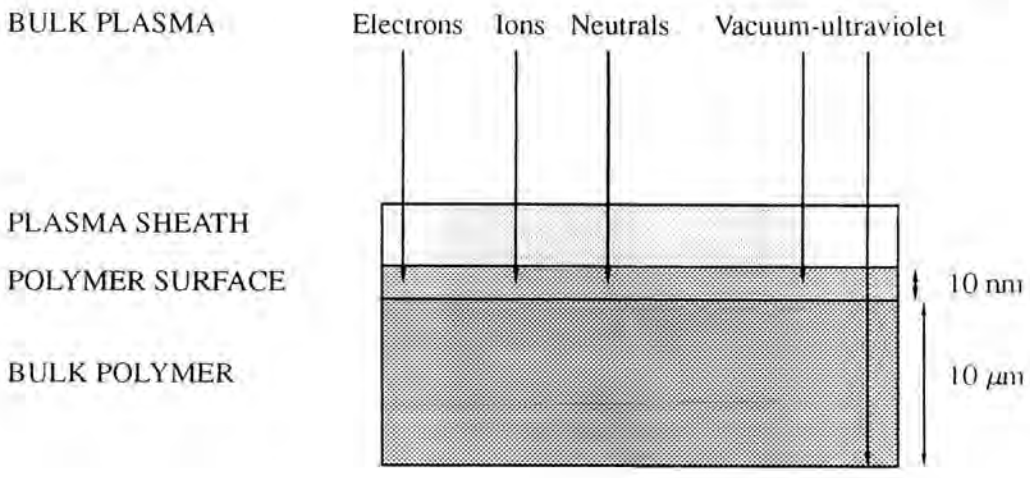

Figure 1.2: Physicochemical processes occurring at the plasma - polymer interface.

1.3.1 Neutrals

Neutral species in the form of atoms, radicals, molecules, and metastables can all take part in reactions at the plasma - solid interface.[5]

1.3.2 Electrons

During plasma modification, electrons can participate in electron capture processes at the surface.[5]

1.3.3 Ion Bombardment

Any surface in contact with a plasma gains a negative charge due to the constituent electrons being more mobile than the ions. This leads to the build up of a space-charge

layer at the plasma - solid interface, which is known as the plasma sheath. The resultant electric field repels electrons away from and accelerates incident ions towards the surface. For floating substrates and chemically reactive plasmas, ion bombardment does not play a significant role. However in the case of noble gases, the absence of chemical interactions makes ion induced surface modification a major reaction pathway.[17]

1.3.4 Electromagnetic Radiation

The main source of electromagnetic radiation within an electrical discharge is the relaxation of metastables.[18] Vacuum-UV irradiation of the substrate can lead to the formation of free radicals followed by their reaction with incident plasma species.[19] All organic polymers exhibit a strong absorbance below 160 nm,[20,21] hence penetration of VUV radiation into the subsurface results in chain scission and crosslinking.[22] By placing a VUV transparent window between the electrical discharge and the polymer substrate it is possible to block out all of the reactive species apart from the VUV component;[23] such experiments have demonstrated the important role played by VUV radiation during plasma modification. However the extent of treatment is critically dependent upon the absorption characteristics of the gas.[24]

1.4 POLYMER BEHAVIOUR

The individual constituents of a plasma (i.e. electrons, ions, neutrals, and photons) are capable of interacting with an underlying polymer substrate in either an isolated or synergistic fashion to result in cleaning, etching, crosslinking, activation, and functionalisation.[25] Such changes can be used to alter the surface energy, polymer molecular weight distribution, chemical composition, and topography at a polymer surface.

1.4.1 Chain Scission

Chain scission can lead to the formation of low molecular weight chains[26,27] which can be washed off with solvent.[28] If this material is incompatible with the substrate then it tends to form droplets on the polymer surface.[29]

1.4.2 Chain Mobility

The movement of chain segments at the surface of some polymers can lead to dynamic behaviour during or following plasma treatment.[30] This may result in migration of polymer chains into the subsurface,[31,32] desorption[29,33] or solublisation into an adjacent medium.[31] Polymer tacticity can also play an important role during plasma modification since it can influence chain mobility.[34]

1.4.3 Crosslinking

Reactive and noble gas plasmas have been shown to be capable of inducing crosslinking down to depths of 3 μm as a result of direct and radiative transfer mechanisms.[19] The direct component consists mainly of ions and metastables interacting with the outermost layers, whereas radiative vacuum-UV radiation penetrates into the subsurface and bulk.[22] Typically, a lower level of crosslinking is found for chemically reactive plasmas compared to inert gas plasmas.[35] The structural nature of the polymer under investigation can be an important factor, for instance polyethylene tends to undergo crosslinking whereas polypropylene prefers chain scission.[36] Typically, a chemically modified top layer covers underlying crosslinked material; the density of the latter drops with increasing depth.[35] The crosslinked layer can limit polymer chain mobility and thereby provide stability to the overlying treated layer,[35] this can improve its heat resistance, frictional behaviour, cohesive strength, and form a diffusion barrier layer.

1.4.4 Surface Activation

Polymer surface activation occurs as a result of the impingement of plasma species. Free radicals are created which can further react with incident plasma species, alternatively

they can participate in chemical reactions upon termination of the plasma, e.g. surface grafting, crosslinking, oxidation upon exposure, etc.

1.4.5 Synthon Approach

Structure-behaviour relationships can prove to be a reliable guide for predicting and designing interfacial behaviour. Clearly the type of gas and polymer employed during plasma modification governs what kind of treated surface is generated. For instance, in the case of oxygen plasma removal of polymer, strong linkages (e.g. aromatic and polar functional groups) inhibit etching, whereas weak bonds within the chain (e.g. C-C bonds) can enhance degradation.[37] This rationale can be extended to plasma modification of polymer surfaces, where the type of functionality generated at the substrate can be correlated to the structure of the parent polymer.[38,39,40,41,42]

1.5 CHARACTERISATION METHODS

Surface analysis has been widely used to help understand the changes taking place at polymer surfaces during plasma modification. Many techniques have been employed, these include: X-ray photoelectron spectroscopy (XPS), secondary ion mass spectrometry (SIMS), ion scattering spectroscopy (ISS), electron microscopy, scanning probe microscopy, contact angle measurements, and infrared spectroscopy. Each technique has its inherent advantages and disadvantages, therefore it is vital that a multitechnique approach is used. Mass spectrometry has also been used as an in situ diagnostic technique to study the plasma - polymer interface during treatment. The effectiveness of some of the more informative analytical techniques is outlined below:

1.5.1 X-ray Photoelectron Spectroscopy

X-ray photoelectron spectroscopy (XPS) is a surface sensitive analytical technique. XPS is based upon the photoejection of a single electron during X-ray irradiation of the substrate, Figure 1.3.

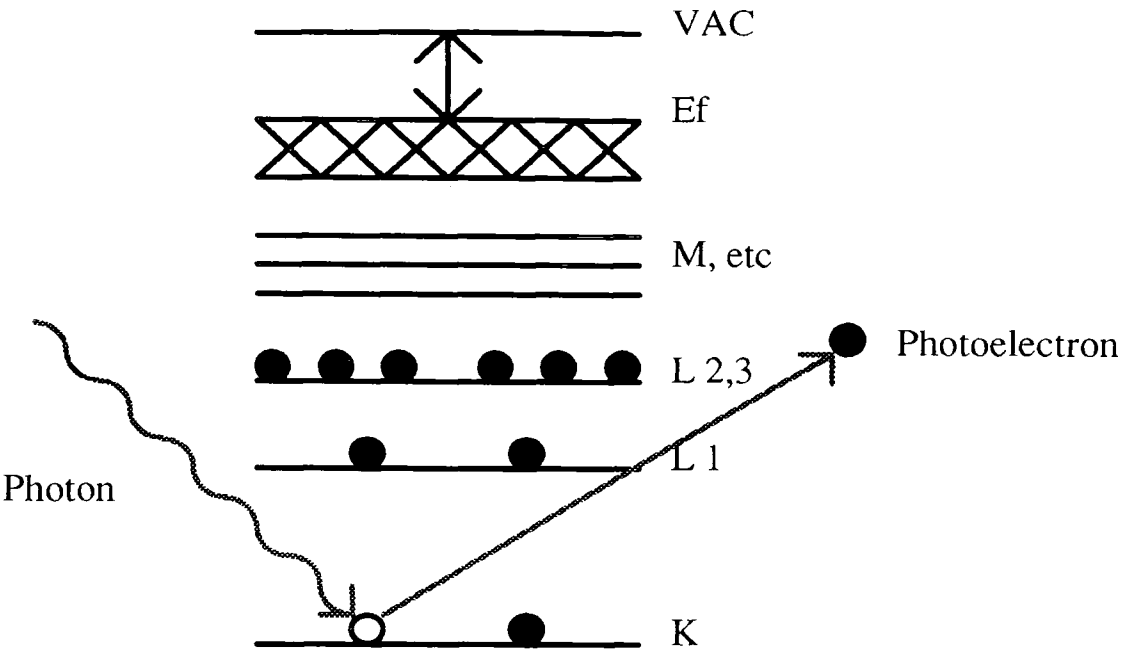

Figure 1.3: A schematic of the ejection of a photoelectron in XPS.

The X-rays with energy hυ cause electrons with a binding energy E_b to be ejected from the core level. As $h\upsilon > E_b$ these electrons must have kinetic energy, E_k. E_k can be measured and since hυ is known E_b can be calculated.

$$h\upsilon = E_b + E_k$$

By suitable selection of the X-ray source, photoelectrons can be generated which originate from less than 5 nm below the surface, Figure 1.4.

Each atom in the periodic table has its own characteristic core energy levels, and hence identification of the elements present at the surface is possible (apart from hydrogen).[43] Signal intensities provide information concerning elemental concentration.[44] For an individual atom, different chemical environments can give rise to a shift in the core level binding energy. For instance, different types of oxidised carbon environment (e.g. alcohol versus ester) can be distinguished.[38] Various standard polymers and reference compounds are normally used to assist in the identification of unknown surface species created during plasma modification.[45] Sometimes it is not possible to unambiguously identify functional groups present at a plasma treated polymer

surface (e.g. alcohol versus ether), in this case, derivatisation of the surface using labelling reagents can help to resolve these issues.[46,47]

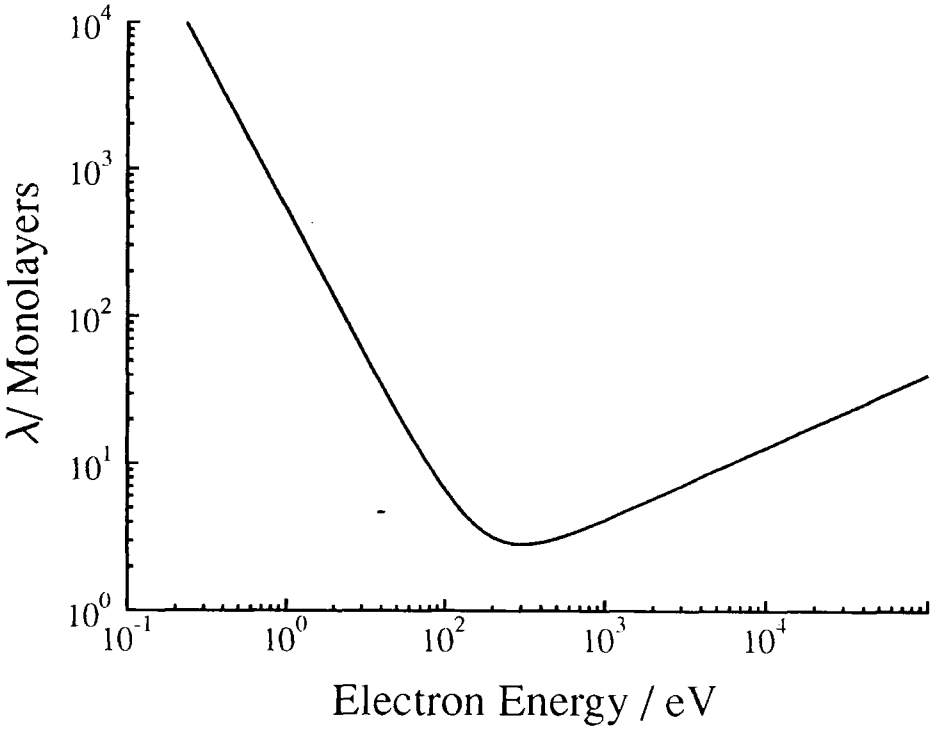

Figure 1.4: The dependence of attenuation length (monolayer) on the energy of the emitted electrons.

Valence band XPS (XPS-VB) spectra provide a qualitative insight into changes occurring in molecular structure during plasma treatment (e.g. crosslinking[19,48,49]). It can also be helpful for differentiating between groups with the same core level shift (e.g. phenyl versus methyl, etc.[45]). Another attribute of this technique is that chemical changes within specific functional groups along the polymer backbone can be followed.[19,48,50]

1.5.2 Mass Spectrometry

In mass spectrometry, molecules in the vapour phase are ionised.[51] The resulting fragmentation pattern of these ions separated by their mass to charge ratio (*m/z*) allows

molecular weight and molecular formula deduction.[51] There are several types of mass spectrometry such as magnetic and time of flight but only quadrupole mass spectrometry will be discussed in more detail here.

1.5.2.1 Quadrupole Mass Spectrometry

The quadrupole mass spectrometer (QMS) consists of three items, the ion source, the mass analyser and the ion detector; each responsible for a particular function. Ions are produced by the bombardment of the gas as it enters the spectrometer with electrons emitted from a hot filament (e.g. Tungsten) source.[52] The positive ions are then accelerated towards the quadrupole analyser where they are separated on the basis of their *m/z* ratio.[51] The analyser consists of four symmetrically arranged, parallel, electrically conducting rods which produce fields which approximate those from hyperbolic surfaces, Figure 1.5

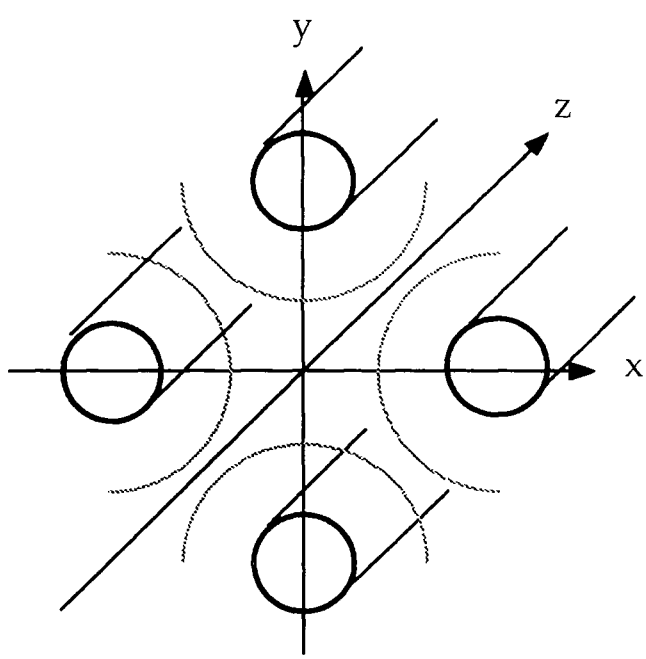

Figure 1.5 Schematic of the quadrupole mass analyser.

Opposite rods are connected together electrically, and to each pair a combination of superimposed RF and DC potentials are applied,[51] described by,

$$P(t) = \pm [U + V \cos(2\pi ft)]$$

where U is the DC voltage, V is the peak amplitude of a RF voltage at frequency f and time t. An ion entering the analyser will experience complex oscillations and only ions with one particular *m/z* ratio at a given set of conditions will have a stable path to traverse the length of the rods (the other *m/z* ratios will be defocused and lost by collisions with the rod or spectrometer casing).[51] The *m/z* ratio can be altered by varying U or V, or by changing f. Keeping U/V constant means that the resolution of the quadrupole mass spectrometry is also constant, as seen by,

$$m / \Delta m = 0.126 / (0.16784 - U/V)$$

Infinite resolution is possible by fixing U/V at 0.16784 or it can be changed by variations in U/V. Most systems keep f constant and simultaneously vary U and V.

After being analysed the ions are detected using a secondary electron multiplier, where the ions are accelerated into the first dynode initiating a cascade of electrons to be produced. A computer is often used to measure this current.

Secondary ion mass spectrometry (SIMS) uses mass spectrometry to study secondary ions emitted from a surface during bombardment by energetic primary particles.[53] A high primary particle beam current leads to dynamic SIMS, whereas a low beam current provides static SIMS (SSIMS). The former is destructive and often used for depth profiling, whilst SSIMS can provide structural chemical information and high surface sensitivity. SSIMS has been extensively used to study polymer surfaces in a qualitative manner,[54] it is molecular specific, can easily differentiate between polymers,[55] and is able to identify branching, or unsaturation.[56]

1.5.3 Atomic Force Microscopy

The relatively recent invention of atomic force microscopy (AFM) works by scanning a very sharp tip attached to a lightly sprung cantilever, across the sample surface whilst keeping the repulsive force between the probe and surface constant. Nanometer resolution of non-conducting substrates can routinely be achieved using AFM without

the need for any additional sample preparation. A number of studies have shown that significant changes in surface morphology can occur during plasma treatment.[50,57] Some of the obtained structures are stable,[64] whilst others can be washed off with solvent.[27,58]

1.6 INFLUENCE OF GAS

The chemical nature of the feed gas employed during plasma treatment can have a strong influence upon the surface modification of polymers.

1.6.1 Noble Gases

Noble gas plasma treatment of polymer surfaces creates free radical centres,[59,60,61] which subsequently participate in hydrogen abstraction, crosslinking, or reaction with foreign molecules (e.g. air, polymerisable monomers, etc.[62]), Tables 1.1-1.3. Modelling studies have shown that comparable levels of surface modification can be achieved using low energy noble gas ion beams,[17,63] this is consistent with there being an absence of any chemical interactions between the glow discharge and the surface. Topographical changes also occur during noble gas plasma treatment; their physical appearance and stability strongly depends upon the nature of the polymer substrate under investigation and which inert gas is being used.[64,65,66] For instance, He plasma treatment of polyethersulfone generates cone-like features at the surface.[64]

Inert gas plasma treatments can be used to lower the frictional resistance of a polymer substrate (this can be important for biological applications);[67] however subsequent biaxial orientation of such treated surfaces has been shown to result in the formation of ultra-fine protrusions, which impede good slip behaviour (this can be critical during film processing on the industrial scale).[68] Also inert gas plasma modification can improve the electrical conductivity of a polymer surface.[50]

1.6.2 Nitrogen

Nitrogen plasma treatment of polymers introduces mainly primary amine groups at the surface along with crosslinking,[29,31,69,70] however the rate of surface reaction is found to be slower compared to corresponding oxygen plasma treatments,[19] Table 1.4. In the case of polypropylene, a preferential reaction of the syndiotactic phase is observed.[29] Amine functionalised polymer chains can possess a dynamic mobility which allows them to be transported into the subsurface with the aid of a wetting permeable solvent, and they can also subsequently be pulled back out towards the surface by using an aqueous protonation medium.[31] Some nitrogen plasma treated polymer surfaces slowly oxidise upon exposure to air to form transient oxygenated moieties which gradually disappear with storage time.[33]

1.6.3 Hydrogen

Hydrogen plasma reduction of polytetrafluoroethylene (PTFE) surfaces results in the formation of a 2 nm thick layer of defluorinated material, this is accompanied by a corresponding drop in its contact angle with water, thereby making the substrate more suitable for bonding,[71,72] Table 1.5. The predominant reaction pathway is considered to be fluorine abstraction by atomic hydrogen from the PTFE surface to form HF (this is highly favourable due to its exothermic nature), the free radical centre left behind either undergoes reaction with subsequent incident hydrogen atoms or participates in crosslinking at the surface.[73] Similarly, other types of polymer surfaces are also able to undergo hydrogen plasma reduction.[64]

POLYMER	XPS	SEM	Contact Angle	Adhesion	Other
Polyethylene	[67]	[67]	[67,89]	[89,92]	Friction: [67] Weight loss: [74]
Polypropylene	[50,75]	[74]			AFM: [50] Electrical conductivity: [50,75] Weight loss: [74]
Polystyrene	[67]	[67]	[67,89]	[89,92]	Friction: [67]
Polyethylene terephthalate			[89]	[89,92]	Weight loss: [74]
Polycarbonate			[89]	[89]	
Polymethylmethacrylate	[50]				AFM: [50] Electrical conductivity: [50]
Polysulfone	[65]		[89]	[89]	AFM: [65]
Polyethersulfone	[64]				AFM: [64]
Polytetrafluoroethylene	[100]				AFM: [100]
Polyvinylfluoride			[89]	[89]	
Polyvinylidene fluoride				[92]	
Nylon				[92]	Weight loss: [74]
Polyvinylchloride	[67]	[67]	[67]		Friction: [67]

Table 1.1: Summary of helium plasma treatments.

POLYMER	XPS	Other
Polypropylene	[75]	Electrical conductivity: [75]
Polysulfone	[65]	AFM: [65]
Polyethersulfone	[64]	AFM: [64]
Polytetrafluoroethylene	[100]	AFM: [100]

Table 1.2: Summary of neon plasma treatments.

POLYMER	XPS	FTIR	Contact Angle	Other
Polyethylene	[72,82]	[35]	[35,82,83]	DSC: [35], Elemental analysis: [35] ESR: [74], Langmuir probe: [83], XRD: [35]
Polypropylene	[50,75]			AFM: [50] Electrical conductivity: [75,50]
Polymethylmethacrylate	[50]			AFM: [50] Electrical conductivity: [50]
Polyethersulfone	[64]			AFM: [64]
Polysulfone	[65]			AFM: [65]
Polytetrafluoroethylene	[71,100,76 ,77]		[71,77]	AFM: [100]
Polyvinylidenefluoride	[76]			

Table 1.5: Summary of hydrogen plasma treatments.

POLYMER	XPS	FTIR	SEM	Contact Angle	Adhesion	Other
Polyethylene	[19,74,78]	[35]	[19]	[35, 79]	[79]	DSC: [35] Elemental analysis: [35] XPS-VB: [19] XRD: [35]
Polypropylene	[50,63,75]					AFM: [50] Electrical conductivity: [50,75] XPS-VB: [63]
Polystyrene	[78]					ESR: [59]
Polyethylene terephthalate	[68,78]			[66]		SIMS: [68] TEM: [68]
Polymethylmethacrylate	[50]					AFM: [50] Electrical conductivity: [50] ESR: [60]
Polysulfone	[65]					AFM: [65]
Polyethersulfone	[64]					AFM: [64]
Nylon	[78]					
Polytetrafluoroethylene	[61,62,74,100, 78,80 ,]		[80]	[62,80,81]		AFM: [100] ESR: [61] SIMS: [80]
Silicone rubber				[79]	[79]	

Table 1.3: Summary of argon plasma treatments.

POLYMER	XPS	FTIR	SEM	Contact Angle	Adhesion	Other
Polyethylene	[19,31,69,74,82]		[19]	[82,83]		ESR: [74] Langmuir probe: [83] XPS-VB: [19]
Polypropylene	[29,63,109, 75]	[29]	[29,74]	[109]	[109,84]	AFM: [109,75] Electrical conductivity: [75] SIMS: [29,84] Weight loss: [74] XPS-VB: [63]
Polystyrene	[69]					
Polyethylene terephthalate	[70]	[57]	[57]	[57]		
Polymethylmethacrylate	[50]					AFM: [50] Electrical conductivity: [50]
Polyether etherketone	[33]					
Polytetrafluoroethylene	[100,74,85 ,86]			[81,86]		AFM: [100]

Table 1.4: Summary of nitrogen plasma treatments.

1.6.4 Oxidation

Plasma oxidation can be used to remove contaminants present on a polymer surface.[87] It can also lead to oxygen incorporation (various groups can be formed, these include alcohols, ethers, esters, acids, etc.), which in turn give rise to improved bondability of the substrate[88,89,90] or a change in its dielectric performance.[91] Care needs to be exercised, since an overtreatment of the polymer substrate can produce a weak boundary layer as a result of extensive chain scission, which can have a detrimental effect on the adhesive performance of the treated surface.[92]

1.6.4.1 Oxygen Plasmas

Oxygen plasma treatment of polymer surfaces comprises degradation of the substrate and reaction with ions, atoms, ozone, metastables of atomic and molecular oxygen, electrons, and a broad electromagnetic spectrum, Table 1.6. In the case of floating low pressure RF oxygen plasmas: the concentration of oxygen atoms is of the order of 1% (trace amounts of water can increase this value[93]), ozone concentration is less than 0.02%, the electron density is close to 4×10^{14} m^{-3}, with an electron temperature of approximately 4 eV, the thermal energy of the neutral oxygen atoms is 0.1 eV, and the emission spectrum is dominated by three intense atomic oxygen lines at 130.2, 130.5, and 130.6 nm.[94] Electron impact dissociation of molecular oxygen is considered to be the predominant reaction pathway for the formation of atomic oxygen.[95]

Modelling studies have shown that the reaction probability of ground state molecular oxygen with a polymer substrate in the presence of VUV radiation emitted by an oxygen plasma is low,[24,96] hence it is the attack of atomic oxygen at VUV activated surface sites which gives rise to oxygenation.[24] Surface modification quickly reaches a steady state in terms of chemical composition,[38] this can be attributed to an overall balance between oxygen incorporation and evolution of volatile reaction products (H_2O, CO, CO_2, oligomers, etc.[97]). For a fixed set of experimental parameters, the relative importance of these competing surface processes is dependent upon the type of polymer under investigation. All unstabilised polymers degrade upon exposure to an O_2 plasma but the rates of oxidation are dependent upon their structure. Functional groups which readily react with oxygen without causing extensive chain scission (e.g. phenyl rings[41,98]) help to

generate a more oxidised surface (e.g. carboxylate groups[39,41]), whilst structural units which are highly susceptible to cleavage will encourage ablation, depolymerisation, and the unveiling of fresh polymer.[39,98] This leads to a whole range of chemical functionalities being generated at a polymer surface during oxygen plasma treatment (e.g. oxidised groups, crosslinked centres, unsaturated bonds, etc.).[99] Most polymers tend to experience an increase in oxygen content at the surface during oxygen plasma treatment; two notable exceptions are PTFE for which there is no change (although there is significant surface roughening[100]) and PMMA which suffers a loss in surface oxygen content.[101] The plasma operating conditions can also influence the surface chemistry, for instance oxygen incorporation is greater at low powers in the case of polyethylene, whereas polystyrene does not display this behaviour.[48] High power densities,[96] long treatment times, and heating above the polymer glass transition temperature (T_g)[102] all lead to extensive roughening of the polymer substrate as a result of etching.

Most oxygen plasma treated surfaces are found to undergo ageing effects leading to hydrophobic recovery combined with a decrease in bondability.[103] Any low molecular weight oxidised material present on plasma treated polymer surfaces may be washed off with a solvent.[104] Such low molecular weight oxidised material can be formed via the attachment of atomic oxygen to free radical sites (these may have been created either by hydrogen abstraction or VUV activation), this is followed by chain scission.[27,40]

Extended ageing of oxygen plasma modified polyethylene results in almost a complete loss of oxygenated functionalities from the surface (probably due to desorption of low molecular weight oxidised material) to leave behind a highly crosslinked layer.[48]

Metal-containing polymers (e.g. polysilanes, polysiloxanes, etc.) quickly form an etch resistant inorganic oxide layer[37,105,106] during plasma oxidation. Ageing effects have also been observed for oxygen plasma treated polysiloxane films, this is primarily attributed to cracking of the overlayer oxide film as a consequence of its markedly different mechanical properties[37] and density[107] relative to the underlying polymer substrate.

1.6.4.2 Air

Air and oxygen plasma treated polymer surfaces generally tend to have similar chemical compositions;[108,109] but differing levels of crosslinking, which is to be expected on the basis of each plasma emitting its own unique radiative VUV component, Table 1.7. Air plasmas are found to take longer than oxygen plasmas to achieve the same level of surface modification.

1.6.4.3 Water

Water plasma treatment is normally found to produce higher levels of oxygenation compared to corresponding oxygen plasma treatments,[110] Table 1.8.

1.6.5 Fluorination

Dissociation of CF_4 in a RF electrical discharge can be summarised as follows:[111]

$$CF_x \xrightarrow[\leftarrow M-]{-e\rightarrow} F + CF_{x-1} \qquad \text{(where x = 4 to 1)}$$

Fluorine atoms are reported to be the most chemically reactive species during CF_4 plasma treatment of polymer surfaces,[40] Table 1.9. Ions, electrons, and electronically excited species play a relatively minor role.[112] Permeation of atomic fluorine deep into the subsurface followed by reaction with the substrate is consistent with this viewpoint.[112,113] Extended Huckel molecular orbital calculations have been used to explain why fluorine atoms react via hydrogen abstraction in the case of saturated hydrocarbon polymers, whilst addition to double bonds is the preferred reaction pathway for polymers containing unsaturated centres, thereby yielding a greater level of surface fluorination for the latter.[40,42]

This structure-behaviour relationship has been utilised to introduce differing levels of fluorination along the length of a polymer chain consisting of both aliphatic and aromatic segments.[114]

CF_4 glow discharge modification of polymer surfaces can be used to improve their water repellency.[115] In the case of polyethylene terephthalate and nylon, surface hydrophobicity introduced during CF_4 plasma treatment deteriorates upon immersion in water;[32] this behaviour has been attributed to the rotational and diffusional migration of fluorinated moieties into the polymer subsurface. A way round this is to first deposit a highly immobile crosslinked plasma polymer layer which is subsequently fluorinated by CF_4 plasma treatment.[32]

1.7 CONCLUSIONS

Plasma modification of polymer surfaces can be used to improve their wettability, adhesion, permeability, gas barrier, electrical conductivity, abrasion resistance, biocompatibility, etc. A detailed understanding of structure-behaviour relationships at the molecular level allows the industrial end-user to optimise the macroscopic behaviour of such plasma treated polymer surfaces.

It is the aim of this thesis to examine in greater depth the interactions occurring at the plasma - polymer interface.

POLYMER	XPS	FTIR	SEM	Contact Angle	Adhesion	Other
Polyethylene	[19,36,39,48, 103,72,88,94,98, 82,116 ,117 118 , 119 ,120]	[96, 121]	[19,96,116]	[35,36,103,89 97,79,82, 83, 121,]	[36,103,88,89,92, 97,79]	DSC: [35] Elemental analysis: [35] GPC: [96] Langmuir probe: [83] Mass spectrometry: [96] SIMS: [36,98] XPS-VB: [19,48] XRD: [35]
Polypropylene	[36,38,50,96,90, 75]	[96,121]	[96]	[36,89,97,121]	[36,103,89,97]	AFM: [50,Gross] Electrical conductivity: [50,75] GPC: [96] Mass spectrometry: [96] SIMS: [36] XPS-VB: [90]
Polystyrene	[23,38,39,41,48,2 8,98]	[28]		[89,97]	[89,92,97]	SIMS: [98] XPS-VB: [48]
Polether etherketone	[39,104,108,117]					SIMS: [104]
Polymethylmethacrylate	[50,96,98]	[96]	[96]	[97]	[97]	AFM: [50]: Electrical conductivity: [50] GPC: [96] Mass spectrometry: [96] SIMS: [98]
Polyethylene terephthalate	[96]	[57,96]	[57,96]	[57,89,97]	[89,92,97]	GPC: [96] Mass spectrometry: [96]

Polycarbonate	[103]			[103,89,97]	[103,89,97]	
Polycaprolactone		[121]		[121]		
Polytetrafluoroethylene	[96,100,80,122 , 123]	[96]	[96,80]	[97,80]	[97]	AFM: [100] GPC: [96] Mass spectrometry: [96] SIMS: [80]
Polyvinylfluoride	[96]	[96]	[96]	[97]	[92,97]	GPC: [96] Mass spectrometry: [96]
Polyvinylidenefluoride	[120]			[89]	[89,92]	
Nylon				[97]	[92,97]	
Polysulfone	[65]			[89]	[89]	AFM: [65]
Polyethersulfone	[64]					AFM: [64]
Silicone rubber				[79]	[79]	

Table 1.6: Summary of oxygen plasma treatments.

POLYMER	XPS	FTIR	SEM	Contact Angle	Adhesion	Other
Polyethylene	[124]				[124]	
Polypropylene	[109]			[109]	[109]	AFM: [109]
Polyethylene terephthalate	[124]	[57]	[57]	[57]	[124]	
Polether etherketone	[108]					
Polytetrafluoroethylene	[125]			[125]	[125]	

Table 1.7: Summary of air plasma treatments.

POLYMER	XPS	FTIR	Contact Angle	Other
Polystyrene	[110]			
Polymethylmethacrylate	[126]	[126]		ISS: [126]

Table 1.8: Summary of water plasma treatments.

POLYMER	XPS	SEM	Contact Angle	Other
Polyethylene	[40,42,113, 117[b],127 , 127[a]]	[113]	[113]	Emission spectroscopy: [113,127,127[a]] RBS: [113] SIMS: [113]
Polypropylene	[42,128]		[128]	
Polystyrene	[41,42[b]]			
Polyisoprene	[40,42]			
Polyethylene terephthalate	[32,42,112, 129]	[112]	[32,112]	
Polether etherketone	[42,108]			
Polycarbonate	[115]		[115]	Emission spectroscopy: [115] SIMS: [115]
Polyethersulfone	[64]			AFM: [64]
Polyimide	[40]			

NB All fluorination treatments are based upon CF_4 plasmas, except for: a - SF_6 plasma, and b - F_2 plasma

Table 1.9: Summary of fluorination plasma treatments

1.8 REFERENCES

[1] J.W. Coburn, IEEE Transactions of Plasma Science **19**, 6 (1991).

[2] H.V. Boenig, *Fundamentals of Plasma Chemistry and Technology* (Technomic Publishing Co, Lancaster,1988).

[3] I. Langmuir, Phys. Rev. **33**, 954 (1929).

[4] A. von Engel, *Electric Plasmas: Their Nature and Uses* (Taylor & Francis, London, 1983).

[5] A. Grill, *Cold Plasma in Materials Fabrication: From Fundamentals to Applications* (IEEE Press, New York, 1994).

[6] F.F. Chen, *Introduction to Plasma Physics* (Plenum Press, London, 1974).

[7] S.M. Rossnagel, *Thin Film Processes II*, edited by J.L. Vosen and K. Wernen (Academic Press, London, 1991), Chapter II-1.

[8] F.M. Penning, *Electrical Discharges in Gases* (Philips Technical Library, 1957).

[9] B. Chapman, *Glow Discharge Processess* (Wiley-Interscience, 1980).

[10] R.F. Baddour and R.S. Timmins eds. *The Applications of Plasmas to Chemical Processing* (MIT Press, Cambridge, 1967).

[11] R. Reif and W. Kern, *Thin Film Processes II*, edited by J.L. Vosen and K. Wernen (Academic Press, London, 1991), Chapter IV-1.

[12] S.Veprek, F-A. Sarrot, S. Rambert and E. Taglauer, J. Vac. Sci. Technol. **A7**, 2614 (1989).

[13] H. Biederman and Y. Osada, Plasma Chemistry of Polymers, Advances in Polymer Science **95**, 57 (1990).

[14] D.L. Flamm, V.M. Donnelly and D.E. Ibbotson, J. Vac. Sci. Technol. **B1**, 23 (1983).

[15] S. Veprek, C. Eckmann and J.T. Elmer, Plasma Chemistry and Plasma Processing **8**, 445 (1988).

[16] E.M. Liston, J. Adhesion **30**, 199 (1989).

[17] R.K. Wells, M.E. Ryan and J.P.S. Badyal, J. Phys. Chem. **97**, 12879 (1993).

[18] D.T. Clark, A. Dilks A and D. Shuttleworth, *Polymer Surfaces*, edited by W.J Feast and D.T. Clark (John Wiley & Sons, Bath, 1978) Chapter 9.

[19] L.J. Gerenser, J. Adhesion Sci. **1**, 303 (1987).

[20] R.H. Partridge, J. Chem. Phys. **45**, 1685 (1966).

[21] R.H. Partridge, J. Chem. Phys. **49**, 3656 (1968).

[22] D.T. Clark and A. Dilks, J. Polym. Sci; Polym. Chem. **16**, 911 (1978).

[23] A.G. Shard and J.P.S. Badyal. J. Phys. Chem. **95**, 9436 (1991).

[24] J. Hopkins, S.H. Wheale and J.P.S. Badyal, J. Phys. Chem. **100**, 14062 (1996).

[25] C. Mayoux, IEEE Trans. Dielectrics and Electrical Insulation **1**, 785 (1994).

[26] F. Ponicin-Epaillard, B. Chevet and J-C. Brosse, Eur. Polym. J. **26**, 333 (1990).

[27] J. Hopkins, R.D. Boyd and J.P.S. Badyal, J. Phys. Chem. **100**, 6755 (1996).

[28] E.C. Onyiriuka, L.S. Hersh and W. Hertl, J. Colloid and Interface Sci. **144**, 98 (1991).

[29] F. Poncin-Epaillard, B. Chevet and J-C. Brosse, Makromol. Chem. **192**, 1589 (1992).

[30] J.D. Andrade, *Polymer Surface Dynamics* (Plenum, New York, 1988).

[31] D.S. Everhart and C.N. Reilley, Surf. Interface Anal. **3**, 126 (1981).

[32] T. Yasuda, K. Yoshida and T. Okuno, J. Polym. Sci; Polym. Phys. **26**, 2061 (1988).

[33] C. Jama, O. Dessaux, P. Goudman, L. Gengembre and J. Grimblot, Surf. Interface Anal. **18**, 751 (1992).

[34] T.J. Hook, J.A. Gardella and L. Salvati, J. Mater. Res. **2**, 117 (1987).

[35] Y. Yao, X. Liu and Y. Zhu, J. Appl. Polym. Sci. **48**, 57 (1993).

[36] M. Morra, E. Occhiello, L. Gila and F. Garbassi, J, Adhesion **33** 77 (1990).

[37] G.N. Taylor and T.M. Wolf, Polymer Engineering and Science **20** 1087 (1980).

[38] D.T. Clark and A. Dilks, J. Polym. Sci; Polym. Chem. **17**, 957 (1979).

[39] A.G. Shard and J.P.S. Badyal, Macromolecules **25**, 2053 (1992).

[40] S.R. Cain, F.D. Egitto and F. Emmi, J. Vac. Sci. Technol. **A5**, 1578 (1987).

[41] I. Tepermeister and H.H. Sawin, J. Vac. Sci. Technol. **A10**, 3149 (1992).

[42] J. Hopkins and J.P.S. Badyal, J. Phys. Chem. **99**, 4261 (1995).

[43] C.D. Wagner, W.M. Riggs, L.E. Davis, J.F. Moulder and G.E. Muilenberg, *Handbook of X-Ray Photoelectron Spectroscopy* (Perkin-Elmer Corp, USA, 1979).

[44] *Practical Surface Analysis by Auger and X-Ray Photoelectron Spectroscopy*, edited by D. Briggs and M.P. Seah (John Wiley and Sons, Chichester, 1983).

[45] G. Beamson, D. Briggs, *High Resolution XPS of Organic Polymers, The Scienta ESCA 300 Database* (John Wiley and Sons, Chichester, 1992).

[46] S. Tasker, S.C.E. Backson, R.W. Richards and J.P.S. Badyal,. Polymer **35**, 4717 (1994).

[47] R.A. Dickie, J.S. Hammond, J.E. deVries and J.W. Holubka, Anal. Chem. **54**, 2045 (1982).

[48] R.K. Wells, J.P.S. Badyal, I.W. Drummond, K.S. Robinson and F.J. Street, J. Adhesion Sci. Technol. **7**, 1129 (1993).

[49] R. Foerch, G. Beamson and D. Briggs, Surf. Interface Anal. **17**, 842 (1991).

[50] M. Collaud, P. Groenig, S. Nowak, and L. Schlapbach. J. Adhesion Sci. **8**, 1115 (1994).

[51] R.M. Silverstein, G.C. Bassler and T.C. Morrill, *Spectrometric Identification of Organic Compounds* (Wiley, Singapore, 1991) Chapter 2.

[52] D.W. Floyd, A.J. Floyd and M. Sainsbury, *Organic Spectroscopy* (Wiley, Bath, 1988) Chapter 5.

[53] A. Brown and J.C. Vickerman, Surf. Interface Anal. **8**, 75 (1986).

[54] D. Briggs, A. Brown, and J.C. Vickerman, *Handbook of Static Secondary Ion Mass Spectrometry* (John Wiley and Sons, Chichester, 1989).

[55] D. Briggs, Surf. Interface Anal. **4**, 151 (1982).

[56] D. Briggs, Surf. Interface Anal. **15** 734 (1990).

[57] A.M. Wrobel, M. Kryszewski, W. Rakowski, M. Okoniewski and Z. Kubacki, Polymer **19**, 908 (1978).

[58] M. Strobel, C. Duntatov, J.M. Strobel, C.S. Lyons, S.J. Perron and M.C. Morgen, J. Adhesion Sci. Technol. **3**, 321 (1989).

[59] M. Kuzuya, A. Noguchi, H. Ito, S-I. Kondo and N. Noda, J. Polym. Sci; Polym. Chem. **29**, 1 (1991).

[60] M. Kuzuya, A. Noguchi, M. Ishikawa, A. Koide, K. Sawada, A. Ito and N. Noda, J. Phys. Chem. **95**, 2398 (1991).

[61] Y. Momose, T.M. Ogino, S. Okazaki and M. Hirayama, J. Vac. Sci. Technol. **A10**, 229 (1992).

[62] K.L. Tan, L.L. Woon, H.K. Wong, E.T. Kang and K.G. Neoh, Macromolecules **26**, 2832 (1993).

[63] M. Collaud, S. Nowak, O.M. Kuttel, P. Groning and L. Schalpbach, Appl. Surf. Sci. **72**, 19 (1993).

[64] J. Hopkins and J.P.S. Badyal, Macromolecules **27**, 5498 (1994).

[65] J. Hopkins and J.P.S. Badyal, J. Polym. Sci; Polym. Chem. **34**, 1385 (1996).

[66] Y-L. Hseih, D.A. Timm and M. Wu, J. Appl. Polym. Sci. **38**, 1719 (1989).

[67] P. Triolo and J.D. Andrade, J. Biomedical Materials Research **17**, 129 (1983).

[68] Y. Nakayama, F. Soeda, A. Ishitani and T. Ikegami, Polymer Engineering and Science; **31**, 812 (1991).

[69] R. Foerch, N.S. McIntyre, R.N.S. Sodhi and D.H. Hunter, J. Appl. Polym. Sci. **40**, 1903 (1990).

[70] B. Mutel, O. Dessaux, P. Goudman, L. Gengenbre and J. Grimblot, Surf. Interface Anal. **20**, 283 (1993).

[71] Y. Yamada, T. Yamada, S. Tasaka and N. Inagaki, Macromolecules **29**, 4331 (1996).

[72] D.T. Clark and R. Wilson, J. Polym. Sci; Polym. Chem. **25**, 2643 (1987).

[73] T.N. Gallaher, T.C. DeVore, R.O. Carter III and C. Anderson, Applied Spectroscopy **34**, 408 (1990).

[74] H. Yasuda, J. Macromol. Sci. Chem. **A10**, 383 (1976).

[75] M. Collaud Couen, P. Groenig, G. Dielter and L. Schalpbach, J. Appl. Phys. **77**, 5695 (1995).

[76] D.T. Clark and D.R. Hutton, J. Polym. Sci; Polym. Chem. **25**, 2643 (1987).

[77] Y. Yamada, T. Yamada, S. Tasaka and N. Inagaki, Macromolecules **29**, 4331 (1996).

[78] H. Yasuda, H.C. Marsh, S. Brandt, C.N. Reilley, J. Polym. Sci; Polym. Chem. **15**, 991 (1977).

[79] R.R. Sowell, N.J. DeLollis, H.J. Gregory and O. Montoya, J. Adhesion **4**, 15 (1972).

[80] M. Morra, E. Occhiello and F. Garbassi, Surf. Interface Anal. **16**, 412 (1990).

[81] M.G. Fessehaie, S. McClain, C.L. Barton, G.S. Swei and S.L. Suib, Langmuir **9**, 3077 (1993).

[82] A. Hollander, J. Behnisch and H. Zimmermann, J. Appl. Polym. Sci. **49**, 1857 (1993).

[83] J. Behnisch, A. Hollander and H. Zimmermann, J. Appl. Polym. Sci. **49**, 117 (1993).

[84] F. Arefi, V. Andre, P. Montazer-Rahmati and J. Amouroux, Pure & Appl. Chem. **64**, 715 (1992).

[85] M.A. Golub, E.S. Lopata and L.S. Finney, Langmuir **9**, 2240 (1993).

[86] M. Kusabiraki, Japanese Journal of Applied Physics **29**, 2809 (1990).

[87] N.H. Ladizesky and I.M. Ward, J. Mater. Sci. **18**, 533 (1983).

[88] U. Plawky, M. Londshien and W. Michaeli, Acta Polymer **47**, 112 (1996).

[89] W.L. Wade Jr., R.J. Mammone and M. Binder, J. Appl. Polym. Sci. **43**, 1589 (1991).

[90] J.M. Burkstrand, J. Vac. Sci. Technol. **15**, 223 (1978).

[91] S-H. Wu, D.D. Denton and R.J. De Souza-Machad, J. Vac. Sci. Technol. **A11**, 291 (1993).

[92] J.R. Hall, C.A.L.Westerdahl, M.J. Bodnar and D.W. Levi, J. Appl. Polym. Sci. **16**, 1463 (1972).

[93] J.T. Herron and H.I. Schiff, Can. J. Chem. **36**, 1159 (1958).

[94] A.F. Whitaker and B.Z. Jang, SAMPE Journal **30**, 30 (1994).

[95] P. Friedel and S.J. Gourier, Phys. Chem. Solids **44**, 353 (1983).

[96] A.F. Whitaker and B.Z. Jang, J. Appl. Polym. Sci. **48**, 1341 (1993).

[97] R.H. Hansen, J.V. Pascale, T. De Benidictis and P.M. Rentzepis, J. Polym. Sci; Polym. **3**, 2205 (1963).

[98] L. Lianos, D. Parrat, T.Q. Hoc and T.M. Duc, J. Vac. Sci. Technol. **A12**: 2491 (1994).

[99] T. Gross, A. Lippitz, W.E.S. Unger, Friedrich and Ch. Woll, *Polymer 35*, 5590 (1994).

[100] M.E. Ryan and J.P.S. Badyal, Macromolecules **28**, 1377 (1995).

[101] P. Groning, M. Collaud, G. Dietler and L. Schlapbach, J. Appl. Phys. **76**. 887 (1994).

[102] O. Joubert, P. Paniez, M. Pons and J. Pelletier, J. Appl. Phys. **70**, 977 (1991).

[103] M. Morra, E. Occhiello and F. Garbassi, *Metallised Plastics 2*, edited by K.L. Mittal (Plenum Press, New York, 1991).

[104] D.J. Pawson, A.P. Ameen, R.D. Short, P. Denison and F.R. Jones, Surf. Interface Anal. **18**, 13 (1991).

[105] C.W. Jurgensen and A. Rammelsberg, J. Vac. Sci. Technol. 7; 3317 (1989).

[106] J.L.C. Fonseca, C.P. Barker and J.P.S. Badyal, Macromolecules **28**, 6112 (1995).

[107] S. Packirsamy, D. Schwam and M.H. Litt, J. Mater. Sci. **30**, 308 (1995).

[108] E.C. Onyiriuka, J. Vac. Sci. Technol. **A11**, 2941 (1993).

[109] S.O. O'Kell, T. Henshaw, G. Farrow, M. Aindow and C. Jones, Surface and Interface Analysis **23**, 319 (1995).

[110] J.F. Evans, J.H. Gibson, J.F. Moulder, J.S. Hammond and H. Goretzki, Fresenius. Z Anal. Chem. **319**, 841 (1984).

[111] E.A. Truesdale and G. Smolinsky, J. Appl. Phys. **50**, 6594 (1979).

[112] T. Yasuda, T. Okuno, M. Miyama and Y. Yasuda, J. Polym. Sci; Polym. Chem. **32**, 1829 (1994).

[113] Y. Khairallah, F. Khonsari-Arefi F and J. Amouroux, Thin Solid Films **241**, 295 (1994).

[114] F. Emmi, F.D. Egitto and L.J. Matienzo, J. Vac. Sci. Technol. **A9**, 786 (1991).

[115] E. Occhiello, M. Morra and F. Garbassi, Die Angewandte Makromolekulare Chemie **173**, 183 (1989).

[116] R. Foerch, N.S. McIntyre and D.H. Hunter, J. Polym. Sci; Polym. Chem. **28**, 193 (1990).

[117] F. Emmi, F.D. Egitto and L.J. Matienzo, J. Vac. Sci. Technol. **A9**, 786 (1991).

[118] D.T. Clark and A. Dilks, J. Polym. Sci; Polym. Chem. **17**, 957 (1979).

[119] H.S. Munro and H. Beer, Polym. Commun. **27**, 79 (1986).

[120] M.A. Golub and R.D. Cormia, Polymer **30**, 1576 (1989).

[121] F. Normand, A. Granier, P. Leprince, J. Marec, M.K. Shi and F. Clouet. Plasma Chemistry and Processing **15**, 173 (1995).

[122] T. Wydeven, M.A. Golub and N.R. Lerner, J. Appl. Polym. Sci. **37**, 3343 (1989).

[123] M.A. Golub, T. Wydeven and R.D. Cormia, Polymer **30**, 1571 (1989).

[124] S. Saphieha, J. Cerny, J.E. Klemberg-Sapieha and L. Martinu, J. Adhesion **42**, 91 (1993).

[125] T. Kasemura, S. Ozawa and K. Hattori, J. Adhesion **33**, 33 (1990).

[126] T.J. Hook, J.A. Gardella Jr. and L.S. Salvati, J. Mater. Res. **2**, 117 (1987).

[127] Y. Khairallah, F. Khonsari-Arefi and J. Amouroux, Pure and Appl. Chem. **66**, 1353 (1994).

[128] M. Strobel, S. Corn, C.S. Lyons and G.A. Korba, J. Polym. Sci; Polym. Chem. **23**, 1125 (1985).

[129] E. Krentsel, S. Fusselman, H. Yasuda, T. Yasuda and M. Miyama, J. Polym. Sci. Polym. Chem. **32**, 1839 (1994).

CHAPTER 2

MASS SPECTROMETRY AT THE PLASMA - POLYMER INTERFACE

2.1 INTRODUCTION

Non-isothermal plasma modification of polymer surfaces has been of scientific and technological interest for over 30 years, since it can improve wettability, adhesion, hydrophobicity, oleophobicity, biocompatibility, permeability, etc. Short treatment times combined with negligible environmental waste have made this technique an important industrial tool.[1] In the past, mainly indirect analytical methods have been utilised to gain an insight into processes occurring at the plasma - polymer interface.[2] For instance, characterisation of the substrate prior to and following plasma treatment using X-ray photoelectron spectroscopy (XPS),[3-14] infrared spectroscopy (IR),[10] secondary ion mass spectrometry (SIMS),[4,5] ion scattering spectroscopy (ISS),[9] contact angle measurements,[4,6,7] and atomic force microscopy (AFM)[11-14] has helped to identify physicochemical changes taking place at the surface. However as yet, it has not been possible to pinpoint and monitor the actual chemical processes occurring within the vicinity of the plasma - polymer interface in real-time. This lack of progress can primarily be attributed to it being experimentally difficult to discriminate between bulk plasma chemistry and reactions occurring at the plasma - substrate interface using in-situ diagnostic techniques, e.g. optical emission spectroscopy (OES),[15] mass spectrometry,[16] electrical and magnetic probes,[17] quartz microbalances,[18,19] or laser induced fluorescence (LIF)[20].

This chapter describes how the major stumbling blocks previously encountered regarding interfacial diagnostics during plasma modification of polymer surfaces can be overcome by exploiting the pressure drop across the substrate. Quadrupole mass spectrometry has been used to detect permeant species, thereby gaining access to interfacial reaction products and intermediates. A comparison is made between N_2, O_2 and air plasma modification of polyethylene, due to the commercial importance of these treatments.

$$-\left(CH_2-CH_2\right)_n-$$

Polyethylene

2.2 EXPERIMENTAL SECTION

Circular pieces of low-density polyethylene film (Goodfellows; 48 mm diameter, thickness 15 μm, density 0.92 gcm^{-3}) were ultrasonically cleaned in a 50 / 50, polar / non-polar solvent mixture of isopropyl alcohol / cyclohexane for 30 s and allowed to dry in air. Oxygen (BOC 99.9%), nitrogen (BOC 99.9%) and air were used as feed gases for the respective plasma exposures.

Low pressure electrical discharge treatments were carried out using an electrodeless cylindrical reactor (39 mm diameter, 826 cm^3 volume, and a leak rate of less than 2.5 x 10^{-5} cm^3s^{-1}) enclosed in a Faraday cage.[21] This was fitted with a gas inlet, an active thermocouple pressure gauge and a mechanical rotary pump. A copper coil (4 mm diameter, 13 turns, spanning 9 cm) wound around the glass reactor was inductively coupled to a 13.56 MHz radio frequency generator via an LC matching network. All joints were grease free. For each experiment, a new piece of polymer film supported on a perforated metal flange was sandwiched between the plasma chamber and a Vacuum Generators Micromass QX200 quadrupole mass spectrometer (0 - 200 amu range; base pressure 2 x 10^{-10} mbar) multiplexed to a computer, Figure 2.1. The plasma reactor side of the polymer membrane was pumped down to a base pressure of better than 2 x 10^{-3} mbar, and then 6 x 10^{-1} mbar of gas was introduced at a flow rate of 0.016 cm^3s^{-1}; this resulted in a rise in the measured mass signal intensity on the other side of the polymer film corresponding to gas permeation.[22] Subsequently, the electrical discharge was ignited at 30 W, and species permeating across the plasma - polymer interface were identified using previously reported mass fragmentation patterns.[23] Additional experiments, where a small amount of O_2 was pulsed into the reactor during N_2 plasma treatment, were undertaken using a General Valve Iota one, series 9, pulse valve system.

Prior to each experiment, it was established that the polymer film required in-situ heating at 60 °C to remove any absorbed water present in the bulk of the substrate, Figure 2.2. Subsequent exposure to D_2O (Goss Scientific, 99.9 %), at a pressure of 6 x 10^{-1} mbar for 30 s followed by N_2 / O_2 plasma treatment, confirmed this requirement. X-ray photoelectron spectroscopy (XPS) was used to check if any chemical changes had taken place at the polymer surface during annealing. XPS spectra were obtained on a Kratos ES300 electron spectrometer equipped with a Mg Kα X-ray source (1253.6 eV) and a concentric hemispherical electron analyser operating in the fixed retarding ratio

mode (FRR, 22:1). Instrumentally determined sensitivity factors were taken for C(1s) : O(1s) as being equal to 1.00 : 0.55.

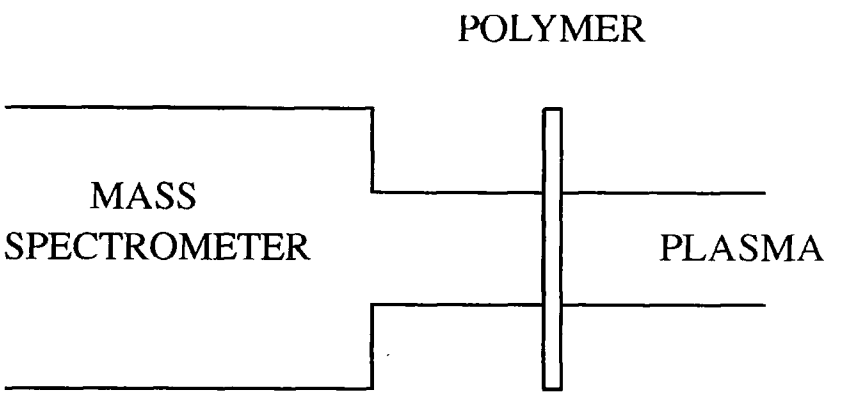

Figure 2.1: Apparatus used for mass spectrometric analysis of species permeating across the plasma - polymer interface.

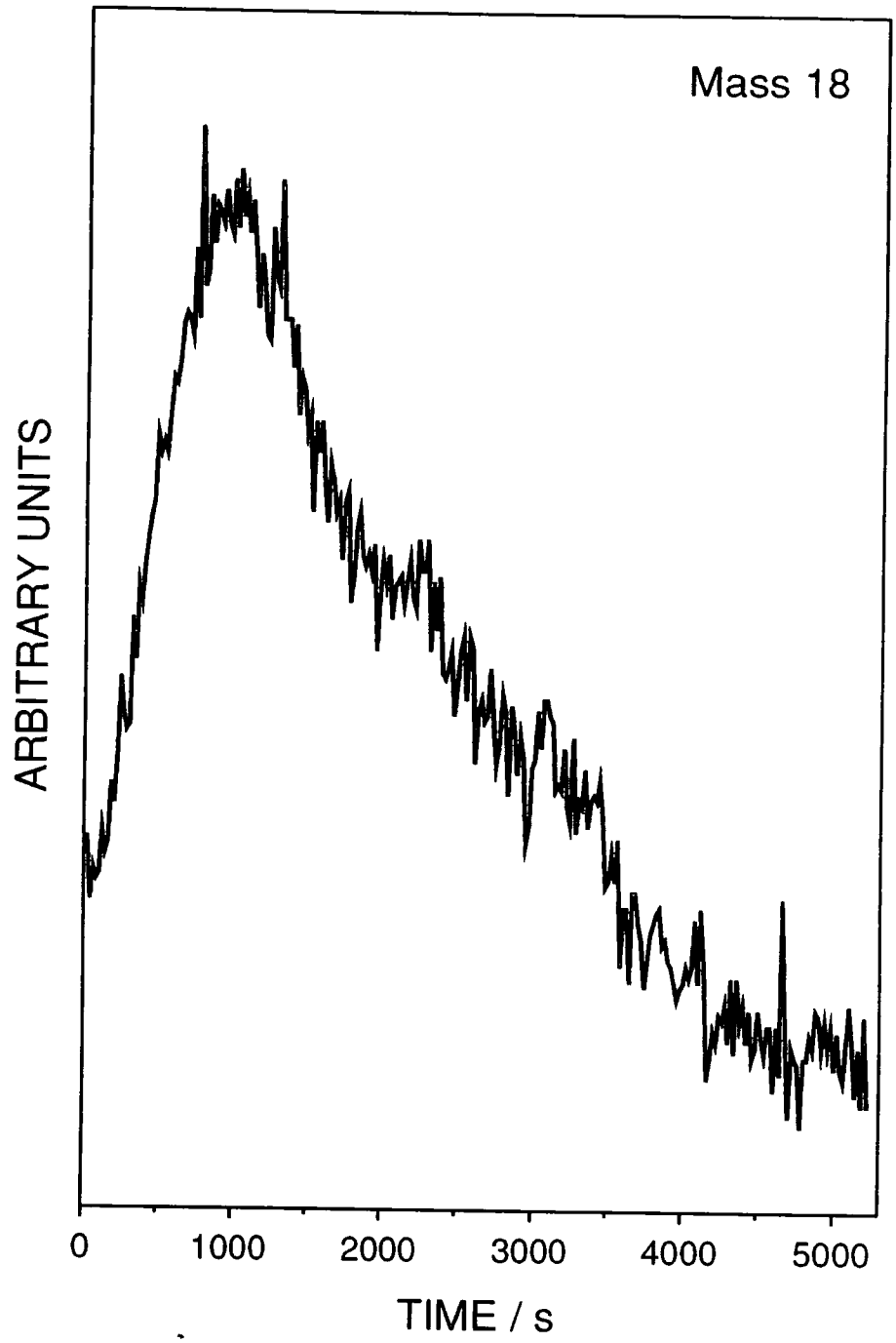

Figure 2.2: Water loss profile (m/z 18) during the heating of polyethylene film.

2.3 RESULTS

O:C XPS ratios obtained prior to and following in-situ heating of the polyethylene substrate at 60 °C are reported in Table 2.1. Annealing was found to lower the amount of oxygen detected at the surface of untreated polyethylene and a corresponding decrease was also noted following nitrogen plasma treatment. This demonstrates that any water trapped within a polymer film can contribute towards surface oxygenation during plasma modification even when the feed gas is free of oxygen.

Treatment	O : C ± 0.02
PE (as received)	0.11
Solvent cleaned	0.02
Heated	0.01
O_2 plasma	0.31
Heated O_2 plasma	0.30
N_2 plasma	0.19 (0.15)*
Heated N_2 plasma	0.10 (0.16)*

*Numbers in brackets represent N : C ratio

Table 2.1: O : C XPS ratios for unannealed and heated polyethylene substrates.

Typical mass profiles of species permeating through the polymer substrate during plasma treatment were acquired using a standard "off/on/off" sequence (20/60/120 s respectively), Figure 2.3. The maximum variations in mass signal intensities for N_2, O_2 and air feed gases are summarised in Figure 2.4. During each experiment the pressure measured on the mass spectrometer side of the polymer film increased on glow discharge ignition and dropped to below its initial starting value upon termination of the plasma.

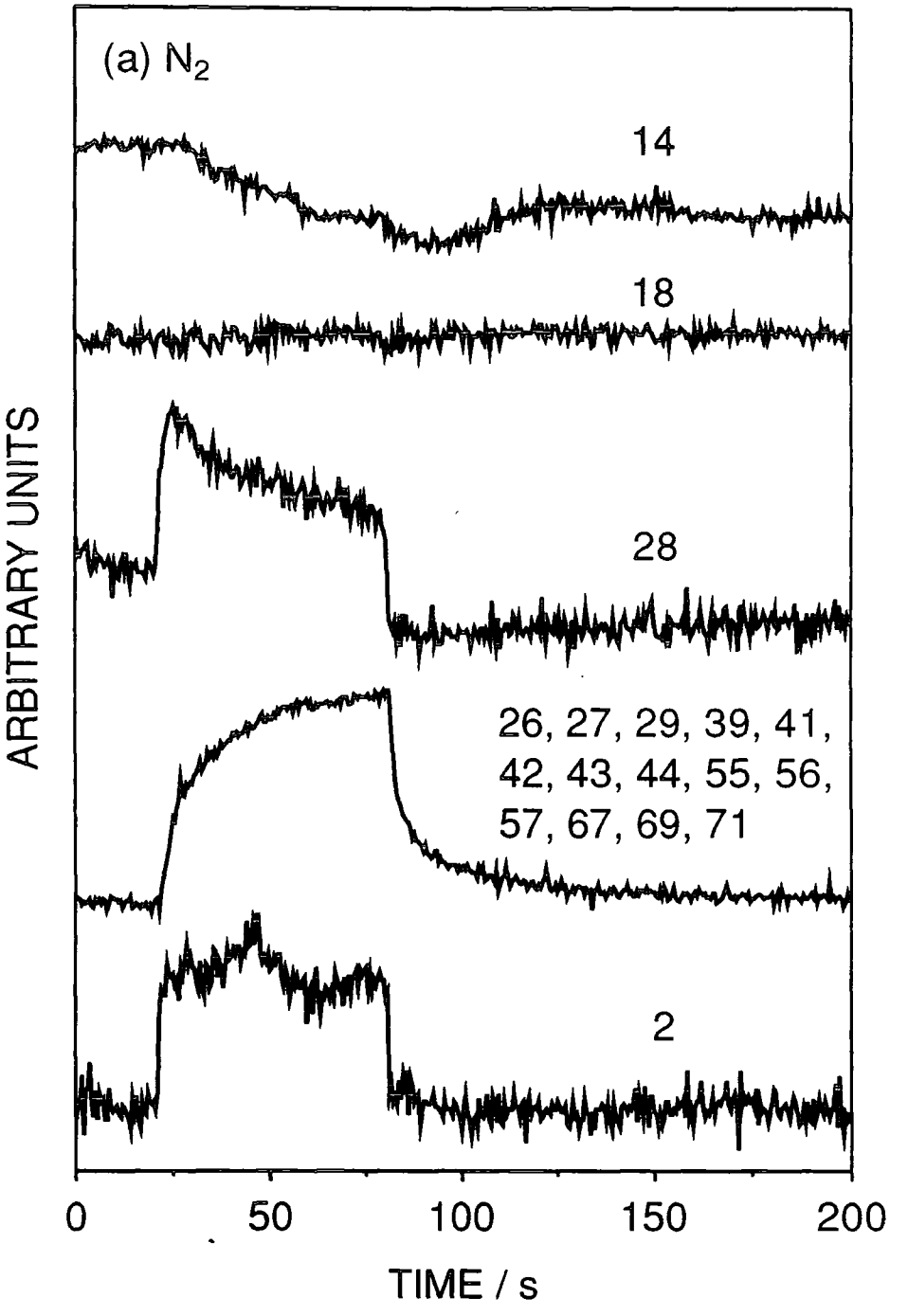

Figure 2.3(a): Mass profiles obtained using a 20/60/120 s, off/on/off sequence for the N_2 electrical discharge (all profiles typical for the relevant masses).

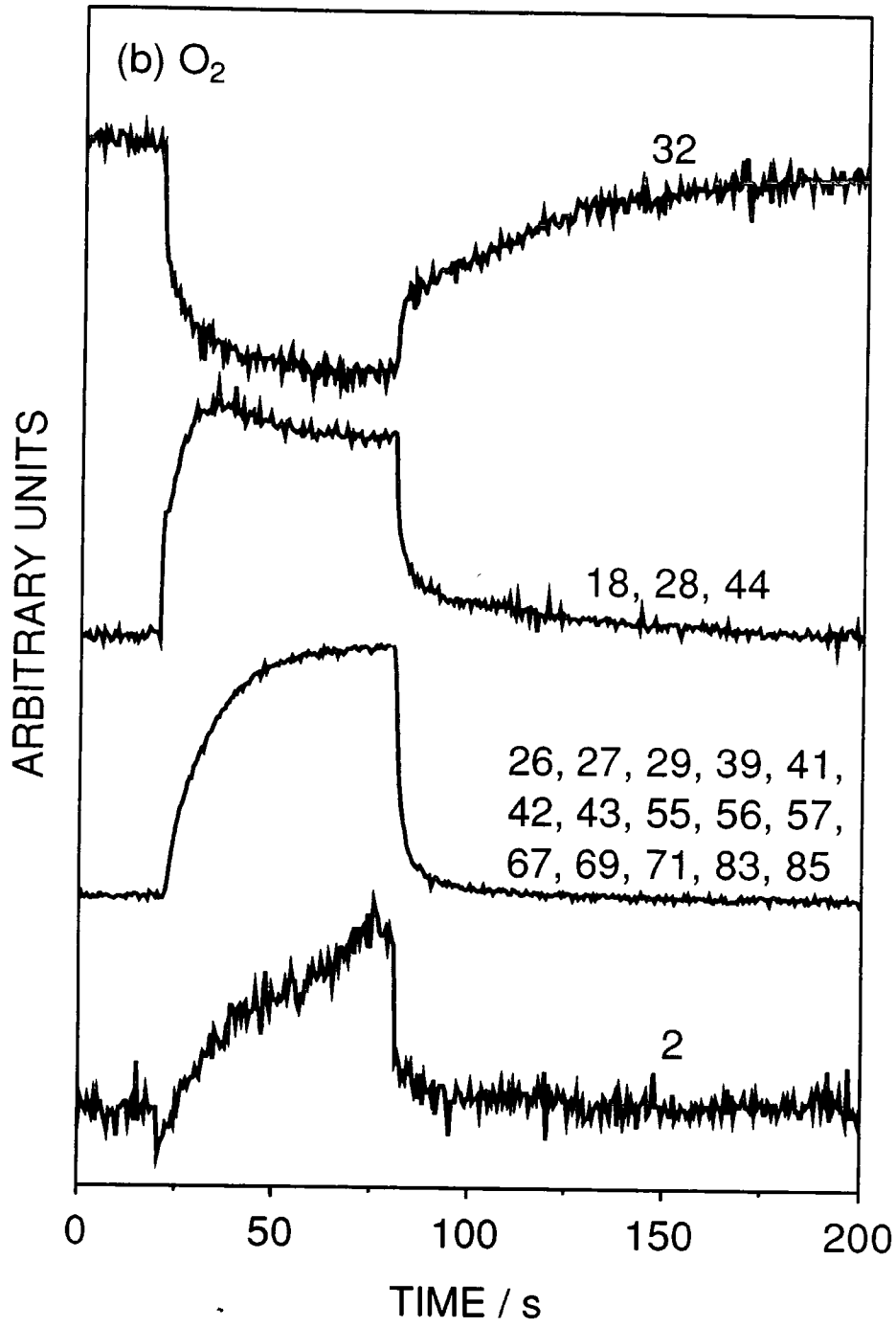

Figure 2.3(b): Mass profiles obtained using a 20/60/120 s, off/on/off sequence for the O_2 electrical discharge (all profiles typical for the relevant masses).

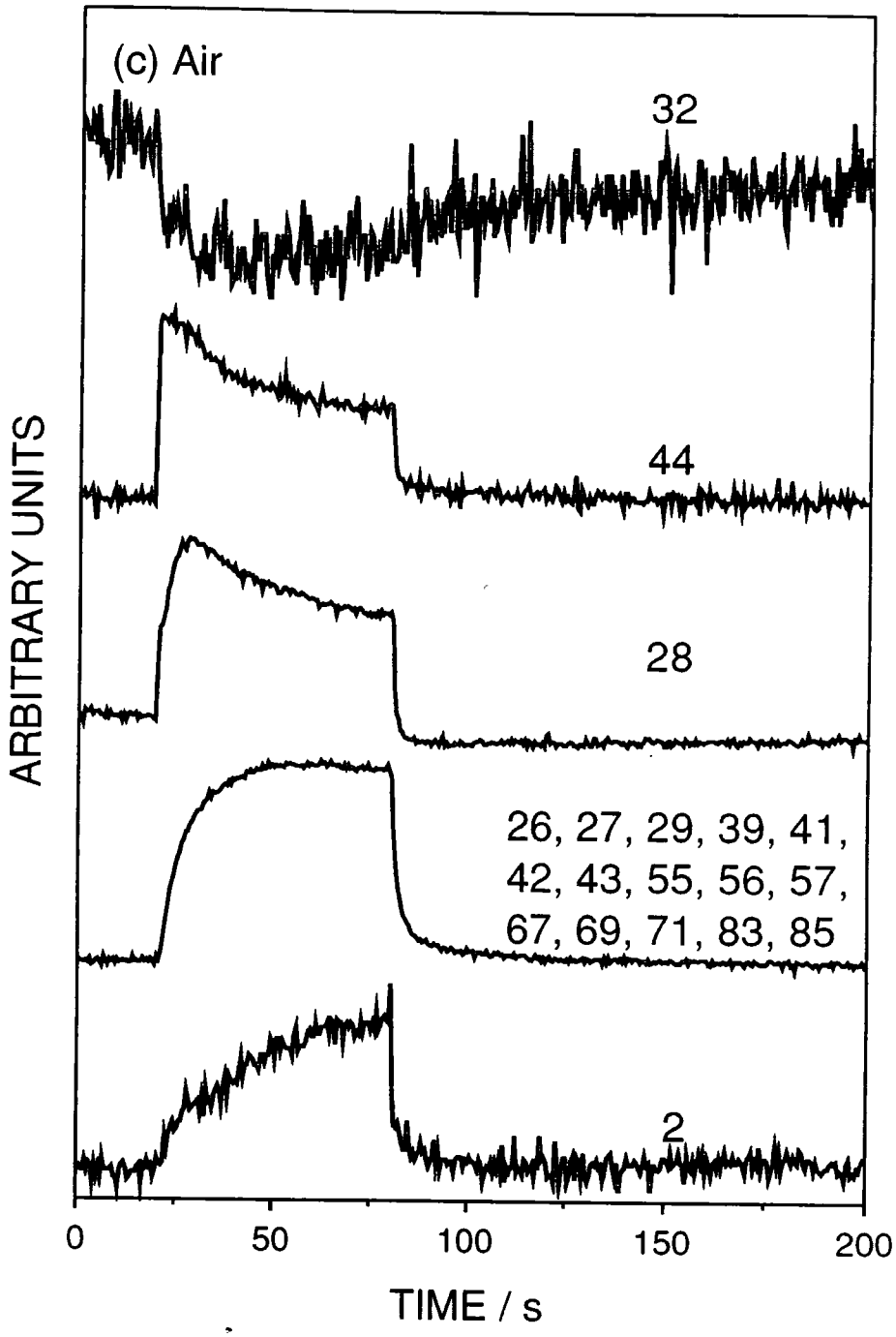

Figure 2.3(c): Mass profiles obtained using a 20/60/120 s, off/on/off sequence for the Air electrical discharge (all profiles typical for the relevant masses).

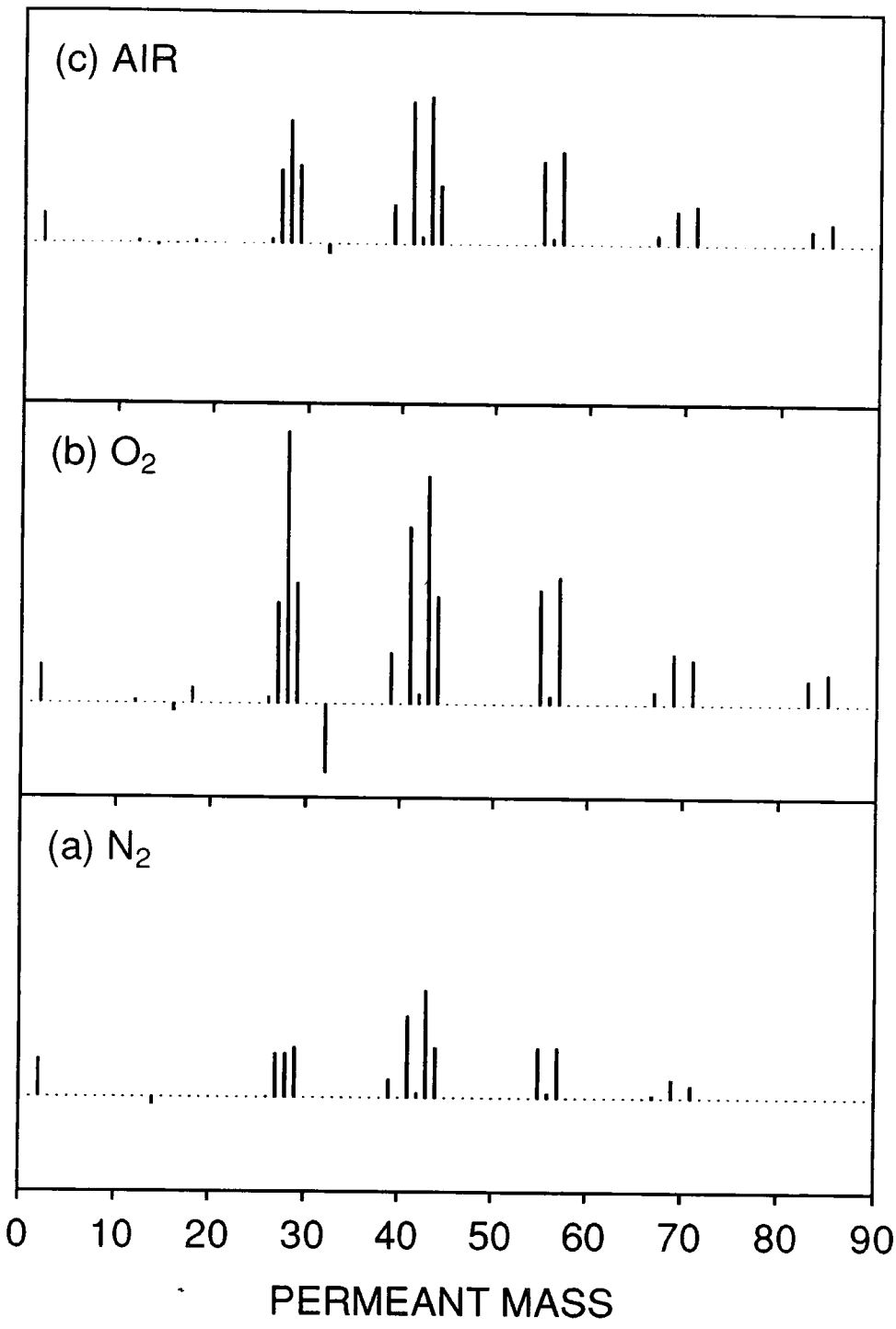

Figure 2.4: Maximum variation in mass signal intensities during plasma treatment: (a) N_2; (b) O_2; and (c) Air.

Mass spectrometric measurements taken during nitrogen electrical discharge treatment of annealed polyethylene displayed a rapid rise in *m/z* 28 which can be attributed to hydrocarbon fragment formation (predominantly propane and butane[23]), followed by a gradual fall in intensity due to a superimposed drop in nitrogen permeation through the polymer (as confirmed by the variation in the *m/z* 14 fragment of molecular nitrogen), Figure 2.3(a). In addition, other hydrocarbon fragments (*m/z* 26, 27, 29, 39, 41, 42, 43, 44, 55, 56, 57, 67, 69, 71) were detected; these were assigned to predominantly straight chain alkanes with more than 2 carbon atoms,[23] i.e. propane (*m/z* 29, 28, 27, 44, 43, 39, 41, 26), butane (*m/z* 43, 29, 27, 28, 41, 39, 42), pentane (*m/z* 43, 42, 41, 27, 29, 39), hexane (*m/z* 57, 43, 41, 29, 27, 55, 56), etc. All of these hydrocarbon species exhibited a sharp initial rise on lighting the plasma and continued to increase slowly until extinction, Figure 2.3. Mass fragments characteristic of methane, ethane and alkene formation were present at either very low or negligible concentrations (e.g. *m/z* 16, 30, 25, 40, 56, 42 for methane, ethane, ethene, propene, butene, and pentene respectively). A fairly steady amount of molecular hydrogen (*m/z* 2) loss was also measured throughout the duration of the electrical discharge exposure. Upon switching the nitrogen plasma off, all of the mass profiles displayed an instantaneous drop, followed by a further gradual decay towards the baseline; *m/z* 28 was the only exception due to it falling to below its original starting value.

During oxygen plasma treatment of annealed polyethylene, CO_2 (*m/z* 44), CO (*m/z* 28 after correction for CO_2) and H_2O (*m/z* 18) evolution were observed in addition to H_2 (*m/z* 2) and hydrocarbon fragments, Figure 2.4. The intensity of the oxidised species (CO_2, H_2O and CO) reached a maximum value approximately 10 s following contact with the glow discharge, and then began to slowly decrease with time, Figure 2.3(b). A corresponding drop and then plateauing in *m/z* 32 (molecular O_2) was noted. Molecular hydrogen and hydrocarbon production (same *m/z* fragments as previously seen for nitrogen plasma exposure plus 83 and 85) were also found to rise rapidly within these first 10 s, however these moieties then continued to increase in concentration at a slower rate. No oxygen containing hydrocarbon chain fragments were detected e.g. aldehydes, alcohols, ketones etc.[23] Plasma termination after 60 s treatment caused a rapid drop in all of the mass signal intensities, to eventually level off. Mass 32 was an exception, since it mirrored this behaviour and returned to just below its initial value.

Air plasma treatment of annealed polyethylene produced both the oxidised and hydrocarbon mass fragments, i.e. a combination of the N_2 and O_2 plasma treatments, Figures 2.3(c) and 2.4.

Exposure of the annealed polymer substrate to D_2O or H_2O prior to N_2 / O_2 plasma treatment confirmed that absorbed water interferes with the surface chemistry, Table 2.2. No visible difference was evident in the hydrocarbon mass profiles. Whereas, the presence of water in the polymer resulted in a marked increase in the rate of oxidation. In the case of the D_2O experiments isotopically exchanged products were also detected (e.g. HD, D_2 and HDO).

Gas pulsing experiments were undertaken in order to gain a deeper insight into the mechanistic details governing plasma modification. Firstly, a series of control experiments were carried out where O_2 was pulsed into the 0.6 mbar N_2 gas feed stream passing through the plasma reactor in the absence of an electrical discharge. These showed that a 1000 μs pulse of oxygen resulted in a 0.01 mbar rise in total pressure (i.e. less than 2 % change) and an accompanying amount of oxygen (*m/z* 32) permeating through the polymer could be detected. No change in the level of N_2 permeation was observed, Figure 2.5. This gas pulsing sequence was then repeated during nitrogen plasma treatment (i.e. 20 s off / 30 s on / O_2 pulse / 30 s on / 120 s off), Figure 2.6. The initial oxygen permeation (*m/z* 32) dropped to a slightly lower intensity than previously seen during the control experiment and subsequently decayed more rapidly; this behaviour coincided with the formation of oxidised species (CO_2, CO and H_2O) in addition to an enhancement in the rate of hydrocarbon and hydrogen evolution, Figure 2.6. Clearly, it can be seen that the trends previously noted for oxygen plasma treatment (Figure 2.3(b)) have been superimposed onto the nitrogen plasma treatment mass profiles (Figure 2.3(a)). The oxidised products (CO_2, CO and H_2O) all diminished following the decay of the O_2 pulse, whilst the hydrocarbon species continued to be formed at a higher rate throughout the rest of plasma treatment. A control experiment where a 1000 μs pulse of N_2 was employed instead of the O_2 pulse gave no observable difference in the N_2 plasma treatment, and therefore the possibility of a slight change in pressure being responsible for the observed chemistry during O_2 pulsing can be ruled out. Finally, it was found that if oxygen was pulsed into the reactor immediately after termination of the N_2 plasma, i.e. at t = 80 s, no consumption of oxygen was detectable, Figure 2.5(d).

PLASMA	PRETREATMENT	MASS SIGNAL INTENSITY (± 5, arbitrary units)						
		2 (H_2)	3 (HD)	4 (D_2)	18 (H_2O)	19 (HDO)	20 (D_2O)	44 (CO_2)
O_2	Annealing	60	0	0	100	0	0	170
	Annealing / H_2O	70	0	0	135	0	0	235
	Annealing / D_2O	60	10	0	130	30	0	225
N_2	Annealing	50	0	0	0	0	0	80
	Annealing / H_2O	60	0	0	35	0	0	120
	Annealing / D_2O	50	35	5	30	5	2	115

Table 2.2: Maximum variations in non-hydrocarbon mass signal intensities during N_2 / O_2 plasma treatment of annealed polyethylene substrates.

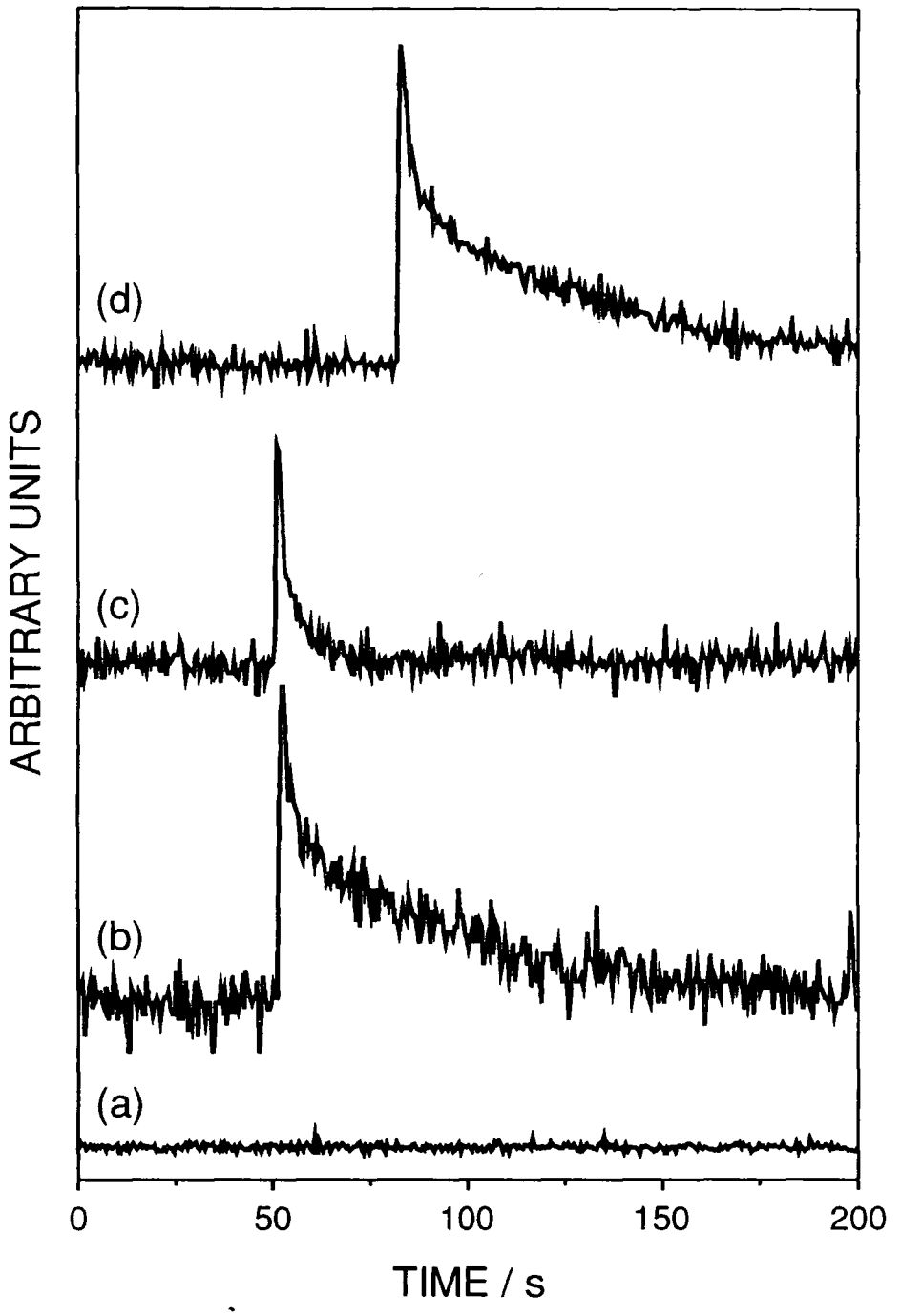

Figure 2.5: (a) Change in *m/z* 28 signal (N_2) upon pulsing a 1000 μs pulse of molecular O_2 at t = 50 s; (b) *m/z* 32 (O_2) signal corresponding to (a); (c) *m/z* 32 (O_2) signal upon pulsing a 1000 μs pulse of molecular oxygen at t = 50 s into a 0.6 mbar N_2 plasma; and (d) *m/z* 32 (O_2) signal upon pulsing a 1000 μs pulse of molecular oxygen upon extinction of the 0.6 mbar N_2 plasma, i.e. at t = 80 s.

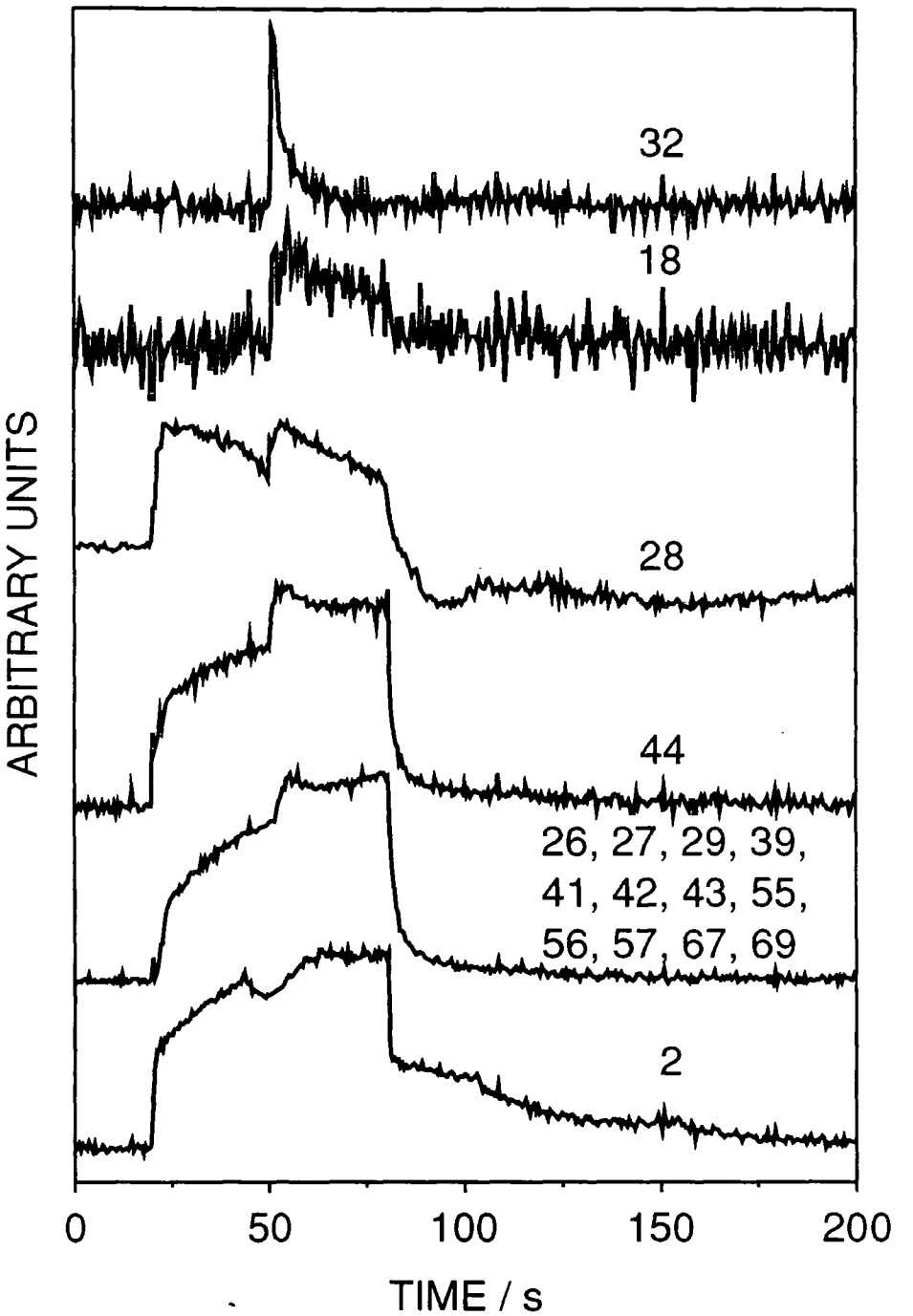

Figure 2.6: Mass profiles obtained during the following sequence: 0.6 mbar of N_2 passing through reactor from t = 0 s, ignition of plasma at t = 20 s, injection of 1000 μs pulse of O_2 at t = 50 s, termination of plasma at t = 80 s (all profiles typical for the relevant masses).

2.4 DISCUSSION

Non-isothermal electrical discharges contain a wide variety of species: ground state atoms, molecules, metastables, ions of either polarity, electrons, and electromagnetic radiation (infrared - vacuum ultraviolet). Two types of interaction can occur at the plasma - polymer interface:[24] direct reactions at the surface due to incident neutral species, ions, photons, and electrons; and indirect processes in the subsurface region as a result of VUV radiation penetrating down to 1-10 μm. As a consequence, free radical centres are created in the surface region via atom abstraction,[25,26] ion bombardment,[26] and photo-excitation.[27] Subsequently these radical species can either react with the adjacent plasma medium or undergo crosslinking. The former is predominant in the case of oxygen plasma treatment on the basis of thermodynamic factors;[28] whereas the latter tends to be more likely for nitrogen plasma exposure as a consequence of less favourable energetics for chemical reaction.[29] VUV photodegradation processes will also be prominent in the near-surface region of polyethylene leading to chain scission accompanied by the formation of atomic hydrogen, Scheme 2.1.[30] Since hydrogen free radicals are likely to be shortlived within the polymer subsurface, formation of molecular hydrogen and crosslinking are to be expected,[30] Scheme 2.1.

In the case of nitrogen plasma exposure, hydrocarbon formation was found to be the predominant reaction pathway (despite the absolute amount evolved being lower compared to oxygen plasma treatment). The continuous rise in hydrocarbon intensity is an indication of how polymer backbone cleavage results in a gradual increase in the number of oligomeric moieties at the surface in conjunction with a decrease in average molecular weight.[31] The *m/z* 28 profile (which is a combination of nitrogen and hydrocarbon species) increases with an initial slope which is similar to that seen for the other hydrocarbon species; upon plasma extinction, it drops to below its starting value, thereby exhibiting a lowering (by 25 $\pm$ 2%) of nitrogen permeability through the polymer film as a result of plasma induced crosslinking (as confirmed by the *m/z* 14 signal). Alkene products were not observed, this is probably as a consequence of the abundant supply of atomic hydrogen promoting termination reactions in preference to double bond formation at free radical sites along the polymer backbone, Scheme 2.1. The sharp drop in hydrocarbon evolution upon plasma extinction confirms the importance of VUV photochemistry within the subsurface region.[32]

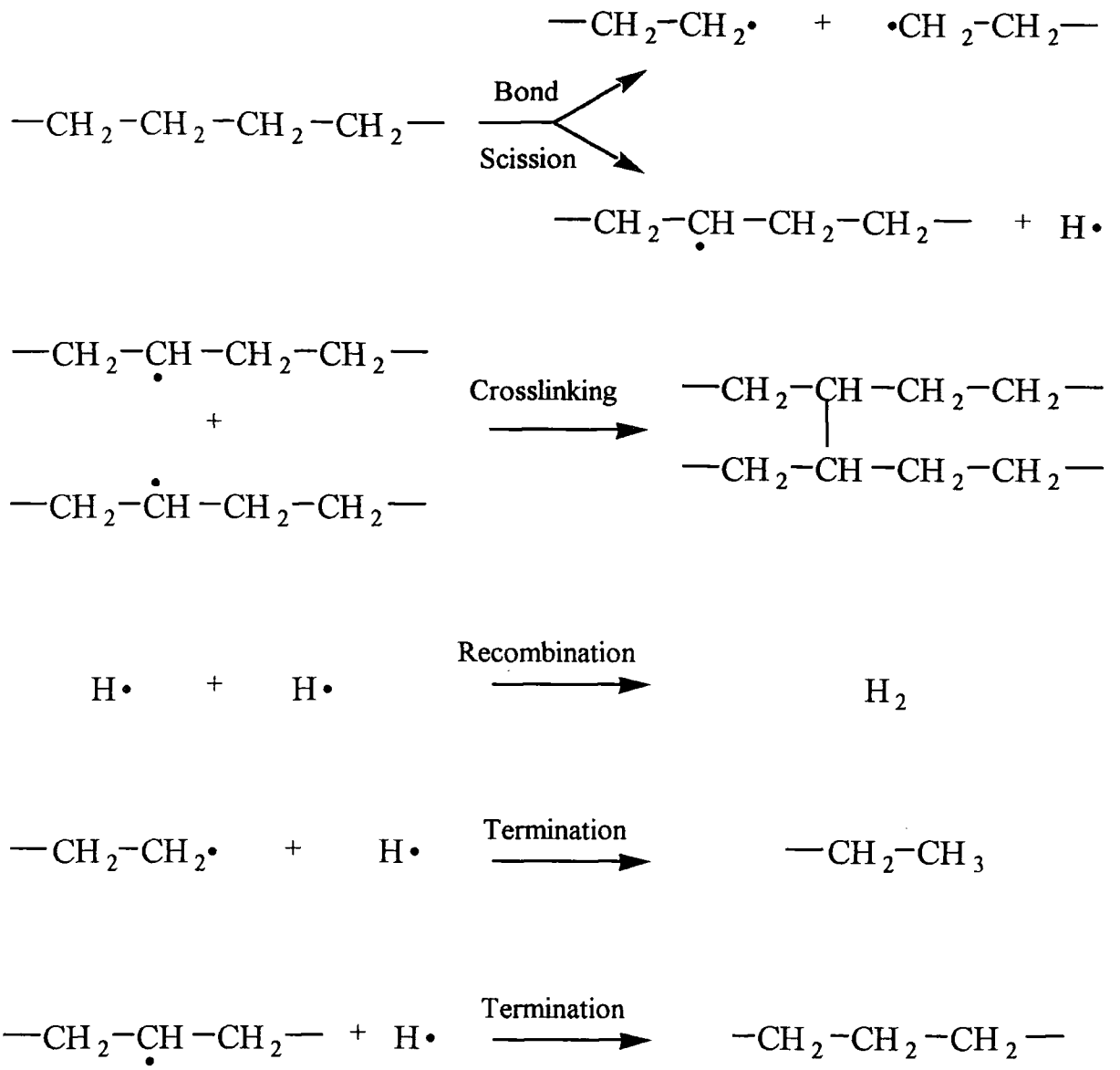

Scheme 2.1: VUV photodegradation reactions along the polyethylene backbone.

A rapid rise in oxidised permeant species (*m/z* 18 (H_2O), 28 (CO) and 44 (CO_2)) was evident during oxygen plasma treatment of polyethylene, thus indicating that oxidation processes coincide with plasma ignition. The subsequent decrease in concentration of these moieties during plasma modification implies that the rate of oxidation is greatest for the clean polymer surface. In contrast, hydrocarbon species gradually rise in intensity throughout plasma exposure. A corresponding consumption of molecular oxygen (*m/z* 32) occurs during the whole 60 s of plasma treatment. It can be deduced from these observations that oxidation is localised at the plasma - polymer interface, and therefore not initially rate limited (i.e. total combustion to H_2O, CO and

CO_2), whilst hydrocarbon formation also occurs in the subsurface region (akin to nitrogen plasma treatment) as a consequence of VUV assisted photochemical chain scission, Scheme 2.1. The additional reactive oxygen species (ions, atoms and metastables) are responsible for oxidation reactions at the polymer surface,[30] which give rise to the evolution of oxidised molecules H_2O, CO and CO_2,[33] Scheme 2.2. The lack of any oxygen containing hydrocarbon chain fragments (in the 0-200 amu range) could either be due to their much longer chain lengths (slow permeation), lower solubilities (compatibility) in the bulk polyethylene host medium or their rapid decomposition.

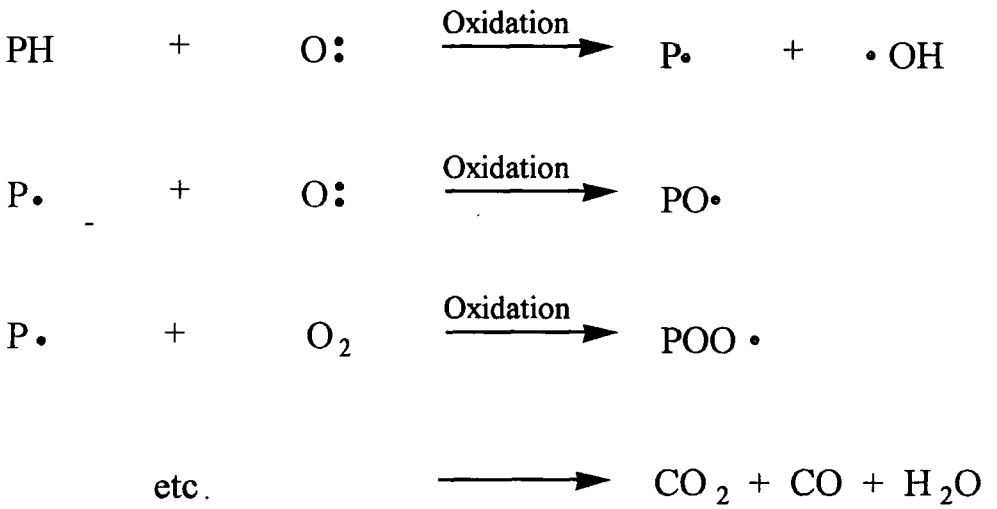

Scheme 2.2: Typical oxidative reaction pathways occurring during oxygen plasma treatment of polyethylene.

A synergistic reaction of atomic oxygen and VUV irradiation with the polymer surface causes polymer backbone cleavage and the formation of low molecular weight oxidised species,[34] Scheme 2.3. This type of additional reaction pathway helps to explain why there is greater chain scission (i.e. increase in the amount of hydrocarbon mass fragments and also the formation of higher *m/z* 83 and 85) during plasma oxidation compared to corresponding experiments with nitrogen,[12,25] and has been verified by the dramatic rise and sustained rate of hydrocarbon fragment evolution upon pulsing a small amount of O_2 during N_2 plasma treatment, Figure 2.6.

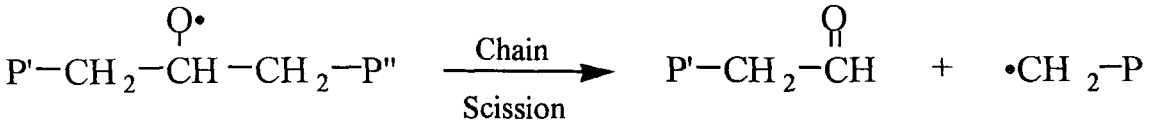

Scheme 2.3: Additional weakening and cleavage of the polymer backbone adjacent to oxygenated centres.[25]

Oxygen glow discharge extinction produces a rapid decline in the evolution of oxidised species in conjunction with a sharp rise in the oxygen profile, followed by a gradual plateauing in the molecular oxygen signal (not observed for nitrogen). The latter behaviour could be potentially attributed to oxidation continuing after the plasma has been turned off (i.e. trapped free radical centres at the polymer surface undergoing reaction with vicinal ground state molecular oxygen), however, this can be ruled out since no oxygen consumption was detected on pulsing in oxygen upon extinction of the nitrogen plasma, Figure 2.5(d). A more likely explanation is the gradual deterioration of O_2 gas barrier due to relaxation of polymer crosslinking via chain scission as depicted in Scheme 2.3. In comparison, the much more rapid disappearance of hydrocarbon fragments correlates to the instantaneous termination of VUV irradiation, thereby halting any photo-chemical cleavage of the polymer backbone. The overall net drop in oxygen permeation by $10 \pm 1\%$ following plasma treatment implies that the polymer surface has been modified to yield a less permeable film. Again this can be attributed to crosslinking hindering the segmental motion of polymer chains to cause an attenuation in gas permeability.[35] The observation that nitrogen plasma treatment causes mainly crosslinking (Scheme 2.1) whereas oxygen plasma exposure gives rise to predominantly chain scission and oxidation (Schemes 2.2 and 2.3) helps to account for the greater drop in gas permeability in the case of N_2 plasma treatment. Such an attenuation in gas permeability must be a contributing factor for the adoption of on-line nitrogen plasma pretreatment prior to metallisation of polymer film for high gas barrier applications.

Air plasma treatment of annealed polyethylene confirms the observations obtained for both the N_2 and O_2 glow discharge exposures. The mass profiles as expected are a combination of both treatments, Figure 2.3(c), with the intensities being less than for O_2 but greater than for N_2 case, Figure 2.4.

Finally, it is important to note that any moisture contained in the polymer substrate can influence the interfacial plasma - polymer chemistry. This factor appears to have

been overlooked in the past. It has been shown that when water is present in the polymer bulk, oxidised mass fragments (CO_2 and H_2O) are produced during N_2 plasma treatment in a similar but milder manner to that seen for oxygen glow discharge exposure. These oxidised species are generated as a result of absorbed water within the polymer subsurface permeating towards the plasma - polymer interface, where it undergoes excitation and reaction, leading to oxygenation of the polymer surface. Heating of the substrate prior to plasma treatment removes any trapped water, Figure 2.2, and thereby avoids surface oxygenation; this is verified by the accompanying drop in O:C XPS ratios, Table 2.1. Exposure of the annealed polymer film to D_2O or H_2O prior to plasma treatment confirms that water absorbed within the polymer substrate can strongly perturb the chemistry occurring at the plasma - polymer interface, Table 2.2. A comparison of the *m/z* 44 profiles shows that any absorbed water causes the typical hydrocarbon profile characteristic of nitrogen plasma treatment to acquire a superimposed $C\bar{O}_2$ component normally associated with oxidation, Figure 2.7.

2.5 CONCLUSIONS

This chapter has shown that a new mass spectrometric technique has been developed which enables the detection of primary reaction products at the plasma - polymer interface. Real time mass spectrometric sampling at the nitrogen plasma - polyethylene interface confirms the importance of VUV initiated reactions (i.e. chain scission leading to hydrocarbon fragments). VUV induced crosslinking in the polymer subsurface restricts polymer chain mobility, which in turn gives rise to an overall improvement in gas barrier performance of the polyethylene substrate. A greater extent of polymer backbone cleavage occurs in the case of oxygen plasma treatment due to oxygenated centres causing a weakening of adjacent carbon-carbon bonds. Finally, it should be noted that any absorbed water within the polymer bulk can lead to an enhancement in oxidation chemistry at the plasma - polymer interface.

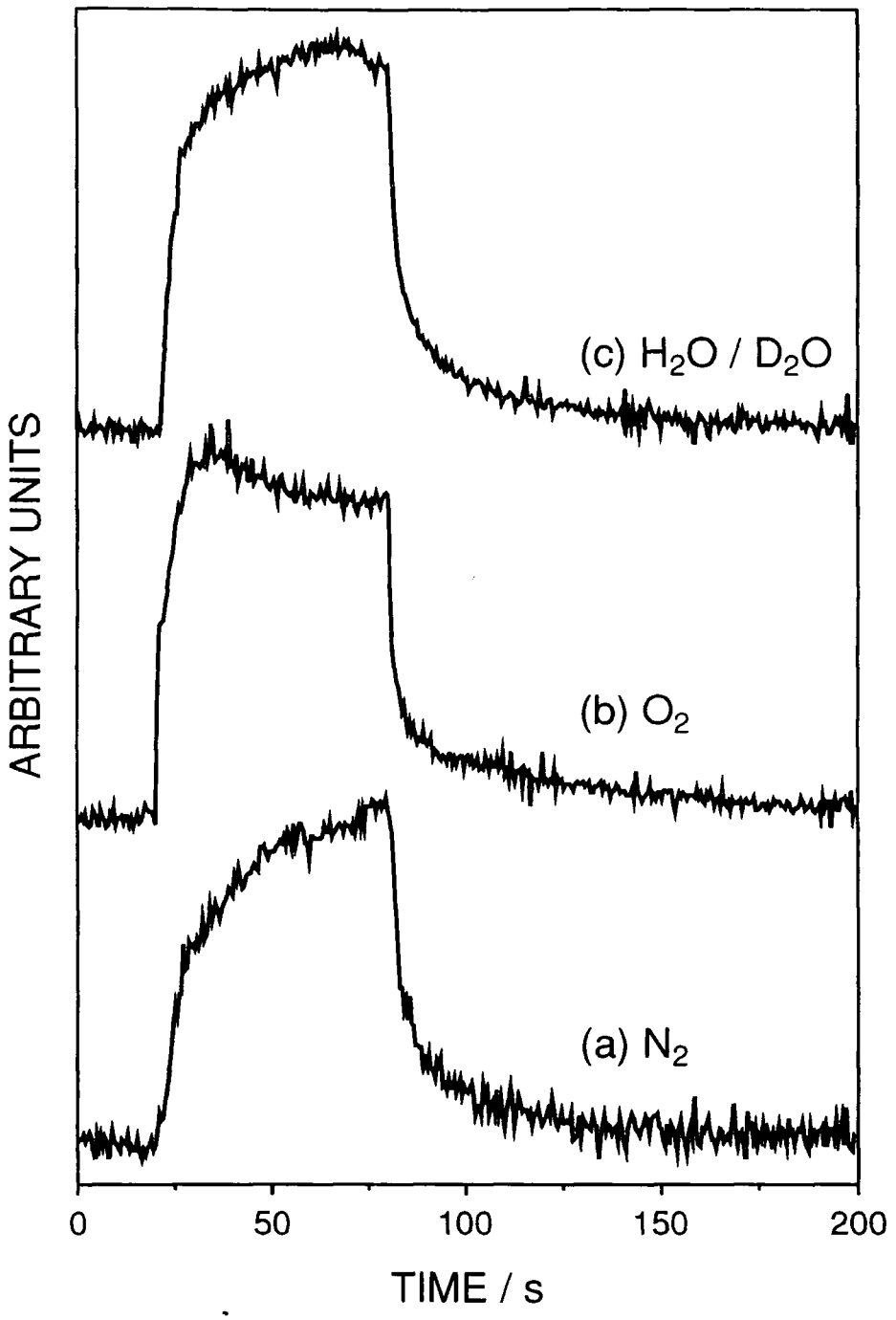

Figure 2.7: Mass 44 profile for: (a) N_2 plasma treatment of annealed polyethylene; (b) O_2 plasma treatment of annealed polyethylene; and (c) N_2 plasma treatment of annealed polyethylene which has been exposed to D_2O or H_2O.

2.6 REFERENCES

[1] A.T. Bell, *Techniques and Applications of Plasma Chemistry*, edited by J.R. Hollahan and A.T. Bell (John Wiley and Sons, New York, 1974), Chapter 10.

[2] D.L. Smith, H.P. Gillis and T.M. Mayer, *Plasma Diagnostics*, edited by O. Auciello and D.L. Flamm (Academic Press, London, 1989), Vol. 2, Chapter 2.

[3] R.K. Wells, J.P.S. Badyal, I.W. Drummond, K S Robinson and F J Street, J. Adhesion Sci. Technol. 7, 1129 (1993).

[4] M. Morra, E. Occhiello, L. Gila and F. Garbassi, J. Adhesion **33**, 77 (1990).

[5] L. Lianos, D. Parrat, T.Q. Hoc and T.M. Duc, J. Vac. Sci. Technol. **A12**, 2491 (1994).

[6] M. Morra, E. Occhiello and F. Garbassi, Langmuir **5**, 872 (1989).

[7] M. Morra, E. Occhiello and F. Garbassi, *Metallized Plastics 2*, edited by K.L. Mittal (Plenum Press, New York, 1991), 363.

[8] D.T. Clark and A. Dilks, J. Polym. Sci., Polym. Chem. Ed. **17**, 957 (1979).

[9] F. Clouet, M.K. Shi, R. Prat, Y. Holl, P. Marie, D. Leonard, Y. Depuydt, P. Bertrand, J.L. Dewez and A. Doren, J. Adhesion Sci. Technol. **8**, 329 (1994).

[10] A.F. Whitaker and B.Z. Jang, J. Appl. Polym. Sci. **48**, 1341 (1993).

[11] O.D. Greenwood, J. Hopkins and J.P.S. Badyal, Macromolecules **30**, 1091 (1997).

[12] J. Hopkins, R.D. Boyd and J.P.S. Badyal, J. Phys. Chem. **100**, 6755 (1996)

[13] J. Hopkins and J.P.S. Badyal, J. Polym. Sci. Polym. Chem. **34**, 1385 (1996).

[14] R.D. Boyd and J.P.S. Badyal, Macromolecules **34** 1385 (1997).

[15] R. d'Agostino, A. Cramarossa and S. DeBenedictis, Plasma Chem. and Process. **2**, 213 (1982).

[16] R. d'Agostino, A. Cramarossa and S. DeBenedictis, Plasma Chem. and Process. **4**, 21 (1984).

[17] P.C. Stangeby, *Plasma Diagnostics*, edited by O. Auciello and D.L. Flamm (Academic Press, London, 1989), Vol. 2, Chapter 5.

[18] J.W. Coburn, *Plasma Diagnostics*, edited by O. Auciello and D.L. Flamm (Academic Press, London, 1989), Vol. 2, Chapter 1.

[19] J.W. Coburn and E. Kay, IBM J. Res. Develop. **23**, 33 (1979).

[20] P.J. Hargis Jr. and N. J. Kushner, Appl. Phys. Lett. **40**, 779 (1982).

[21] A.G. Shard, H.S. Munro and J.P.S. Badyal, Polym. Commun. **32**, 152 (1991).

[22] C.P. Barker, K.H. Kochem, K.M. Revell, R.S.A. Kelly and J.P.S. Badyal, Thin Solid Films **259**, 46 (1995).

[23] A. Cornu and R. Massot, *Compilations of Mass Spectral Data* (Heyden and Sons, London, 1975), 2nd Edition, Vol 1, Part a.

[24] D.T. Clark and A. Dilks J. Polym. Sci. Polym. Chem. **15**, 2321 (1977).

[25] S.R. Cain, F.D. Egitto and F. Emmi, J. Vac. Sci. Technol. **A5**, 1578 (1987).

[26] M. Hudis, *Techniques and Applications of Plasma Chemistry*, edited by J.R. Hollahan and A.T. Bell (John Wiley and Sons, New York, 1974), Chapter 3.

[27] L.J. Gerenser, J. Adhesion Sci. **1**, 303 (1987).

[28] G.N. Taylor and T.M. Wolf, Polym. Eng. Sci. **20**, 1087 (1980).

[29] *CRC Handbook of Chemistry and Physics*, edited by R.C. Weast and M.J. Astle, (CRC Press, Inc., Florida,1982).

[30] B. Ranby and J.F. Rabek, *Photodegradation, Photooxidation and Photostabilization of Polymers* (John Wiley and Sons, London, 1975), Chapter 4.

[31] R.D. Boyd, D. Briggs and J.P.S. Badyal, Macromolecules in press.

[32] A. Hollander and J. Behnisch, Am. Chem. Soc. Div. Polym. Chem. **38**, 1051, (1997).

[33] C. Mayoux, A. Antoniou, B. Ai and R. Lacoste, Eur. Polym. J. **9**, 1069 (1973).

[34] J. Hopkins, S.H. Wheale and J.P.S. Badyal, J. Phys. Chem. **100**, 14062 (1996).

[35] *Membrane Science and Technology*, edited by Y. Osado and T. Nakagawa, (Marcel Dekker, New York, 1992).

CHAPTER 3

MASS SPECTROMETRY AT THE HYDROGEN GLOW DISCHARGE - POLYMER INTERFACE

3.1 INTRODUCTION

Non-isothermal hydrogen glow discharges are a source of atomic hydrogen[1] and are thus used to clean surfaces[2] e.g. semiconductors.[3,4] The flux of incident hydrogen atoms onto the vessel walls / substrates promotes the formation of volatile compounds (CO, H_2O, CH_4, etc.). Hydrogen plasmas are also used to anisotropically etch organic materials,[5] etch diamond films,[6] and to fabricate thin film transistors.[7] Unlike the O_2 plasma the H_2 glow discharge has the advantage of non-oxidising conditions.[8]

Previous work with the hydrogen glow discharge treatment of saturated hydrocarbon polymers has shown that the substrates undergo an increase in molecular weight due to crosslinking,[9,10] with little change in contact angle.[11] Unsaturated polymers also become hydrogenated[12,13] and oxygen and sulphur containing functionalities are reduced and removed as H_2O and H_2S respectively.[12,13] Hydrogen glow discharge treatment has also been used to defluorinate the surface of PTFE[14] to improve its adhesion to other surfaces,[15] and to lower the dielectric losses of plasma-polymerised films.[16]

Hydrogen is often added to fluorinating gas plasmas e.g. CF_4, to decrease the etching and increase the polymerisation behaviour of the electrical discharge.[16,17] The hydrogen atoms react with the F atoms to produce unreactive HF, thus increasing the concentration of CF_x by suppressing the recombination reaction of F and CF_x. Addition of the hydrogen also allows control of the film F:C ratio.[17]

In this chapter the effect of hydrogen glow discharges on polyethylene substrates is studied using the newly developed mass spectrometry technique described in chapter 2.

3.2 EXPERIMENTAL SECTION

Circular pieces of low-density polyethylene film (Goodfellows; 48 mm diameter, thickness 15 μm, density 0.92 g cm^{-3}) were ultrasonically cleaned in a 50 / 50 solvent mixture of isopropyl alcohol / cyclohexane for 30 s and allowed to dry in air. Hydrogen (BOC 99.9%), nitrogen (BOC 99.9 %) and deuterium (BDH, 99.9 %) were used as feed gases for the respective plasma exposures.

Low pressure electrical discharge treatments were carried out as previously described in section 2.2. Prior to each experiment, it was established that the polymer film required in-situ heating at 60 °C to remove absorbed water present in the bulk of the substrate. Additional experiments, where a small amount of gas was pulsed into the reactor during plasma treatment, were undertaken using a General Valve Iota one, series 9, pulse valve system.

3.3 RESULTS

Typical mass profiles of species permeating through the polymer substrate during plasma treatment were acquired using a standard "off/on/off" sequence (20/60/120 s respectively), Figure 3.1. The maximum variations in mass signal intensities for all of the feed gases are summarised in Figure 3.2. During each experiment the pressure measured on the mass spectrometer side of the polymer film increased on glow discharge ignition and dropped to below its initial starting value upon termination of the plasma.

Mass spectrometric measurements taken during the hydrogen electrical discharge treatment of annealed polyethylene displayed a rapid rise in hydrocarbon fragments (*m/z* 27, 28, 29, 39, 41, 42, 43, 44, 55, 57, 67, 69, 71), Figure 3.2. These were assigned to predominantly straight chain alkanes with more than 2 carbon atoms,[18] i.e. propane (*m/z* 29, 28, 27, 44, 43, 39, 41, 26), butane (*m/z* 43, 29, 27, 28, 41, 39, 42), pentane (*m/z* 43, 42, 41, 27, 29, 39), hexane (*m/z* 57, 43, 41, 29, 27, 55, 56), etc. All of these hydrocarbon species exhibited a sharp initial rise on plasma ignition and continued to increase slowly until extinction, Figure 3.1(a). Hydrogen plasma treatment produced similar mass fragments and profiles to nitrogen plasma exposure, (chapter 2) however the intensities were much lower and the range of fragments smaller, Figure 3.1(b) and 3.2(b). A fairly steady amount of molecular hydrogen (*m/z* 2) was also produced throughout the duration of the electrical discharge exposure. Upon switching the plasma off, all of the mass profiles displayed an instantaneous drop, followed by a further gradual decay towards the baseline.

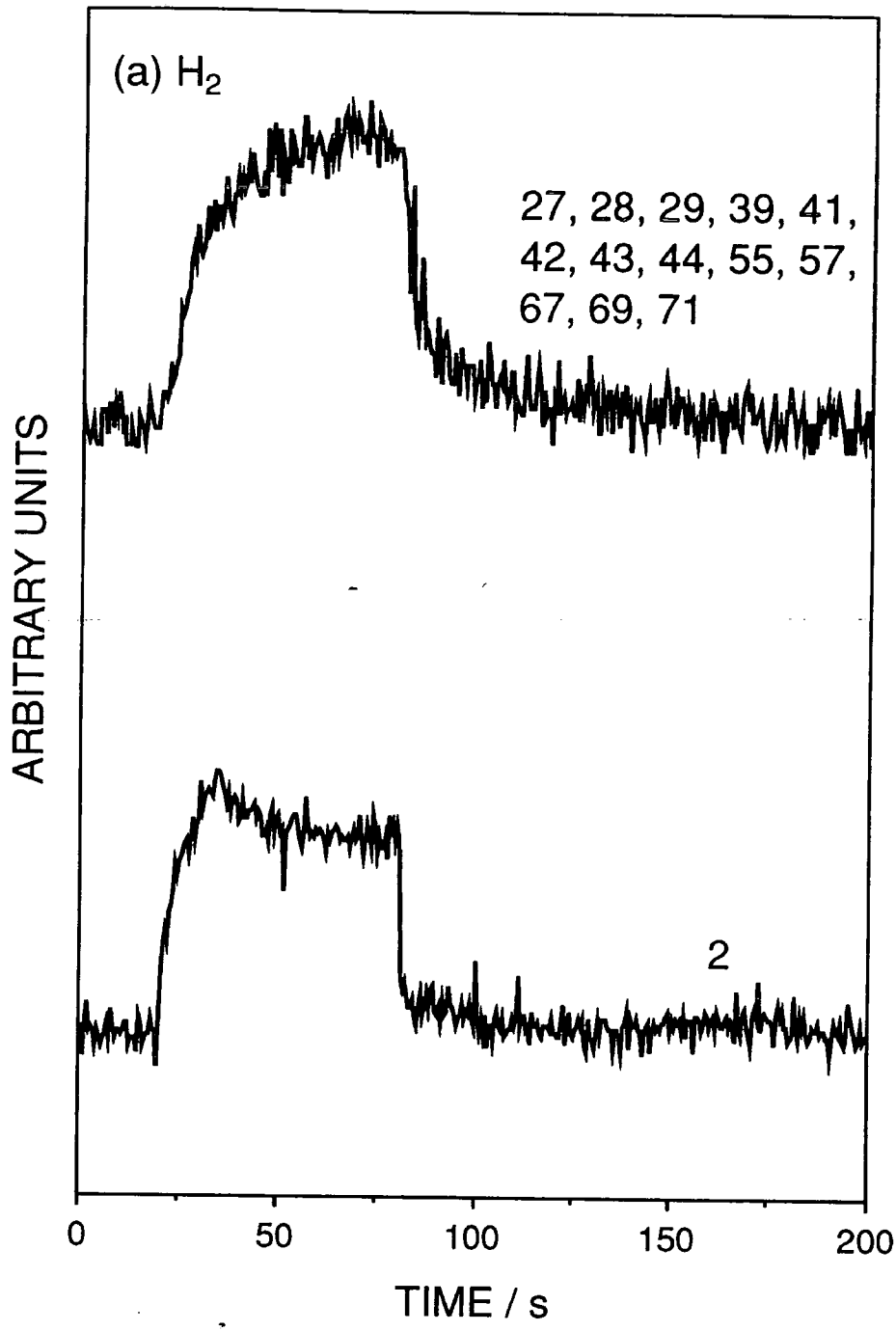

Figure 3.1(a): Mass profile obtained using a 20/60/120 s, off/on/off sequence for the H_2 electrical discharge (all profiles typical for the relevant masses).

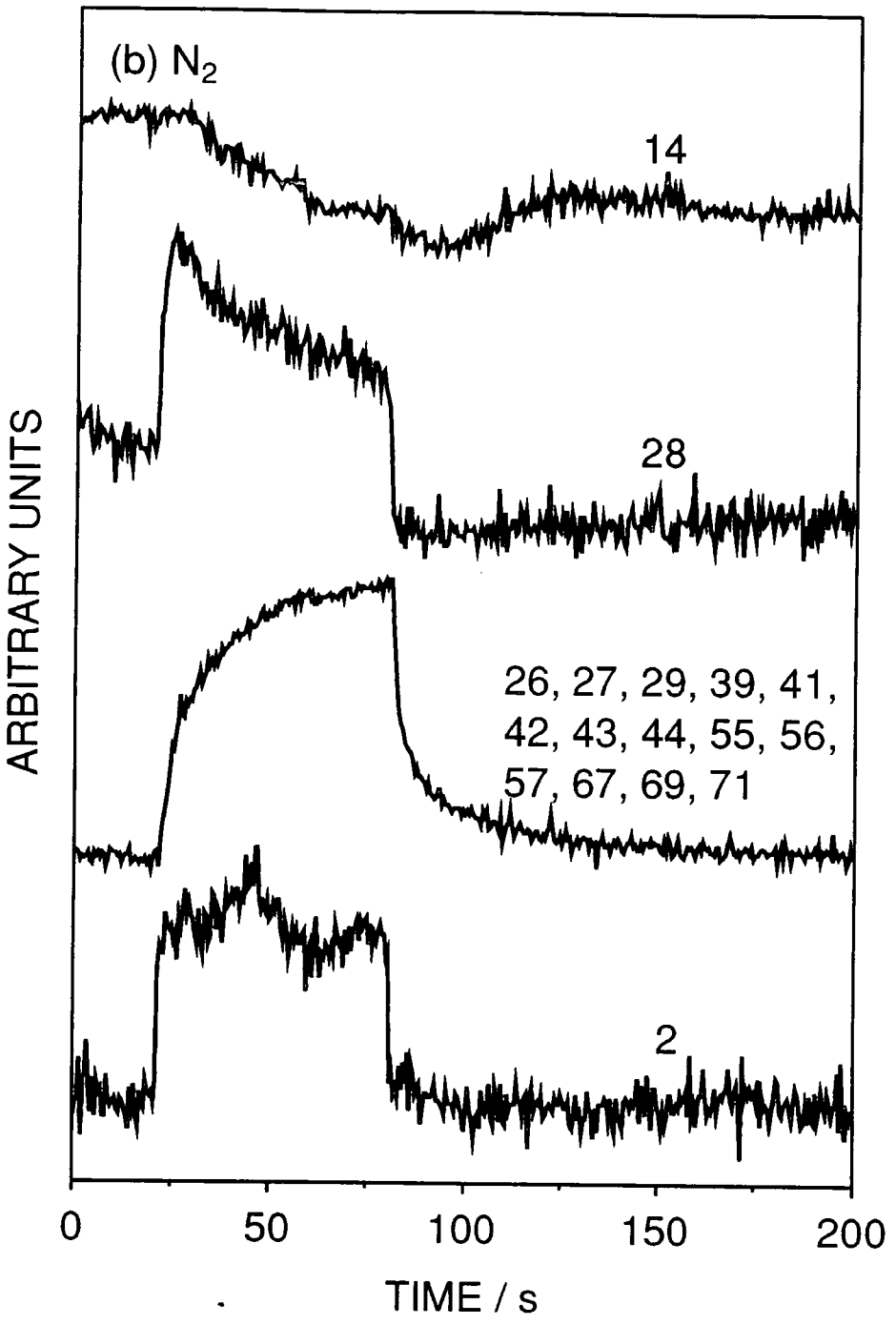

Figure 3.1(b): Mass profiles obtained using a 20/60/120 s, off/on/off sequence for the N_2 electrical discharge (all profiles typical for the relevant masses).

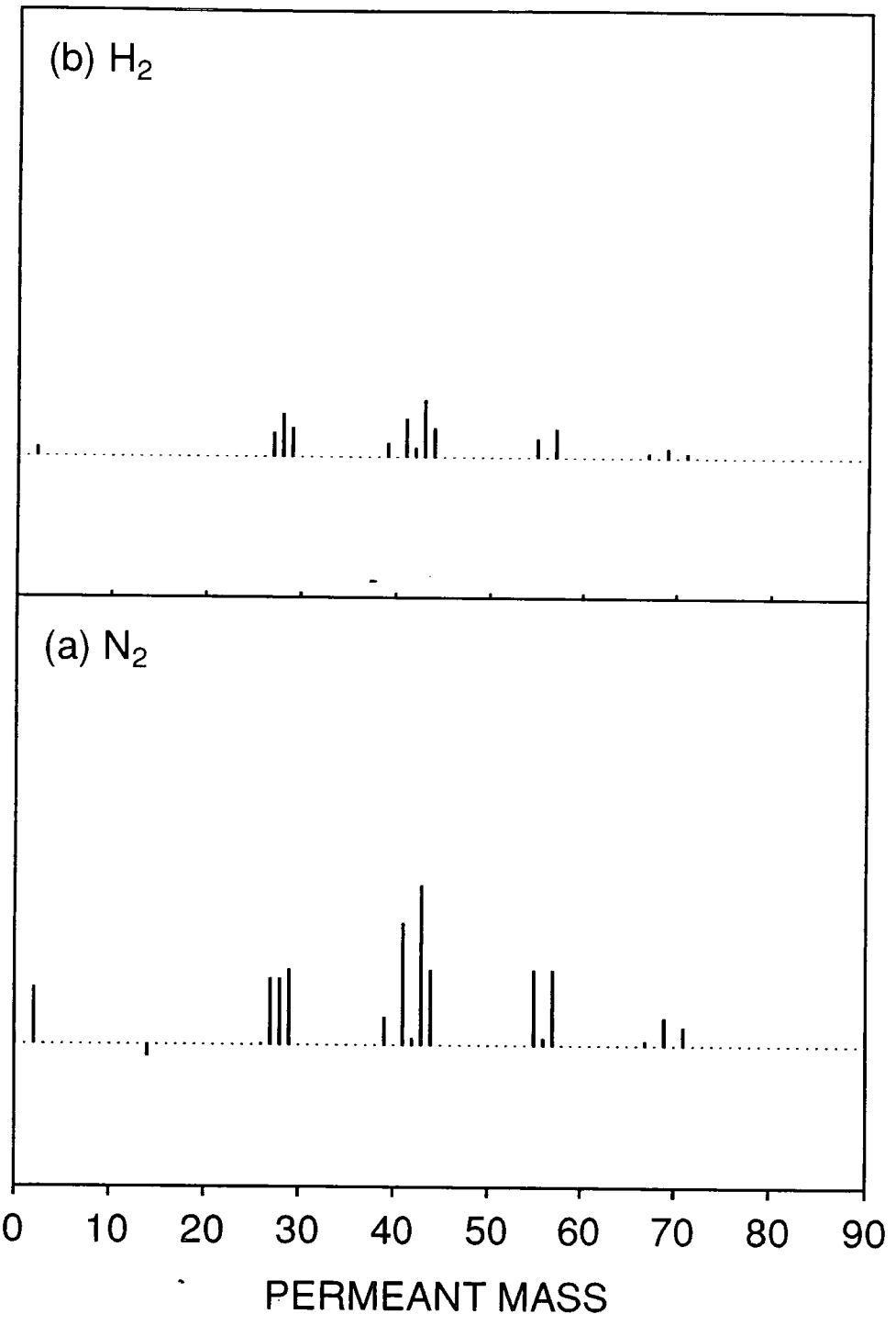

Figure 3.2: Maximum variation in mass signal intensities during plasma treatment: (a) H_2; and (b) N_2.

Further experiments, using the noble gases (Ar, Ne and He) and CF_4 as feed gases for the plasma treatment of polyethylene also produced hydrocarbon mass fragments and profiles similar to that of both the hydrogen and nitrogen electrical discharge treatments, Chapter 8, Appendix A.

Gas pulsing experiments were undertaken in order to gain a deeper insight into the mechanistic details governing plasma modification. Firstly, a series of control experiments were carried out where D_2 was pulsed into the 0.6 mbar H_2 gas feed stream passing through the plasma reactor in the absence of an electrical discharge. These showed that a 1000 μs pulse of deuterium resulted in a 0.01 mbar rise in total pressure (i.e. less than 2 % change) and an accompanying amount of D_2 (*m/z* 4) permeating through the polymer could be detected. No change in the level of H_2 permeation was observed, Figure 3.3(a). This gas pulsing sequence was then repeated during hydrogen plasma treatment (i.e. 20 s off / 30 s on / D_2 pulse / 30 s on / 120 s off), Figure 3.3(b). No change in the hydrocarbon mass profiles or fragment pattern was observed, however, the D_2 pulse was less intense than for the control experiments and decreased more rapidly. Also *m/z* 2 production steadied and *m/z* 3 was formed, Figure 3.3(b).

This procedure was then used for H_2 / D_2 (*m/z* 4) pulsed into a nitrogen plasma, Figures 3.4 and 3.5. No change in the level of N_2 permeation was observed when the gases were pulsed without plasma ignition, Figure 3.4(a) and 3.5(a). During plasma exposure the pulses caused the formation of hydrocarbon to drop dramatically but gave no change in the nitrogen production (*m/z* 14), Figures 3.4(b) and 3.5(b). For the D_2 pulse, HD (m/z 3) was produced and an increase in m/z 2 was observed, Figure 3.5(b). No change in the mass fragment pattern for the hydrocarbons was detected.

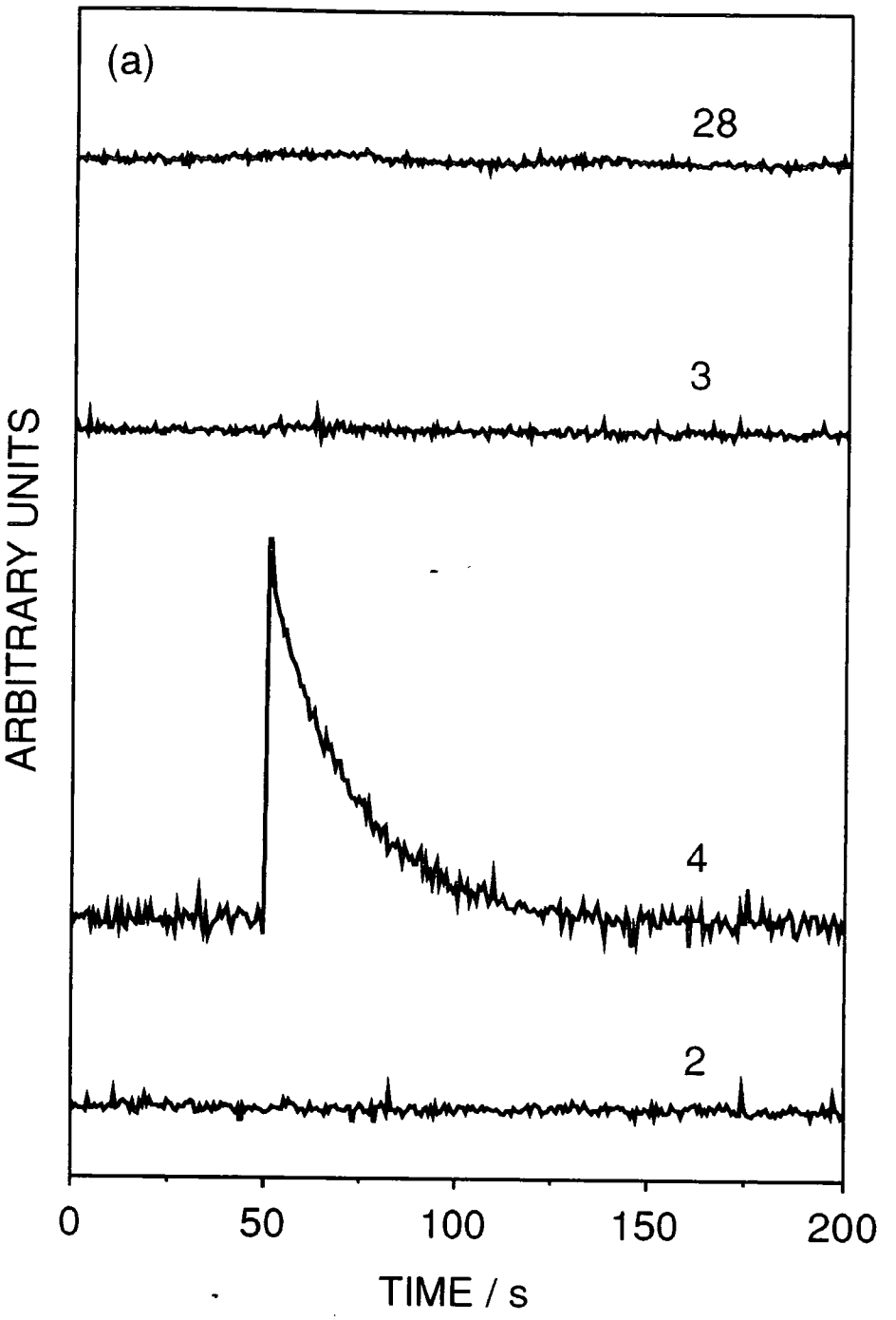

Figure 3.3(a): Mass profiles obtained when a 1000 μs pulse of D_2 is added to 0.6 mbar of H_2 passing through reactor at t = 50 s.

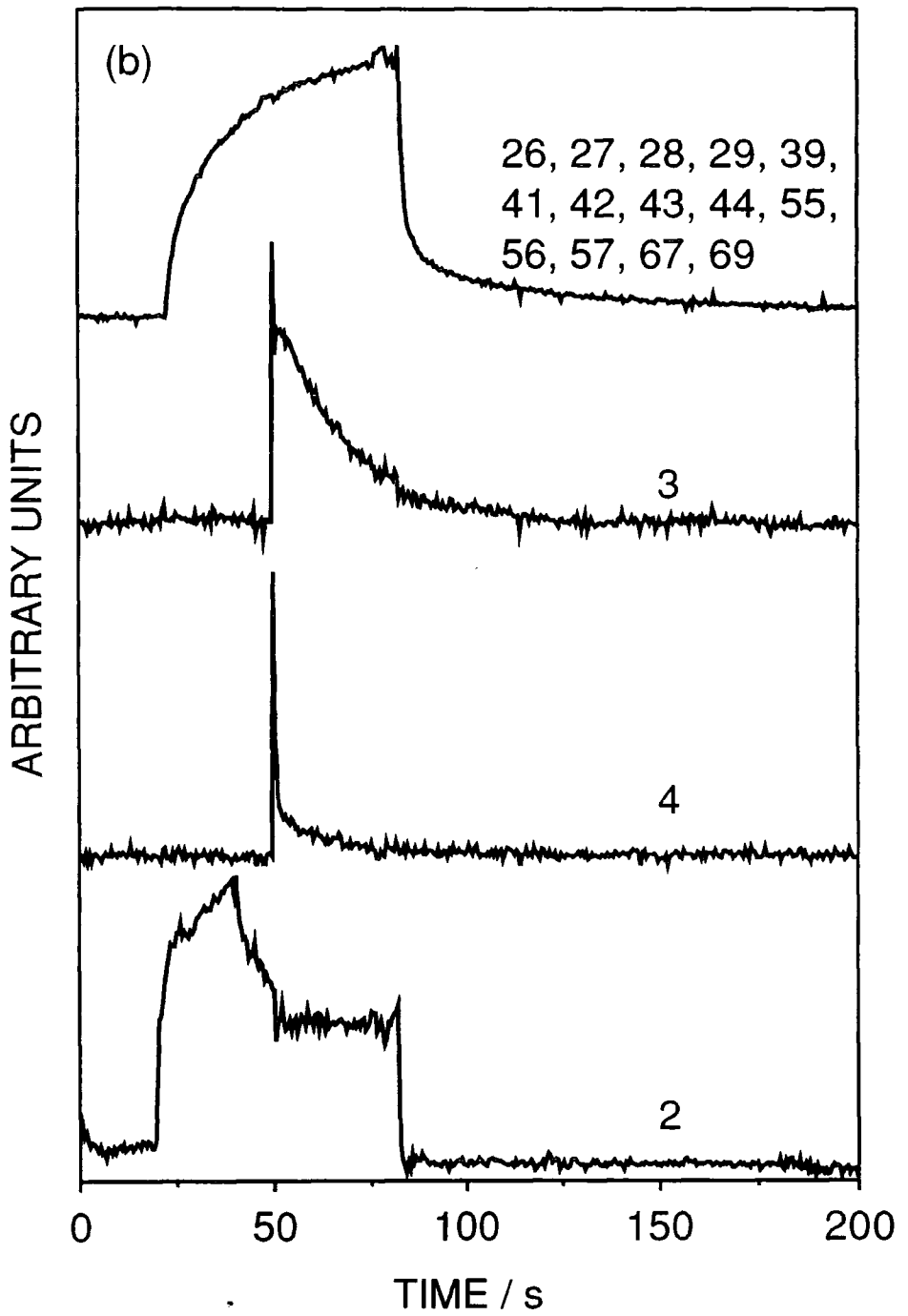

Figure 3.3(b): Mass profiles obtained during the following sequence: 0.6 mbar of H_2 passing through reactor from t = 0 s, ignition of plasma at t = 20 s, injection of 1000 μs pulse of D_2 at t = 50 s, termination of plasma at t = 80 s (all profiles typical for the relevant masses).

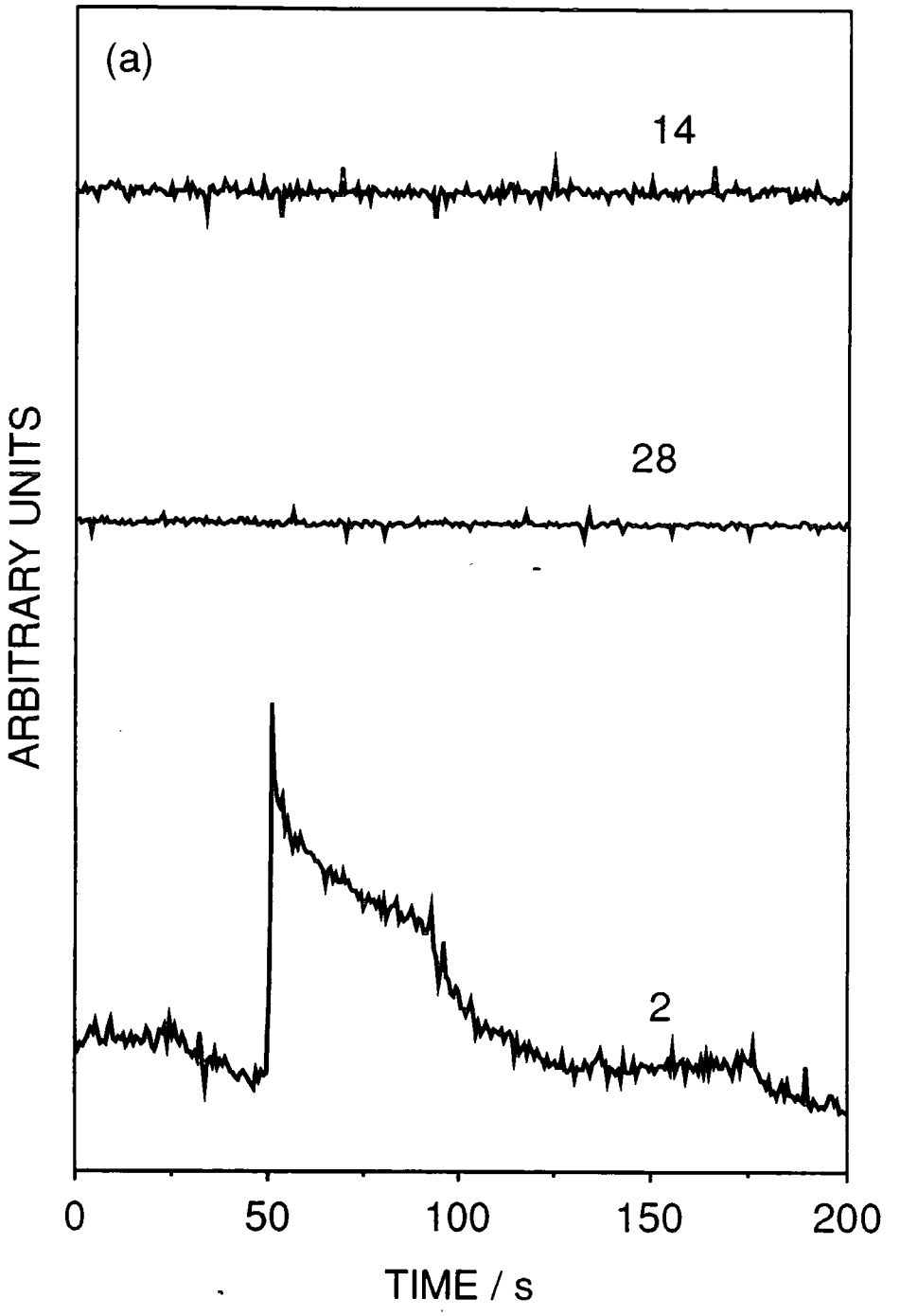

Figure 3.4(a): Mass profiles obtained when a 1000 μs pulse of H_2 is added to 0.6 mbar of N_2 passing through reactor at t = 50 s.

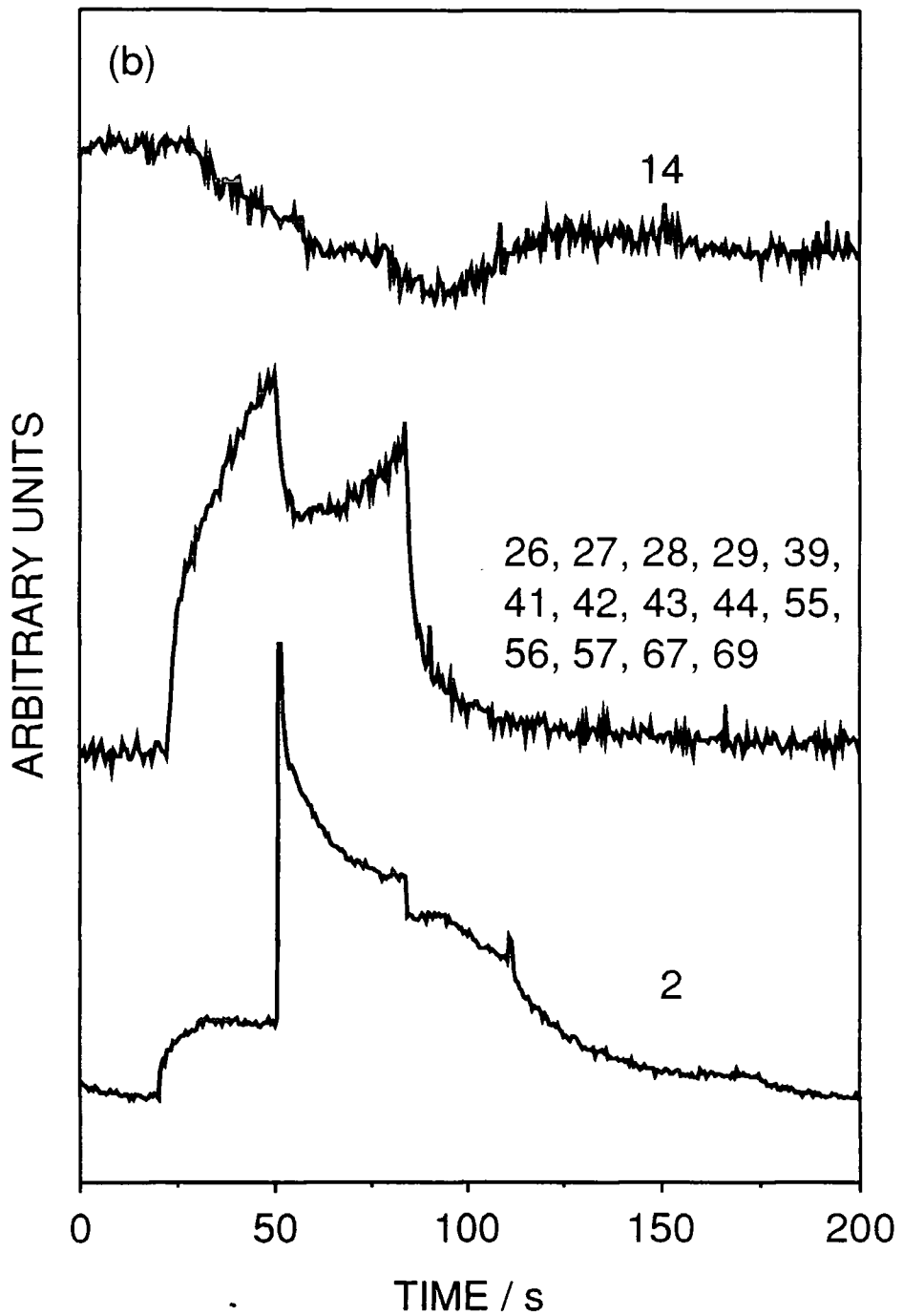

Figure 3.4(b): Mass profiles obtained during the following sequence: 0.6 mbar of N_2 passing through reactor from t = 0 s, ignition of plasma at t = 20 s, injection of 1000 μs pulse of H_2 at t = 50 s, termination of plasma at t = 80 s (all profiles typical for the relevant masses).

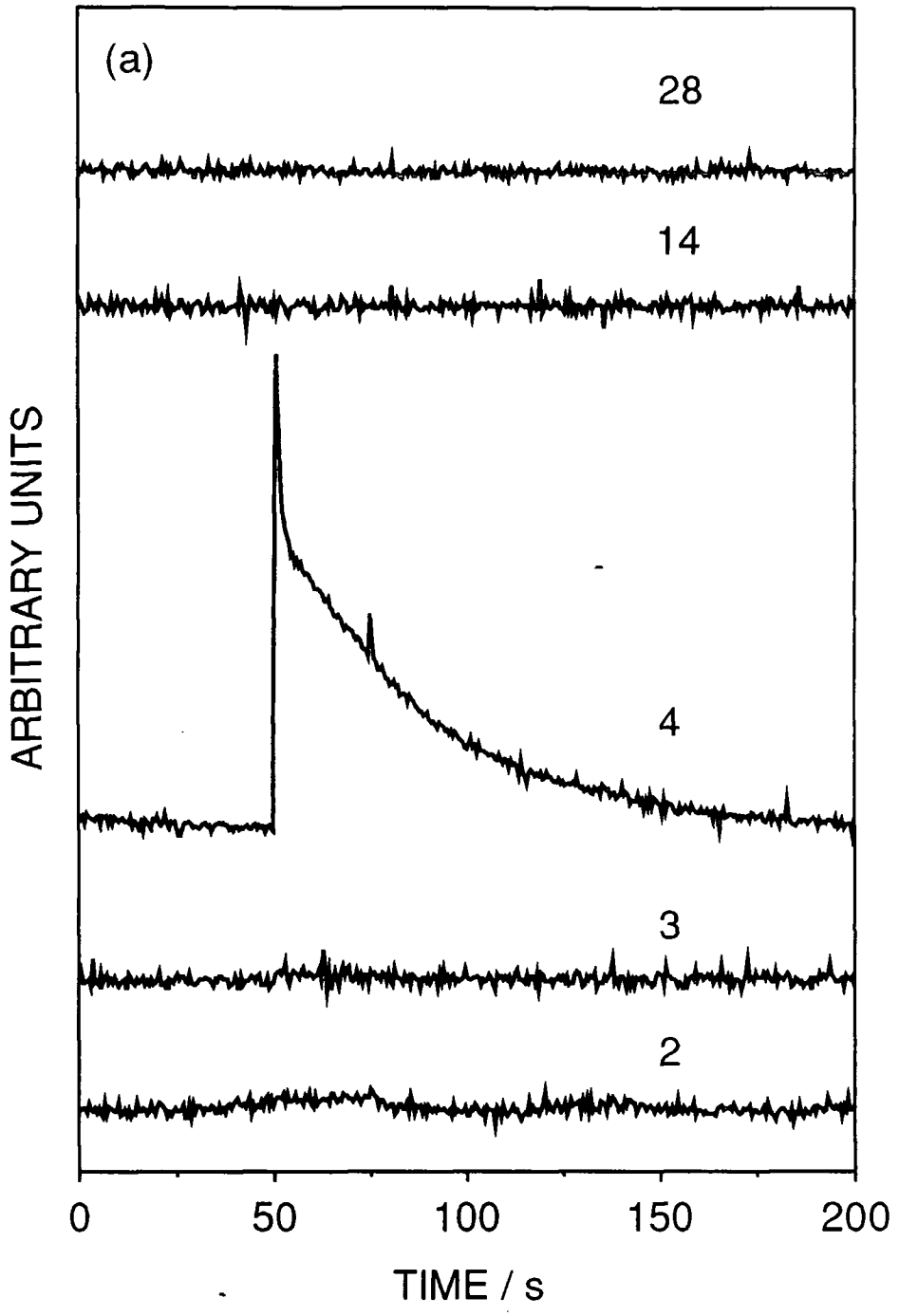

Figure 3.5(a): Mass profiles obtained when a 1000 μs pulse of D_2 is added to 0.6 mbar of N_2 passing through reactor at t = 50 s.

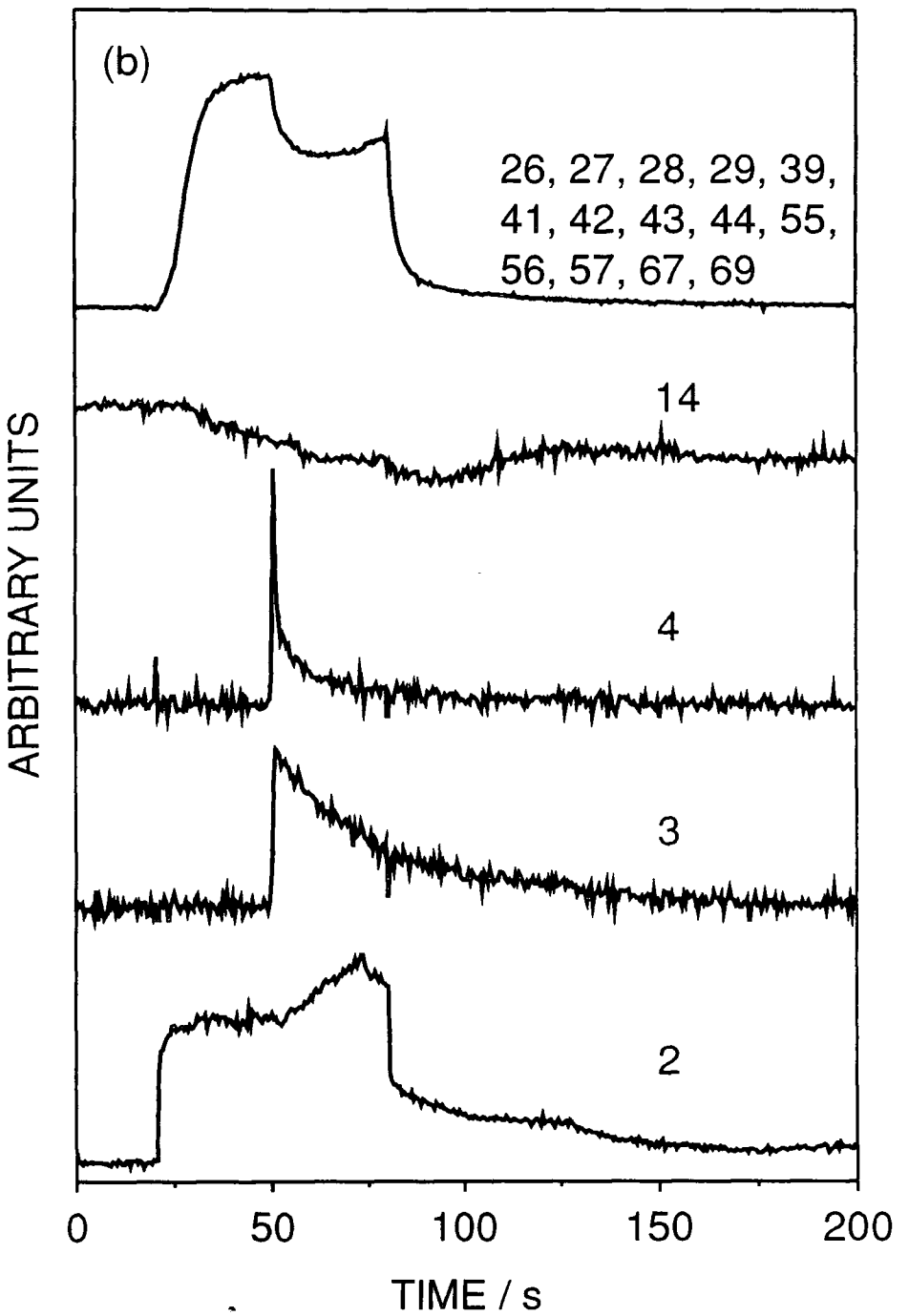

Figure 3.5(b): Mass profiles obtained during the following sequence: 0.6 mbar of N_2 passing through reactor from t = 0 s, ignition of plasma at t = 20 s, injection of 1000 μs pulse of D_2 at t = 50 s, termination of plasma at t = 80 s (all profiles typical for the relevant masses).

3.4 DISCUSSION

Non-equilibrium electrical discharges contain a wide range of species (atoms, molecules, ions, electrons, and electromagnetic radiation) which undergo direct and indirect interactions[19] with polymer surfaces causing the production of free radical centres.[20,21,22] These radical species can either react with the adjacent plasma medium or undergo crosslinking. A hydrogen plasma is a reactive medium (predominant reactive species are H atoms) thus both of these pathways are likely to occur. As for the N_2, O_2 and air plasma treatments (chapter 2) VUV photodegradation processes will be prominent in the near-surface region of polyethylene leading to chain scission accompanied by the formation of atomic hydrogen, Scheme 2.1.[23] Since hydrogen free radicals are likely to be short-lived within the polymer subsurface, formation of molecular hydrogen and crosslinking are to be expected,[23] Scheme 2.1.

For the hydrogen plasma exposure, as reported in previous studies,[24] hydrocarbon formation was found to be the predominant reaction pathway, Figure 3.2. The absolute amount of hydrocarbons produced was much lower than that observed for the nitrogen plasma treatment, Figure 3.2. This is probably due to the termination of the free radicals at the polymer surface with H atoms produced in the plasma.

$$R\bullet + H\bullet \longrightarrow R\text{-}H$$

This effect has been noted in the hydrogen plasma treatment of PTFE, where defluorination occurs and the remaining free radicals in the PTFE backbone react with the H atoms.[15] In this work, the enhanced termination halts chain scission and thus the production of hydrocarbon fragments. Plasma induced crosslinking is also impeded due to the decrease in concentration of the reactive free radical sites. This is shown by the very slight change in hydrogen permeability (by $1 \pm 0.05\%$) compared to the large drop in nitrogen permeability for the N_2 plasma treatment.

As expected, pulsing D_2 into a H_2 plasma had very little effect on hydrocarbon production as both H and D atoms are equally capable of reacting with the polymer free radicals and cause termination of chain scission.

$$R\bullet + D\bullet \longrightarrow R\text{-}D$$

However, new reaction pathways were observed; the formation of HD (*m/z 3*) and the decrease in the production of H_2 (*m/z 2*). HD is produced due the combination of hydrogen and deuterium atoms,[1]

$$D\bullet + H\bullet \longrightarrow HD$$

which in turn leads to a decrease in the formation of H_2. The mass profiles of H_2 (*m/z* 2) and HD (*m/z* 3) combined, Figure 3.3(b), give the original mass profile for H_2 plasma treatment, Figure 3.1(a).

The effect of termination of free radicals with H atoms has been confirmed by the pulsing of H_2 / D_2 into a N_2 plasma. On introduction of the gas pulse into the N_2 plasma the amount of hydrocarbons decreased, Figures 3.4(b) and 3.5(b). This indicates a loss of chain scission due to the capping of the polymer free radicals with H or D atoms.

$$R\bullet + H\bullet \longrightarrow RH \text{ (loss of chain scission)}$$

No deuterated hydrocarbons were detected in either of the D_2 pulsing experiments and no NH_x was observed on H_2 pulsing.

3.5 CONCLUSIONS

Hydrogen electrical discharge treatment of polyethylene causes the formation of free radicals along the polymer backbone. These free radicals can undergo chain scission and produce hydrocarbon fragments in a similar manner to that seen previously for nitrogen plasma treatment. However, the production of these fragments is impeded due to hydrogen atoms in the plasma reacting with the polymer free radicals thus terminating the chain scission. This chapter and chapter two have shown that the processes occurring at the plasma - polymer interface are dependent upon the feed gas used.

3.6 REFERENCES

[1] F.K. McTaggart, *Plasma Chemistry in Electrical Discharges*, (Elsevier Publishing Company, Essex, 1967).

[2] D. Didier, D. Bensahel and J.L. Regolini, U.S. Pat. 5252181, 1993.

[3] D.E. Aspnes and R.P.H. Chang, *Plasma Diagnostics Volume 2*, edited by O. Auciello and D.L. Flamm (Academic Press, London, 1989), Chapter 3.

[4] D.A. Cathey Jr. and I.D. Boise, U.S. Pat. 5354698, 1994.

[5] F.Y. Robb and A.Z. Tempe, U.S. Pat. 4529860, 1985.

[6] G.J. Tessmer, B.R. Stoner and D.L. Dreifus, U.S. Pat. 548733, 1995.

[7] G.E. Possin, R.F. Kwasnick and B.W. Giambattista, U.S. Pat. 5281546, 1994.

[8] J.R. Hollahan, *Techniques and Applications of Plasma Chemistry*, edited by J.R. Hollahan and A.T. Bell (John Wiley and Sons, London, 1974) Chapter 7.

[9] M. Hudis, *Techniques and Applications of Plasma Chemistry*, edited by J.R. Hollahan and A.T. Bell (John Wiley and Sons, London, 1974) Chapter 5.

[10] Y. Yao, X. Liu and Y. Zhu, J. Appl. Polym. Sci. **48**, 57 (1993).

[11] A. Hollander, J. Besnisch and H. Zimmermann, J. Appl. Polym. Sci. **49**, 117 (1993).

[12] J. Hopkins and J.P.S. Badyal, J. Polym. Sci; Polym. Chem. **34**, 1385 (1996).

[13] J. Hopkins and J.P.S. Badyal, Macromolecules **27**, 5498 (1994).

[14] M.E. Ryan and J.P.S. Badyal, Macromolecules **28**, 1377 (1995).

[15] D.T. Clark and D.R. Hutton, J. Polym. Sci; Polym. Chem. **25**, 2643 (1987).

[16] H. Yasuda, *Plasma Polymerisation*, (Academic Press, London, 1985).

[17] R. d'Agostino, F. Cramarossa and F. Fracassi, *Plasma Deposition, Treatment and Etching of Polymers*, edited by R. d'Agostino (Academic Press, London, 1990) Chapter 2.

[18] A. Cornu and R. Massot, *Compilations of Mass Spectral Data* (Heyden and Sons, London, 1975) 2nd Edition, Vol 1, Part a.

[19] D.T. Clark and A. Dilks, J. Polym. Sci. Polym. Chem. **15**, 2321 (1977).

[20] S.R. Cain, F.D. Egitto and F. Emmi, J. Vac. Sci. Technol. **A5**, 1578 (1987).

[21] M. Hudis, *Techniques and Applications of Plasma Chemistry*, edited by J.R. Hollahan and A.T. Bell (John Wiley and Sons, New York, 1974), Chapter 3.

[22] L.J. Gerenser, J. Adhesion Sci. **1**, 303 (1987).

[23] B. Ranby and J.F. Rabek, *Photodegradation, Photooxidation and Photostabilization of Polymers* (John Wiley and Sons, London, 1975), Chapter 4.

[24] T.W. Gallaher, T.C. Devore, R.O. Carter and C. Anderson, Appl. Spectroscopy **34**, 408 (1980).

CHAPTER 4

XENON DIFLUORIDE PLASMA FLUORINATION OF POLYMER SURFACES

4.1 INTRODUCTION

Fluorinated polymer surfaces are widely sought after for their low surface energies[1] and chemical inertness.[2] Direct plasma fluorination is an appealing way of achieving this goal.[1-20] CF_4,[7,13,16,17] SF_6,[13,18] C_2F_6,[16,17] and F_2[4] feed gases have been used in the past for this purpose. Most other types of fluorocarbon monomer tend to undergo fragmentation and polymerisation in the presence of an electrical discharge to form coatings, e.g. CF_3H.[17] In general, surface modification is preferred over thin film deposition, since it offers faster processing speeds, lower consumption of monomer, and less waste.

Xenon difluoride (XeF_2) is another potential reagent for plasma fluorination. At room temperature it is a white solid with a vapour pressure of 4.5 mbar,[21] and is often used for etching silicon[22-28] and silicon compounds,[24,25,29] as well as for the removal of hydrocarbon residue from silicon surfaces.[23] XeF_2 is also renowned as an effective fluorinating reagent for many solution phase organic reactions[29-31] (e.g. addition across carbon-carbon double[31] / triple bonds;[30] hydrogen replacement;[30,31] electrophilic substitution;[31] fluorination of organoelements;[28] fluorodecarboxylation,[30] etc). XeF_2 electrical discharges offer two potential advantages over existing plasma fluorination routes: firstly it is a solid compound and therefore can be easily transported; and secondly no chemically reactive byproducts from the feed gas can interfere with the surface reactions, since xenon is chemically inert towards polymer substrates (whereas other feed gases, e.g. CF_4, SF_6 etc, all generate additional reactive intermediate species, e.g. CF_x, SF_x respectively). In this chapter the susceptibility of a range of polymers containing different types of structural repeat unit towards non-isothermal XeF_2 plasma fluorination is examined.

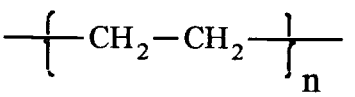

Polyethylene (PE)

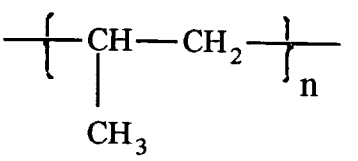

Polypropylene (PP)

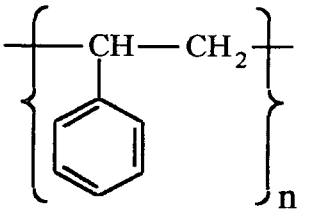

Polystyrene (PS)

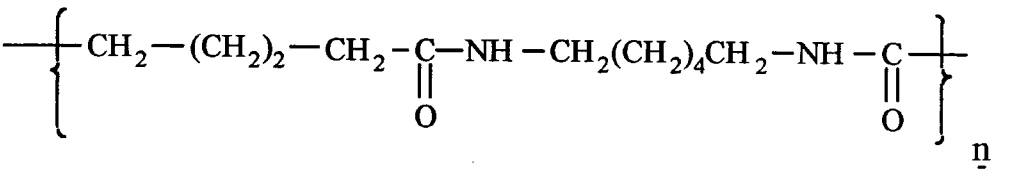

Nylon 6,6 (N-66)

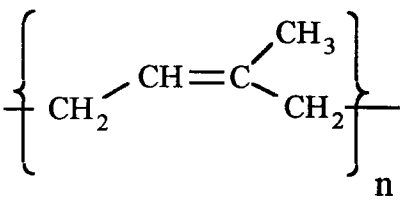

Polyisoprene (PIP)

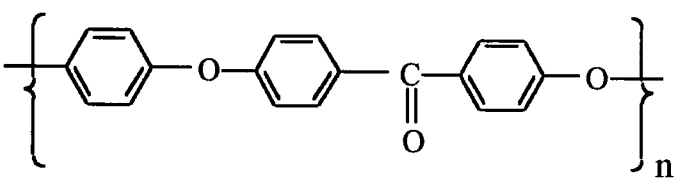

Polyetheretherketone (PEEK)

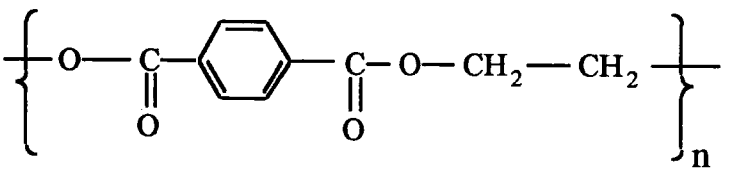

Polyethylene teraphthalate (PET)

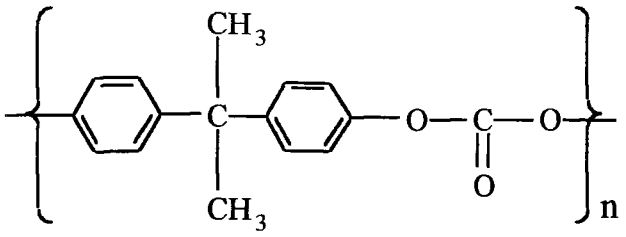

Polycarbonate (PC)

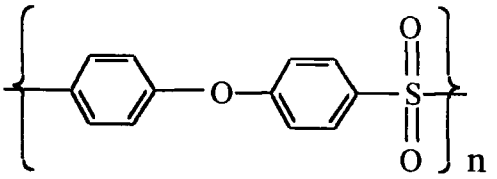

Polyethersulfone (PES)

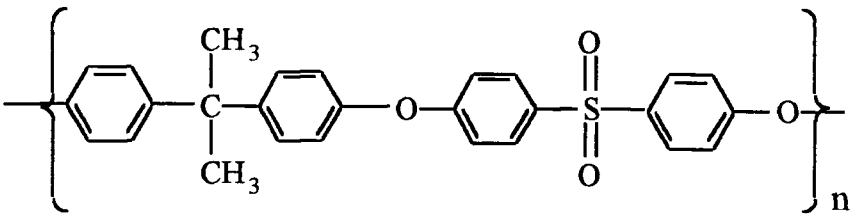

Polysulfone (PSF)

4.2 EXPERIMENTAL

Small strips of additive-free low density polyethylene (ICI), polypropylene (ICI), nylon 6,6 (Goodfellows), polystyrene (Huntsman), polyetheretherketone (ICI), polyethylene teraphthalate (Hoechst), polycarbonate (General Electric Plastics), polyethersulfone (Westlake Plastics Company) and polysulfone (Westlake Plastics Company) were ultrasonically washed in a 50 : 50 mixture of isopropyl alcohol and hexane for 30 s and dried in air. Polyisoprene (Shell) was dissolved in toluene (2% w/v) and spin coated onto glass slides. Xenon difluoride (99%, Fluorochem) and carbon tetrafluoride (99.7 %, Air Products) were used as feed gases for surface plasma fluorination treatments.

Experiments were carried out in a electrodeless cylindrical glass plasma reactor (diameter 5 cm, volume 500 cm^3, base pressure of 6 x 10^{-3} mbar and a leak rate of better than 2 x 10^{-5} cm^3s^{-1}) enclosed in a Faraday cage,[33] Figure 4.1. This was fitted with a gas inlet and a thermocouple pressure gauge. All joints were grease free. RF power from a 13.56 MHz generator was inductively coupled via an LC matching unit to a copper coil (6 cm diameter, 10 turns, and spanning 10 cm) wound around the reactor. Prior to each

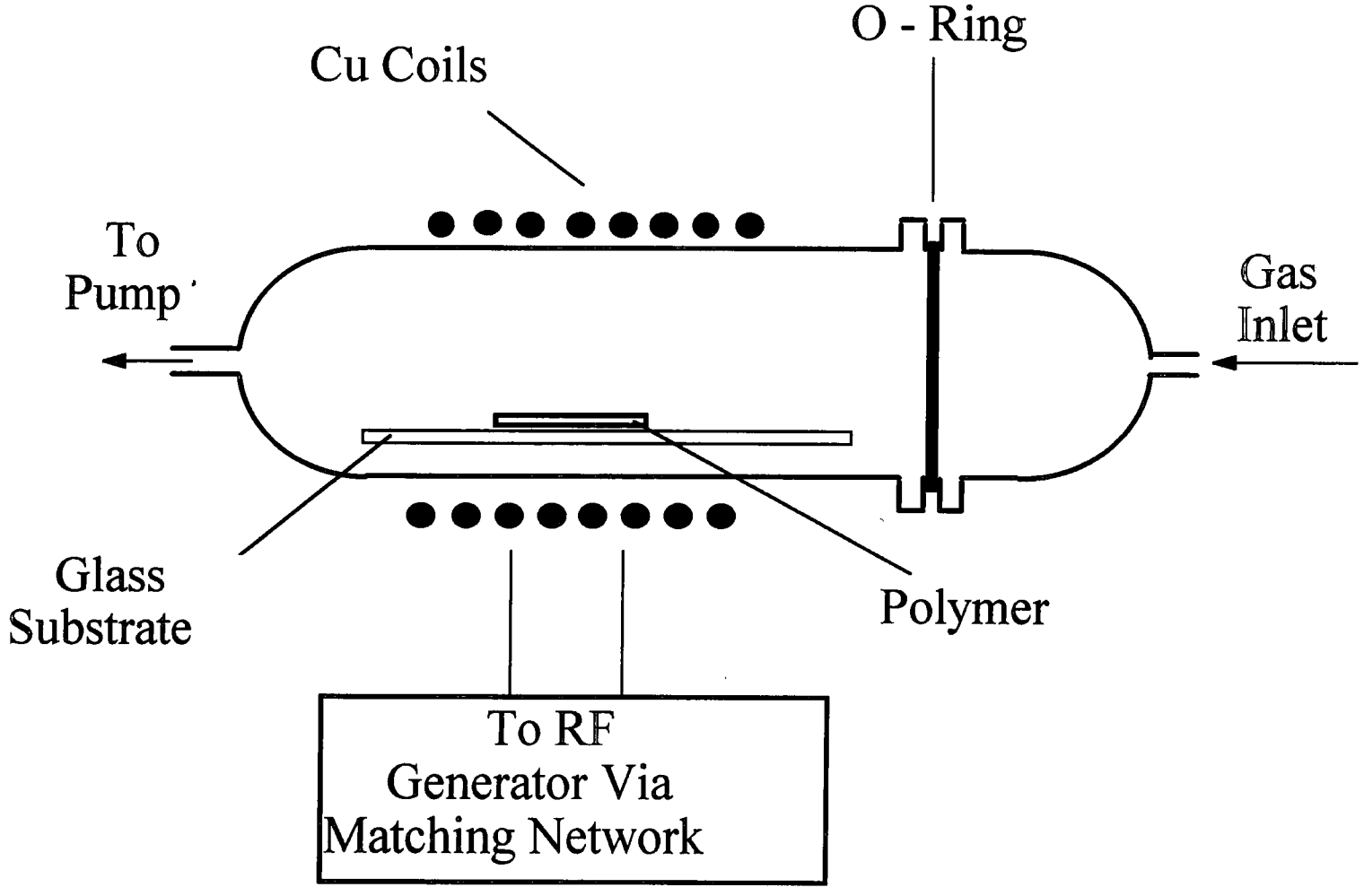

Figure 4.1: Schematic of the plasma fluorination apparatus.

experiment, the inside of the glass reactor was lined with polyethylene film in order to prevent etching of the glass walls by reactive XeF_2 glow discharge species. A typical experimental run comprised inserting a strip of polymer into the centre of the coils and evacuating to base pressure. XeF_2 stored in a steel reservoir heated to 80 °C was introduced into the plasma reactor via a leak valve at a pressure of 0.1 mbar. After 5 mins of purging, the electrical discharge was ignited at 20 W. Upon termination of treatment, XeF_2 was allowed to continue to pass over the substrate surface for a further 5 mins, after which time the apparatus was evacuated back down to base pressure and vented to air. These experiments were repeated using a glass slide substrate in order to check for the absence of etching and subsequent redeposition of polyethylene from the reactor lining:- no fluorinated coating was detected. Control experiments where polymer substrates were exposed to XeF_2 in the absence of an electrical discharge indicated negligible surface fluorination (F:C ratio = 0.11 ± 0.01 for polyethylene, and 0.16 ± 0.01 for polystyrene).

Surface characterisation prior to and following plasma fluorination was carried out using X-ray photoelectron spectroscopy (XPS). A Kratos ES300 electron spectrometer equipped with a Mg Kα X-ray source (1253.6 eV) and a concentric hemispherical electron analyser operating in the fixed retarding ratio mode (FRR, 22:1) was used to acquire XPS spectra. C(1s) XPS peaks were fitted using a Marquardt minimization computer program with Gaussian components having equal full-width-at-half-maximum (FWHM).[34] Instrumentally determined sensitivity factors for C(1s) : O(1s) : S(2p) : N(1s) : F(1s) were taken as being 1.00 : 0.55 : 0.54 : 0.74 : 0.67 respectively.

4.3 RESULTS

C(1s) XPS spectra of untreated polyethylene (PE) and polypropylene (PP) showed a single peak at 285.0 eV corresponding to -$\underline{C}_xH_y$-, Figure 4.2(a). Polyisoprene (PIP) and polystyrene (PS) also displayed a main hydrocarbon peak at 285.0 eV with an additional π-π* shake-up satellite feature at 291.6 eV.[35,36] C(1s) spectra of nylon 6,6 (N-66), polyetheretherketone (PEEK), polyethylene teraphthalate (PET), polycarbonate (PC), polysulfone (PSF) and polyethersulfone (PES) all contained oxidised carbon functionalities:[35] e.g. carbon adjacent to carboxylate ($\underline{C}$-CO_2) at 285.7 eV, ether linkage

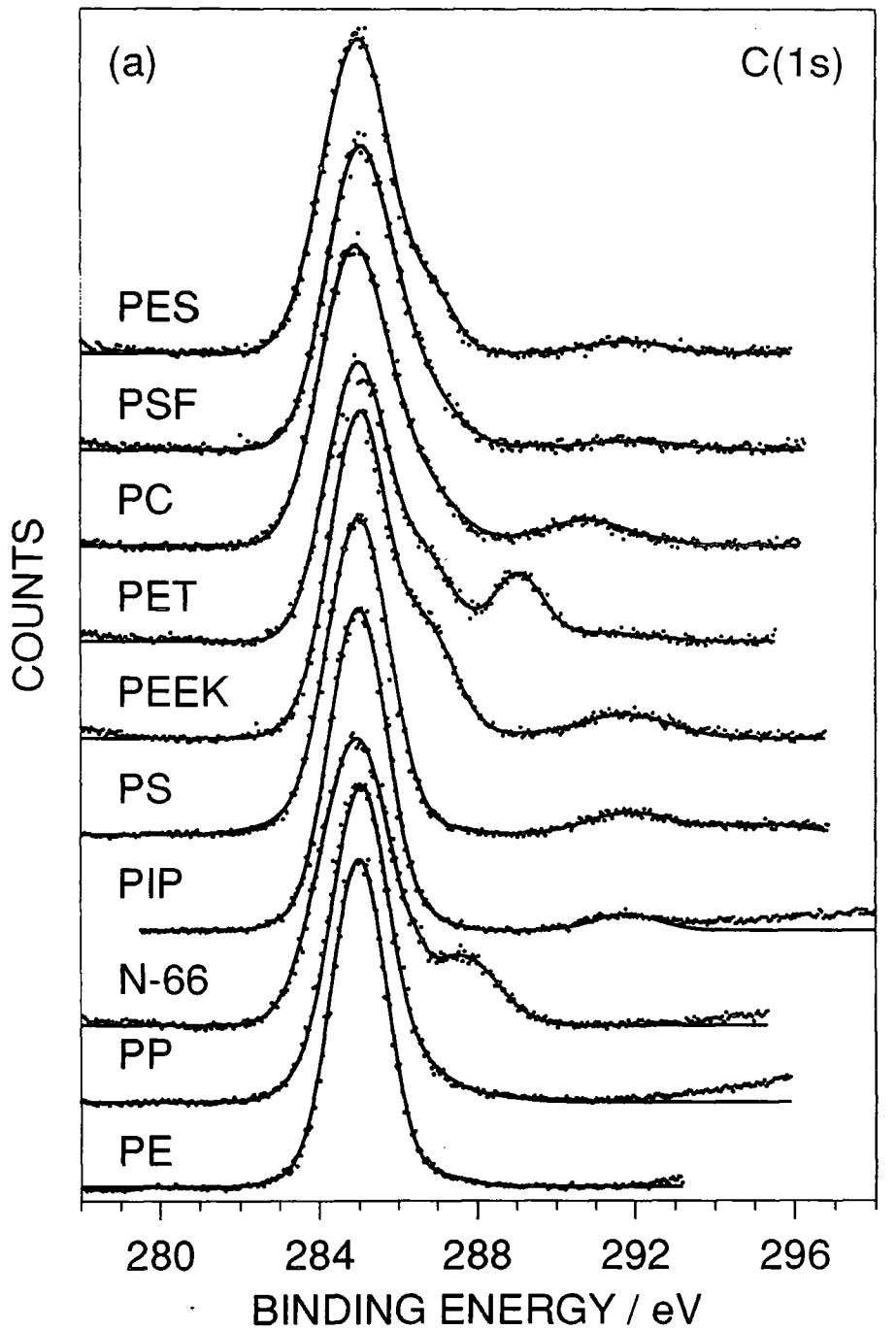

Figure 4.2(a): C(1s) XPS spectra of clean polymers.

(-C-O-) at 286.6 eV, carbonyl (-C=O) at 287.9 eV, carboxylate (-O-C=O) at 289.0 eV, or carbonate (-O-CO-O-) at 290.4 eV. In the case of polyethersulfone (PES) and polysulfone (PSF), carbon centres attached to sulfone groups (C-SO_2-) at 285.6 eV also needed to be included;[35] whilst carbon bonded to nitrogen (-C-NH) at 286.0 eV and carbon located in an amide environment (NH-C=O) at 288.0 eV had to be taken into consideration for nylon 6,6 (N-66).[35]

XeF_2 plasma treatment gave rise to extensive surface fluorination, Table 4.1. A small amount of oxygen incorporation at the surface (~3 %) was found for the non-oxygen containing polymers due to the reaction between trapped surface free radicals and the atmosphere during sample transfer from the plasma chamber to the XPS spectrometer.[18] C(1s) spectra taken for each of the polymers following 1 min of XeF_2 plasma fluorination are shown in Figure 4.2(b). Comparison of Figures 4.1 and 4.2 shows that all the polymer surfaces have been fluorinated greatly, as peaks indicative of highly fluorinated carbon moieties are formed on treatment i.e. spectra shifts to a higher binding energy. Further interpretation of the spectra is limited as there is great number of different fluorinated carbon environments, this gives rise to undefined broad peaks and ambiguity in peak fitting. However, for the purpose of this work values for the main carbon environments were ascertained from tabulated fluorinated polymer standards[18,37] and the C(1s) envelopes were peak fitted to the following carbon environments: C_xH_y at 285.0 eV, C-CF_n at 286.6 eV, CF at 287.8 eV, CF-CF_n at 289.3 eV, CF_2 at 291.2 eV and CF_3 at 293.3 eV,[18,37] Figure 4.3. It is evident that XeF_2 is more effective than CF_4 at surface fluorination, and this difference is more pronounced for polymers containing >C=C< double bonds, Table 4.1 and Figure 4.4. It was found that over 95 % of fluorination occurred within the first 10 s for both types of feed gas.

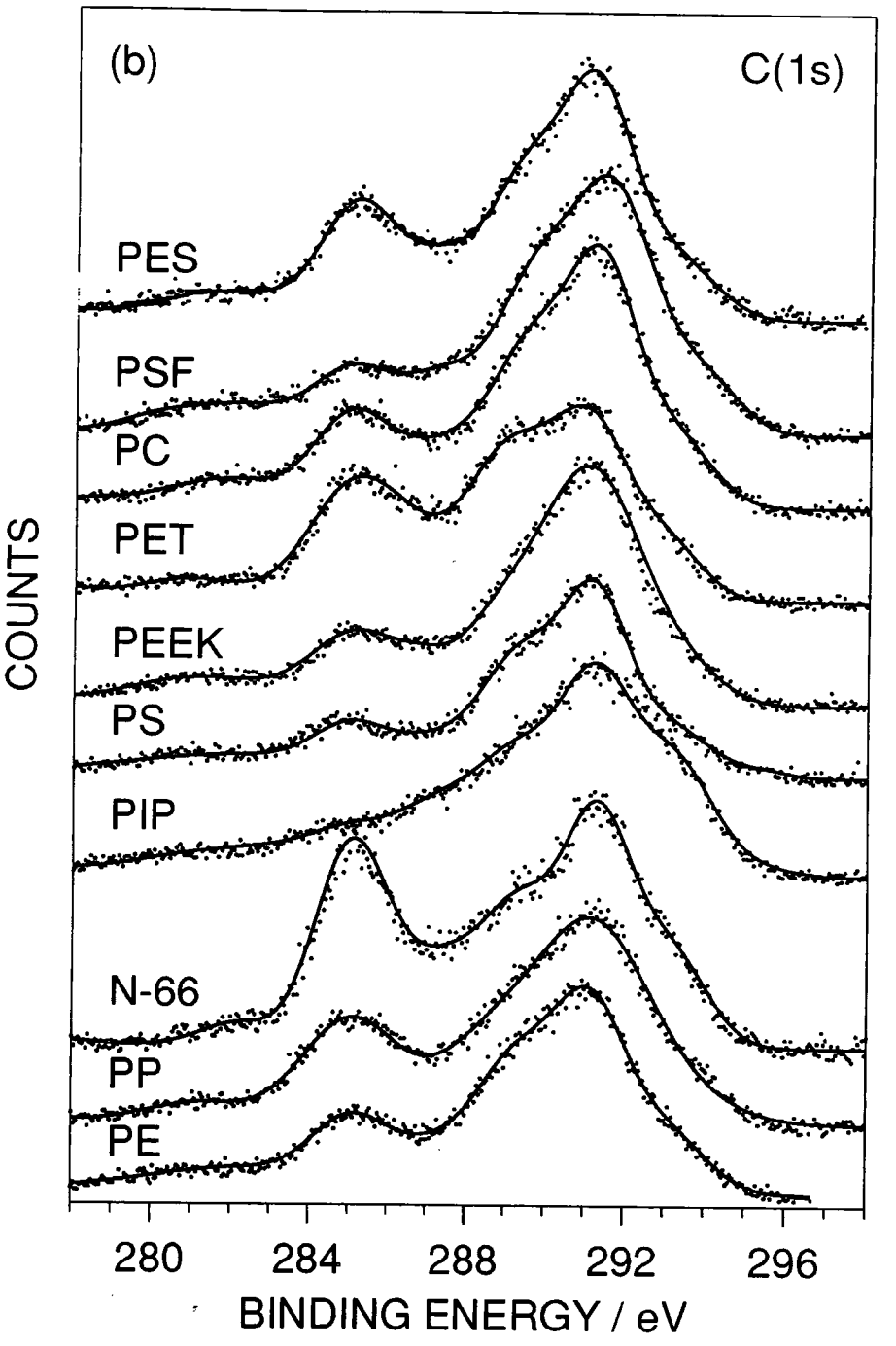

Figure 4.2(b): C(1s) XPS spectra of XeF_2 plasma treated polymers (20 W, 1 min).

POLYMER	XeF_2			CF_4			THEORETICAL†		
	F : C	O : C	S : C / N : C	F : C	O : C	S : C / N : C	F : C	O : C	S : C / N : C
Polyethylene	1.56	0.02	0	1.50	0.03	0	2.00	0	0
Polypropylene	1.41	0.03	0	1.40	0.02	0	2.00	0	0
Nylon 6,6	1.43	0.06	0.14	1.42	0.05	0.08	1.83	0.16	0.16
Polyisoprene	1.67	0.02	0	1.49	0.02	0	1.60	0	0
Polystyrene	1.59	0.08	0	1.40	0.05	0	1.00	0	0
Polyether etherketone	1.29	0.12	0	1.13	0.25	0	0.63	0.16	0
Polyethylene teraphthalate	1.23	0.24	0	0.98	0.41	0	0.83	0.40	0
Polycarbonate	1.57	0.10	0	1.29	0.20	0	0.93	0.19	0
Polysulfone	1.52	0.08	0.01	1.48	0.16	0.01	0.81	0.16	0.04
Polyethersulfone	1.53	0.10	0.03	1.51	0.26	0.04	0.67	0.25	0.08

†Calculated on the basis of straightforward fluorine substitution of C-H bonds.

Table 4.1: A comparison between XeF_2 and CF_4 glow discharge treatment of various polymers.

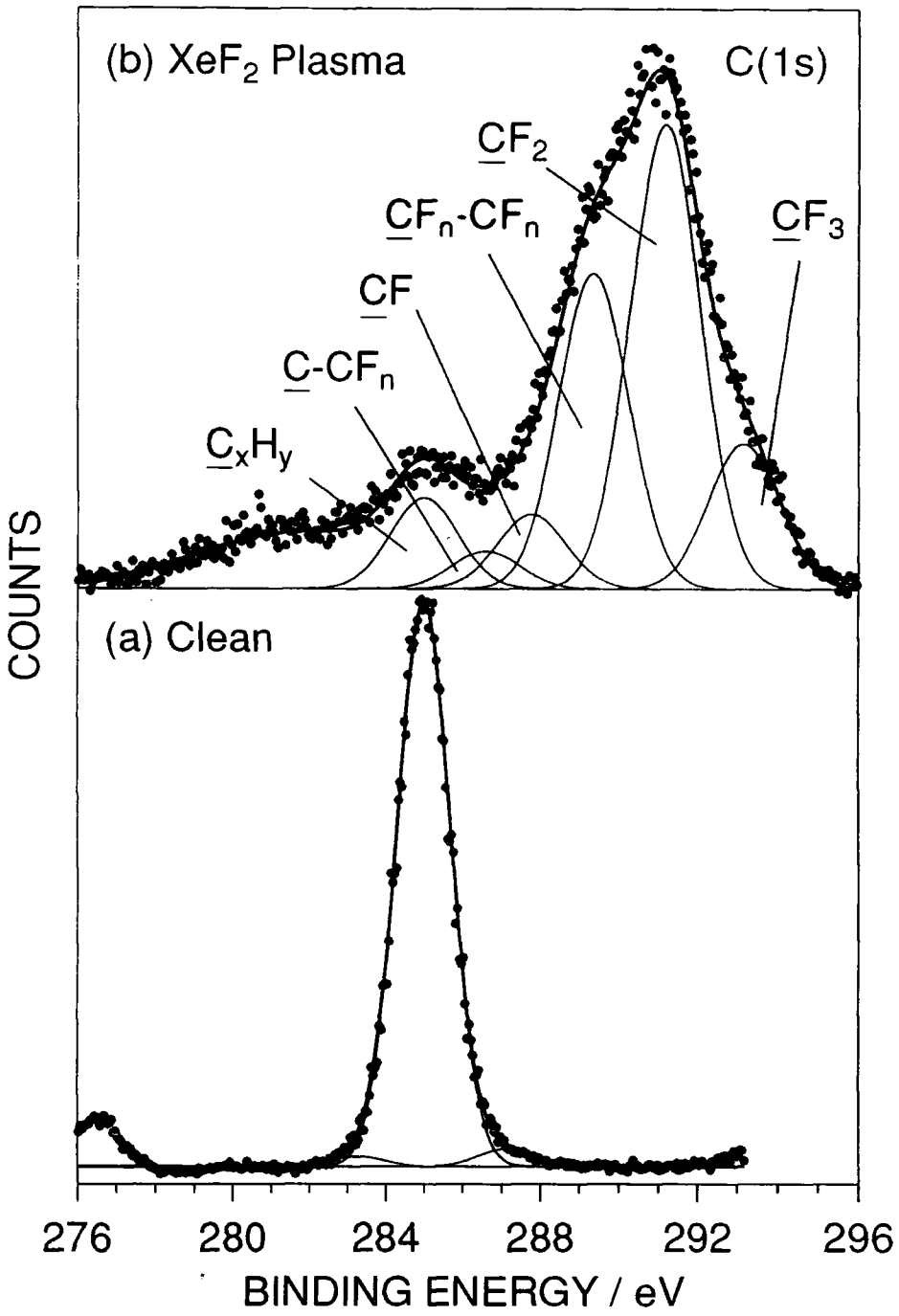

Figure 4.3: C(1s) XPS spectra of: (a) clean polyethylene; and (b) XeF_2 plasma treated polyethylene (20 W, 1 min).

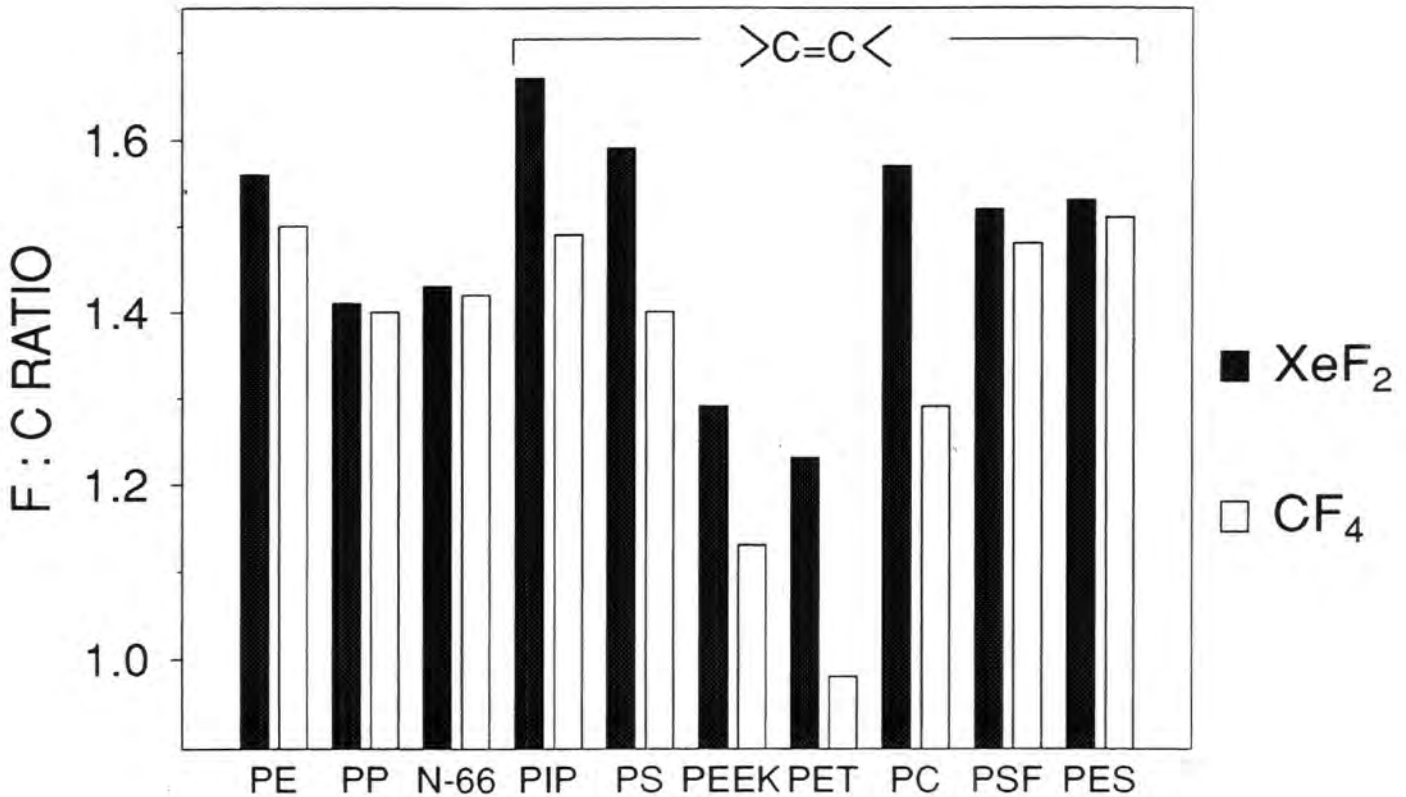

Figure 4.4: Comparison of experimentally measured levels of XeF_2 and CF_4 plasma fluorination (20 W, 1 min).

4.4 DISCUSSION

XeF_2 molecules can undergo fragmentation in the vicinity of an alternating RF field to generate fluorine atoms. Similarly, electrical discharge excitation of CF_4 can also yield chemically reactive fluorine atoms.[2,12] This study shows that the predominant reaction of both these plasma treatments is fluorination of the polymer surfaces. Hydrogen abstraction by fluorine to form HF is a thermodynamically favourable initiation step for saturated polymers,[3] Scheme 4.1. The formation of HF is thermodynamically favourable, since C-H bond strengths are in the 3-4 eV range compared to 5.9 eV for H-F and 5.0 eV for C-F.[12]

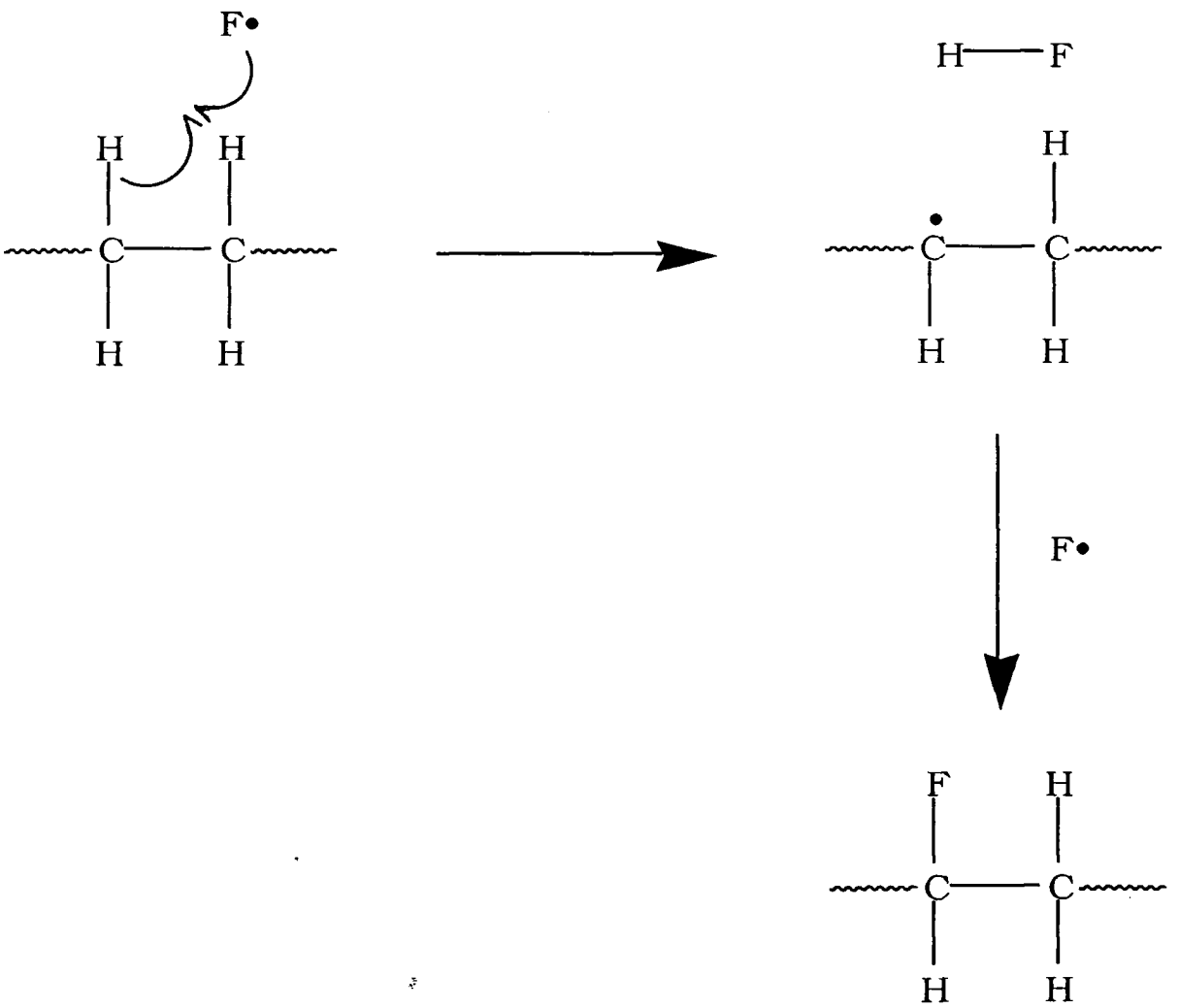

Scheme 4.1: Atomic fluorine attack at saturated hydrocarbon sites.

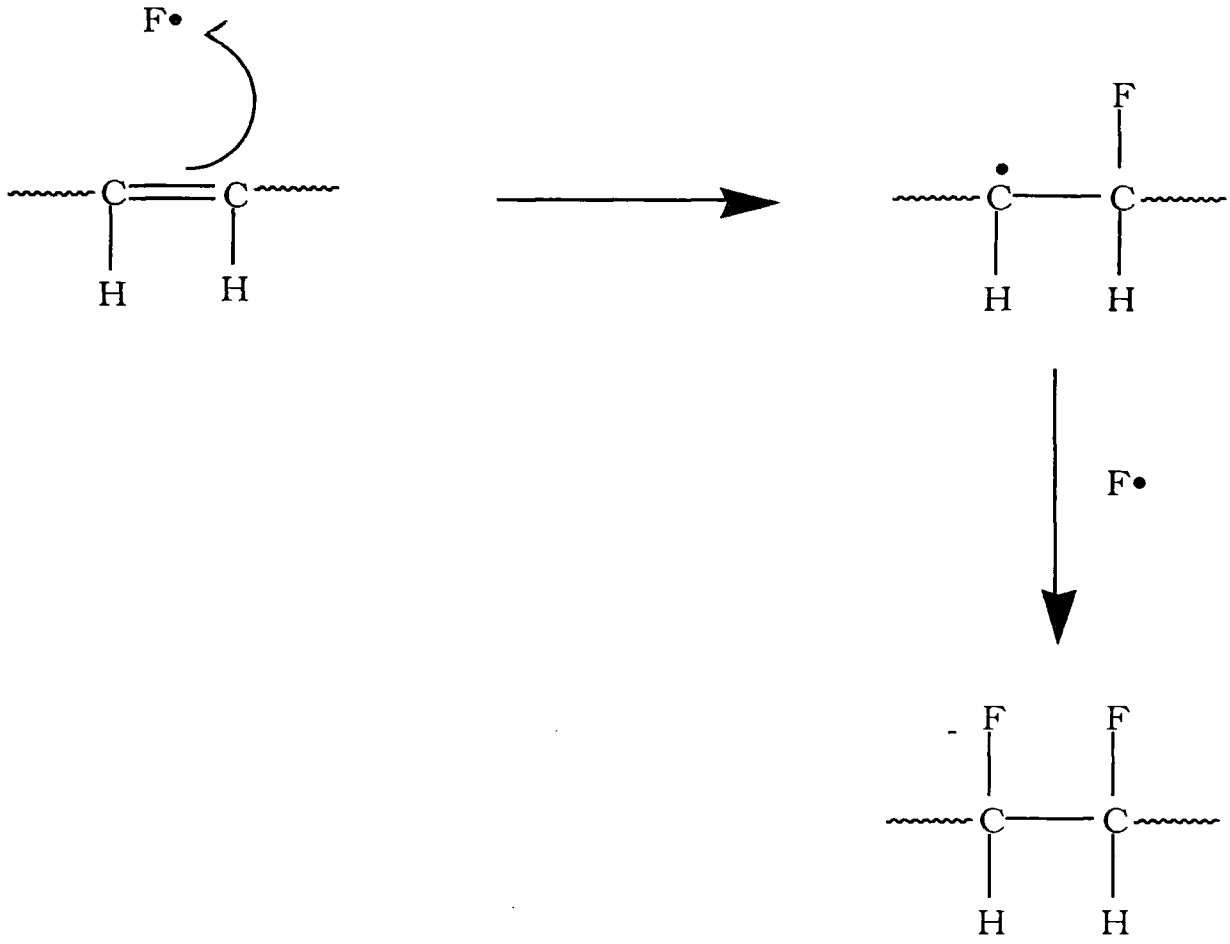

Scheme 4.2: Atomic fluorine attack at unsaturated hydrocarbon functionalities.

The XPS F:C ratios for each treated polymer substrate can be compared with the theoretically expected value based on a straightforward substitution of C-H bonds by C-F, Figure 4.5; it can be seen that polymers containing carbon-carbon double bonds experience a far greater degree of fluorination than might be expected on this basis. Hence, further fluorination via addition must also be occurring for polymers containing carbon-carbon double bonds, Scheme 4.2. This is borne out by Figure 4.5, which shows that there is a good correlation between the proportion of carbon atoms located in >C=C< bonds and the level of fluorination. This effect is more strongly accentuated for XeF_2 compared to CF_4 plasma treatment, Figure 4.6. Extended Huckel molecular orbital calculations[3] also predict that F atoms can participate in reactions at the polymer surface; these include hydrogen substitution and / or addition across carbon-carbon double bonds, Schemes 4.1 and 4.2 respectively.

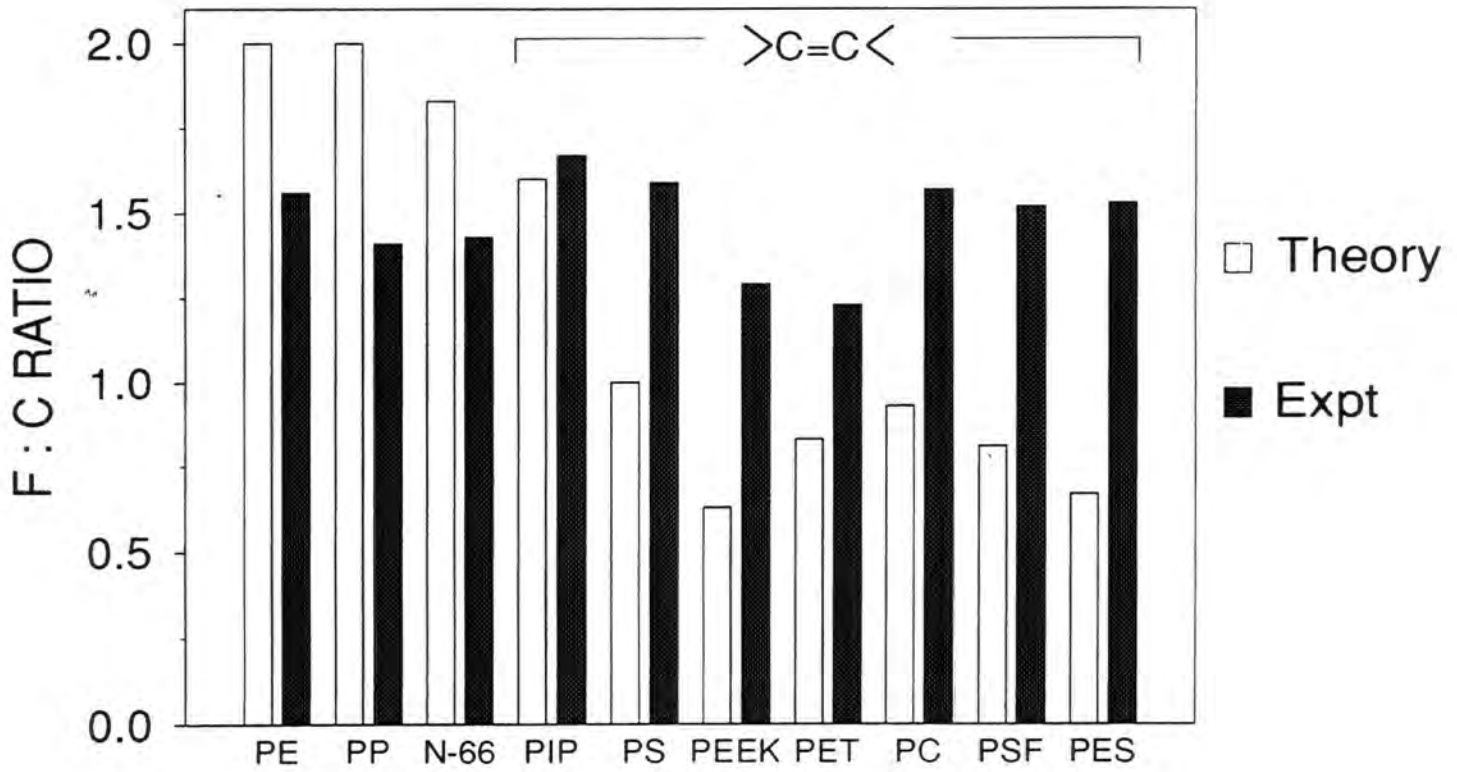

Figure 4.5: Comparison between theoretically calculated (based on fluorine substitution of C-H bonds) and experimentally measured levels of XeF_2 plasma fluorination.

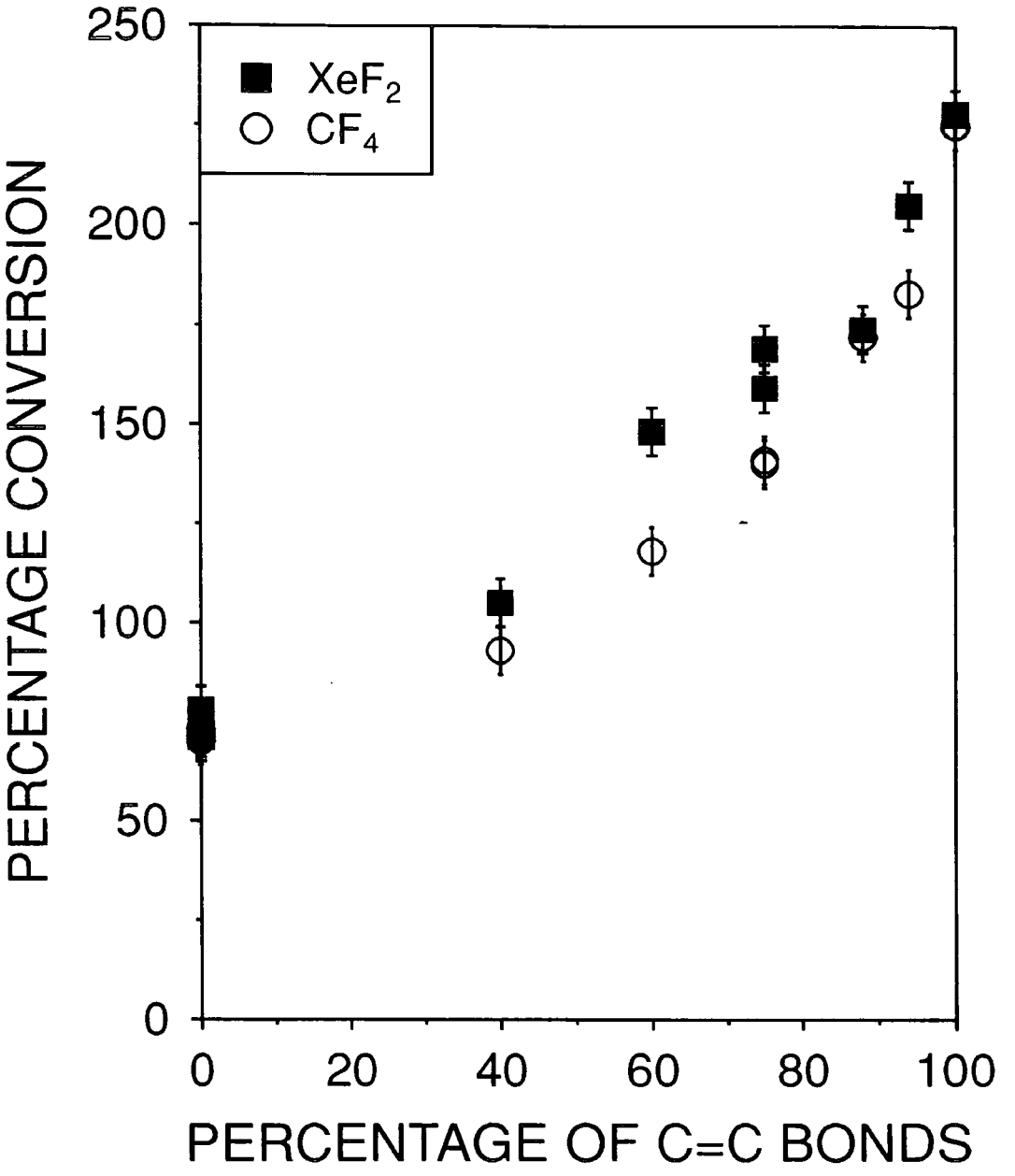

Figure 4.6: Percentage of carbon atoms in >C=C< double bonds versus percentage conversion (based on fluorine substitution of C-H bonds).

The greater susceptibility of polymer substrates towards XeF_2 plasma fluorination compared to CF_4 glow discharge treatment might be due to the stoichiometrically higher concentration of F atoms for the former: XeF_2 dissociates readily into Xe and F atoms, whilst CF_4 also produces CF_x.[12] Another contributing factor might be the absorption of XeF_2 onto the surface prior to and during treatment.

4.5 CONCLUSIONS

The work contain in this chapter proves that XeF_2 glow discharges are a highly effective method for fluorinating polymer surfaces. The extent of fluorine incorporation can be accounted for in terms of a structure-behaviour relationship based on extended Huckel molecular orbital calculations. Greater fluorination occurs if XeF_2 is used as the feed gas for plasma treatment rather than CF_4.

4.6 REFERENCES

[1] E. Occhiello, M. Morra and F. Garbassi, Die Angewandte Makromolekulare Chemie **173**, 183 (1989).

[2] B.E. Smart, *Chemistry of Organic Fluorine Compounds*, edited by M. Hudlicky and A.E. Pavlath, (ACS, Washington, 1995) Chapter 6.

[3] S.R. Cain, F.D. Egitto and F. Emmi, J. Vac. Sci. Technol. **A5**, 1578 (1987).

[4] I. Tepermeister, H.H. Sawin, J. Vac. Sci. Technol. **A10**, 3149 (1992).

[5] J. Hopkins and J.P.S. Badyal, J. Phys. Chem. **99**, 4261(1995).

[6] T. Yasuda, K. Yoshida and T. Okuno, J. Polym. Sci; Polym. Phy. **26**, 2061 (1988).

[7] J. Hopkins and J.P.S. Badyal, Macromolecules **27**, 5498 (1994).

[8] E.C. Onyiriuka, J. Vac. Sci. Technol. **A11**, 2941 (1993).

[9] T. Yasuda, T. Okuno, M. Miyama and Y. Yasuda, J. Polym. Sci; Polym. Chem. **32**, 1829 (1994).

[10] Y. Khairallah, F. Khonsari-Arefi and J. Amouroux, Thin Solid Films **241**, 295 (1994).

[11] F. Emmi, F.D. Egitto and L.J. Matienzo, J. Vac. Sci. Technol. **A9**, 786 (1991).

[12] R. D'Agostino, F. Cramarossa and S. DeBenedictis, Plasma Chem. and Plasma Process. **2**, 213 (1982).

[13] Y. Khairallah, F. Khonsari-Arefi and J. Amouroux, Pure and Appl. Chem. **66**, 1353 (1994).

[14] M. Strobel, S. Corn, C.S. Lyons and G.A. Korba, J. Polym. Sci; Polym. Chem. **23**, 1125 (1985).

[15] E. Krentsel, S. Fusselman, H. Yasuda, T. Yasuda and M. Miyama, J. Polym. Sci; Polym. Chem. **32,** 1839 (1994).

[16] T. Momose, T. Takada and S. Okazaki, Proceedings of the ACS Division of Polymeric Materials: Science and Engineering, Spring Meeting, Denver, Colorado, **56**, 236 (1987).

[17] M. Klausner, I.H Loh, R F Baddour and R.E. Cohen, Proceedings of the ACS Division of Polymeric Materials: Science and Engineering, Spring Meeting, Denver, Colorado, **56**, 227 (1987).

[18] M. Strobel and C.S. Lyons, Proceeedings of the ACS Division of Polymeric Materials: Science and Engineering, Spring Meeting, Denver, Colorado, **56**, 232 (1987).

[19] I.C. Plumb and K.R. Ryan, Plasma Chem. and Plasma Process. **6**, 11 (1986).

[20] B. LaMontagne, O.M. Kuttel and M.R. Wertheimer, Can. J. Phys. **69**, 202 (1991).

[21] J. H. Holloway, *Noble Gas Chemistry* (Metheun, London, 1968) 108.

[22] H.F. Winters and J.W. Coburn, Appl. Phys. Lett. **34**, 70 (1979).

[23] V.S. Aliev, M.R. Baklanov and V.I. Bukhtiyarov, Appl. Surf. Sci. **90**, 191 (1995).

[24] H.F. Winters, J. Vac. Sci. Technol. **B1,** 927 (1983).

[25] Y-Y. Tu, T.J. Chaung and H.F. Winters, Phys. Rev. **B23**, 823 (1981).

[26] H.F. Winters and D. Haarer, Phys. Rev. **B36**, 6613 (1987).

[27] H.F Winters and F.A. Houle, J. Appl. Phys. **54**, 1218 (1983).

[28] M.M. Hills and G.S. Arnold, Appl. Surf. Sci. **47**, 77 (1991)

[29] A.M. Barklund and H.-O. Blom, J. Vac. Sci. Technol. **A11**, 1226 (1993).

[30] V.V. Bardin and Y.L Yagupolskii, *New Fluorinating Agents in Organic Synthesis*, eds L. German and S. Zemskov, (Springer-Verlag, Berlin, 1989) Chapter 1.

[31] M. Hudlicky, *Chemistry of Organic Fluorine Compounds* (Ellis Horwood Ltd., England, 1976) 2nd edition.

[32] M. Tius, Tetrahedron **51**, 6605 (1995).

[33] A.G. Shard, H.S. Munro and J.P.S. Badyal, Polym. Commun. **32**, 152 (1991).

[34] J.F. Evans, J.H. Gibson, J.F. Moulder, J.S. Hammond and H. Goretzki, Fresenius Z. Anal. Chemie, **319**, 841 (1984).

[35] G. Beamson and D.Briggs, *High Resolution XPS of Organic Polymers. The Scienta ESCA300 Database* (John Wiley and Sons, Chichester, 1992).

[36] D.T. Clark, D.B. Adams, A. Dilks, J. Peeling and H.R. Thomas, J. Electron. Spec. **18**, 51 (1976).

[37] D.T. Clark and D. Shuttleworth, J. Polym. Sci; Polym. Chem. Ed. **18**, 27 (1980).

CHAPTER 5

VUV ENHANCED XeF_2 FLUORINATION OF POLYMER SURFACES

5.1 INTRODUCTION

Fluorination of polymer surfaces is a highly effective means for improving water repellency without altering the underlying bulk properties of the substrate.[1,2] A number of different approaches have been utilised in the past to achieve this goal, these include: direct reaction with F_2;[3] conventional solution phase polymerisation of fluoromonomers to produce fluoropolymer coatings;[4] chemical derivatisation of functional groups located at the surface;[5,6] electrical discharge fluorination using fluorine containing gases e.g. CF_4;[7,8] plasma polymerisation of fluoromonomers;[9,10] and sputter deposition of fluorocarbon layers from a PTFE target.[11,12] All of these techniques suffer from some type of drawback: the use of solvents, hazardous gases, expensive vacuum apparatus, etc.

In the previous chapter XeF_2 electrical discharges were used to fluorinate polymer surfaces. This chapter describes another new approach, based on VUV-assisted xenon difluoride (XeF_2) fluorination. XeF_2 is potentially a useful reagent, since it exists as a solid at room temperature and is therefore easily transportable; it also offers the benefit of forming chemically inert xenon as the major waste product species upon reaction. Polyethylene and polystyrene were chosen as substrates. Both polymers have a straight chain hydrocarbon backbone, with the latter also containing pendant phenyl rings; this combination allows a comparison to be made of the relative susceptibilities of saturated versus unsaturated substrates towards VUV-assisted surface fluorination.

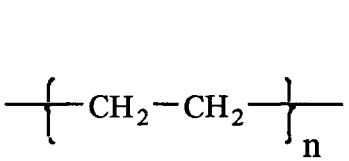

Polyethylene

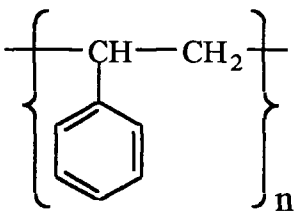

Polystyrene

5.2 EXPERIMENTAL

Small pieces of additive-free low density polyethylene (ICI) and polystyrene (Huntsman), were ultrasonically washed in a 50 : 50 solvent mixture of isopropyl alcohol and hexane for 30 s and dried in air. Oxygen (BOC, 99.6%), nitrogen (BOC, 99.9 %), argon (BOC 99.9 %), krypton (Spectra gases, 99.9 %) and xenon (Spectra gases 99.9 %) were employed as feed gases for generating the various VUV emission lines, in conjunction with a 13.56 MHz inductively coupled cylindrical plasma reactor (diameter 5 cm, volume 500 cm^3, base pressure of 6 x 10^{-3} mbar and a leak rate of better than 2 x 10^{-5} cm^3s^{-1}) enclosed in a Faraday cage.[13] This VUV radiation source was attached via a lithium fluoride window (cut-off wavelength below 104 nm[14,15]) to a gas exposure chamber, Figure 5.1. All joints were grease free. A typical experimental run comprised placing a strip of polymer 1 cm away from the LiF window, and evacuating both sides of the apparatus to base pressure. XeF_2 (99%, Fluorochem) contained in a heated steel reservoir (80 °C) was introduced into the fluorination chamber via a fine control leak valve at a pressure of 0.1 mbar, whilst at the same time the electrical discharge feed gas was released into the other side at 0.1 mbar pressure. After allowing 5 mins for purging, the plasma was ignited at 20 W for 5 mins. Upon termination of VUV exposure, XeF_2 was allowed to continue to pass over the substrate surface for a further 5 mins. Next the reactor was evacuated back down to base pressure and then vented to air. Any potential loss in transmission of the LiF window during VUV exposure was routinely checked by running a control experiment (VUV-assisted fluorination of polyethylene).

X-ray photoelectron spectroscopy (XPS) characterisation prior to and following surface modification was carried out using a Kratos ES300 electron spectrometer equipped with a Mg Kα X-ray source (1253.6 eV) and a concentric hemispherical electron analyser operating in the fixed retarding ratio mode (FRR, 22:1). XPS spectra were accumulated on an interfaced PC computer. C(1s) envelopes were fitted with Gaussian peaks having equal full-width-at-half-maximum (FWHM)[16] using a Marquardt minimisation computer program. Instrumentally determined sensitivity factors were taken as being C(1s) : O(1s) : F(1s) equals 1.00 : 0.55 : 0.67.

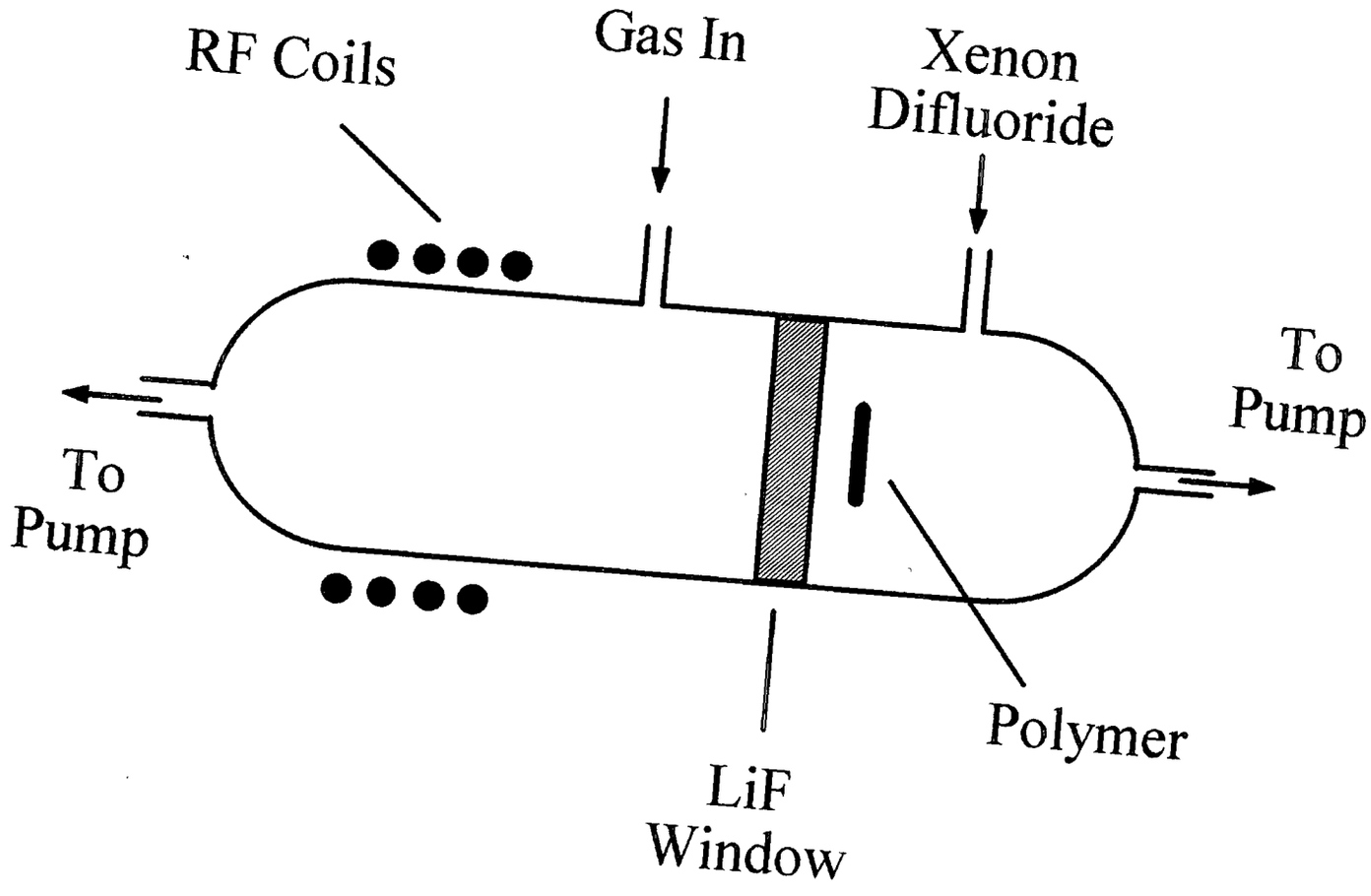

Figure 5.1: Apparatus used for VUV assisted XeF_2 fluorination.

5.3 RESULTS

The C(1s) XPS spectrum for untreated polyethylene (PE) comprises a single peak at 285.0 eV corresponding to -$\underline{C}_xH_y$-, Figure 5.2(a). Polystyrene (PS) displayed an additional π-π^* shake-up satellite feature at 291.6 eV,[17,18] Figure 5.2(b). Control experiments, where XeF_2 was passed over the polymer substrates indicated that very little surface fluorination took place in the absence of VUV irradiation (F:C ratio = 0.11 $\pm$ 0.01 for polyethylene, and 0.16 $\pm$ 0.01 for polystyrene).

C(1s) spectra acquired following 5 min exposure of the polymer surfaces to XeF_2 in the presence of VUV irradiation revealed a significant enhancement in fluorination, Figure 5.2. The C(1s) envelopes could be fitted with the following carbon functionalities: $\underline{C}_xH_y$ at 285.0 eV, $\underline{C}$-CF_n at 286.6 eV, $\underline{C}F$ at 287.8 eV, $\underline{C}F$-CF_n at 289.3 eV, $\underline{C}F_2$ at 291.2 eV and $\underline{C}F_3$ at 293.3 eV;[3,19,28] also the π-π^* shake-up satellite at 291.6 eV was still discernible for XeF_2 fluorination of polystyrene in the presence of VUV irradation emitted by O_2 and N_2 plasmas, Table 5.1. A corresponding variation in the F:C ratios was also noted, with the noble gases causing the greatest level of fluorination, Table 5.1 and Figure 5.3. Furthermore, polystyrene was found to be more susceptible towards VUV assisted XeF_2 fluorination compared to polyethylene for all the electrical discharge feed gases apart from Xe (where similar levels were obtained). A small amount of oxygen incorporation at the surface (~3 %) could be found as a result of reaction between trapped free radicals and the atmosphere during sample transfer from the VUV irradiation chamber to the XPS spectrometer.[19]

A comparative study where XeF_2 was replaced with CF_4 led to no fluorination for any of the VUV electrical discharge sources. This absence of reaction can be attributed to CF_4 only absorbing at wavelengths below the LiF window cut-off of 104 nm[20,21] (the VUV absorption cross-section of CF_4 is very small at $\lambda > 110$ nm).[21]

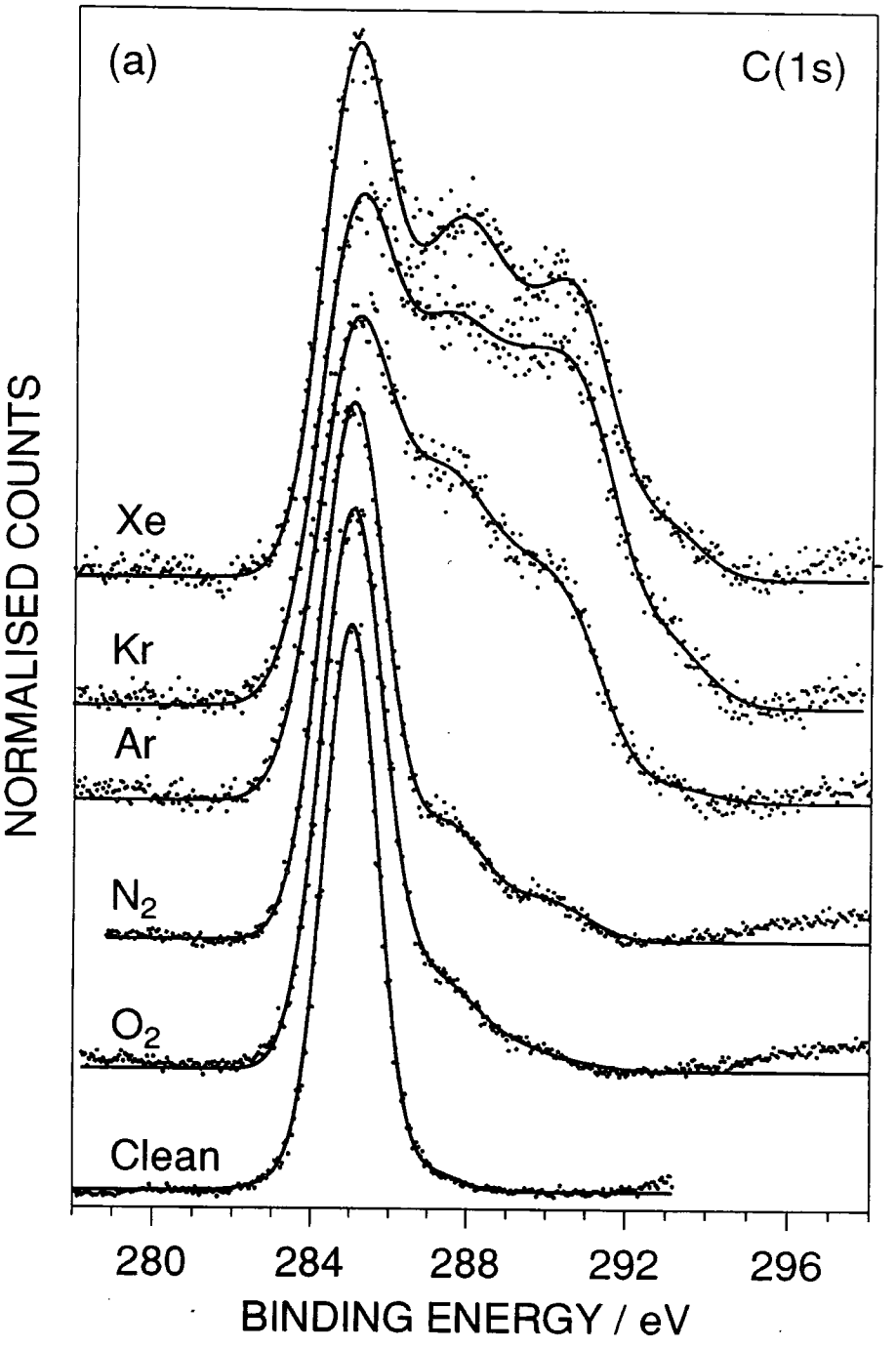

Figure 5.2(a): C(1s) XPS spectra taken following VUV assisted XeF_2 fluorination of polyethylene.

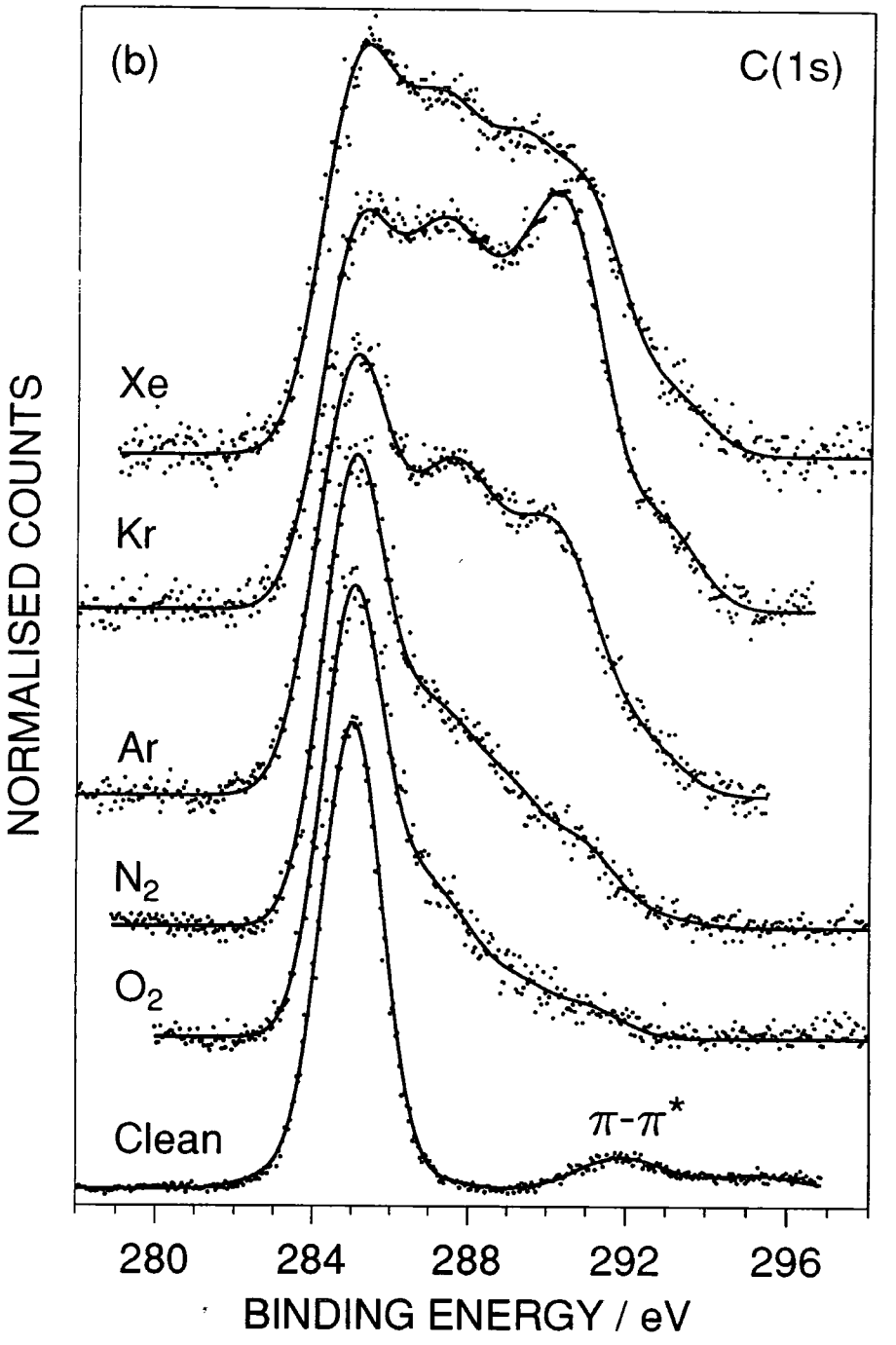

Figure 5.2(b): C(1s) XPS spectra taken following VUV assisted XeF_2 fluorination of polystyrene.

VUV Gas	Percentage Carbon Functionalities (± 0.5 %)						F:C RATIO ± 0.03
	$\underline{C}_x$-H_y	$\underline{C}$-CF_n	$\underline{C}F$	$\underline{C}F$-CF_n	$\underline{C}F_2$	$\underline{C}F_3$	
O_2	78.6	9.3	8.1	2.9	0.96	0	0.13
N_2	73.0	7.8	12.2	4.2	2.9	0	0.29
Ar	39.0	15.5	18.2	13.4	12.8	1.3	0.76
Kr	35.8	13.8	19.6	18.2	20.3	4.5	0.86
Xe	36.2	12.9	18.8	13.5	15.9	2.7	0.82

Table 5.1(a): Summary of XeF_2 fluorination treatments for polyethylene.

VUV Gas	Percentage Carbon Functionalities (± 0.5 %)							F:C RATIO ± 0.04
	$\underline{C}_x$-H_y	$\underline{C}$-CF_n	$\underline{C}F$	$\underline{C}F$-CF_n	$\underline{C}F_2$	$\underline{C}F_3$	π-π^*	
O_2	61.0	16.2	11.4	6.6	3.3	0	1.5	0.29
N_2	49.8	16.2	14.1	11.5	7.0	1.6	1.0	0.48
Ar	32.4	16.2	16.5	13.6	17.0	4.2	0	0.86
Kr	24.1	15.0	17.3	14.9	23.0	5.8	0	1.03
Xe	31.8	15.5	15.5	13.4	20.6	5.9	0	0.81

Table 5.1(b): Summary of XeF_2 fluorination treatments for polystyrene.

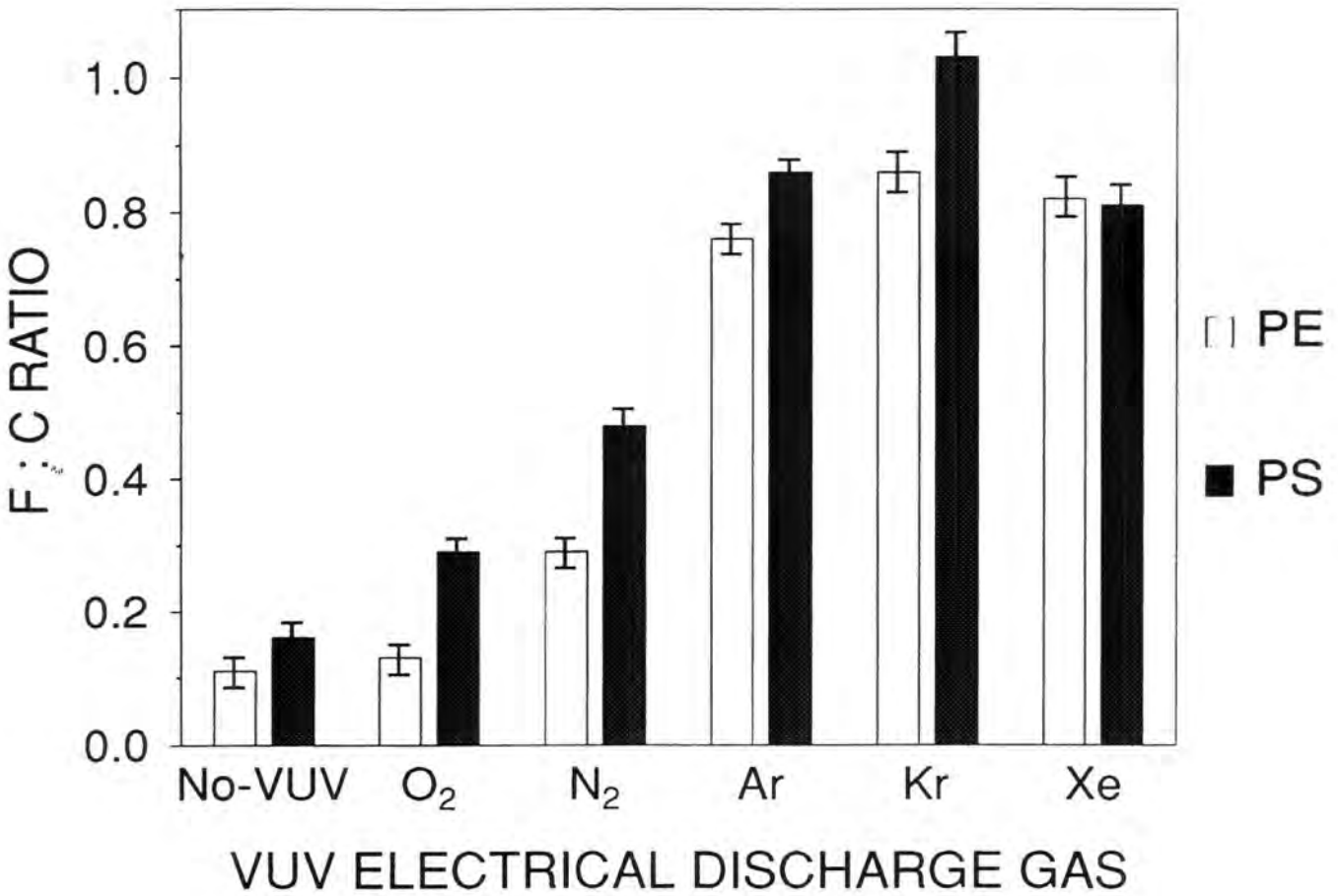

Figure 5.3: XPS F:C ratios for VUV assisted XeF_2 fluorination of polyethylene and polystyrene.

DISCUSSION

Photo-assisted XeF_2 etching of silicon has been extensively studied in the past.[22,23,24,25,26] XeF_2 spontaneously reacts with silicon to form a fluorosilyl layer accompanied by the loss of SiF_4. Concurrent VUV irradiation is found to enhance the rate of silicon etching (greatest efficiency occurring at wavelengths below 120 nm).

In the present study with polymer substrates, VUV wavelengths greater than 104 nm are transmitted by the LiF window.[14,15] The strongest VUV emission lines for the noble gas plasmas are the M(I) series,[15,27] (where M is the noble gas atom); these correspond to the transition between the lowest lying excited electronic state and the ground state of each atom (e.g. Ar $3s^23p^54s^1$ to $3s^23p^6$).[28] Less intense M(II) lines are also emitted arising from transitions between the lowest lying excited singly ionised state and its ground state (e.g. Ar^+ $3s3p^6$ to $3s^23p^5$). Any accompanying UV and visible radiation produced by these glow discharges is at least two orders of magnitude lower in intensity.[27] The emission spectrum associated with low pressure N_2 plasmas is dominated by the atomic lines N(I) at 174 and 149 nm,[27,29] whilst O_2 glow discharges emit a strong O(I) line at 130 nm.[27,30,31] In both of these cases, the VUV flux is at least a factor of 10 lower in intensity compared to the noble gas plasmas under similar experimental conditions,[27] Table 5.2.

VUV irradiation during exposure of the polymer substrates to XeF_2 gas leads to an enhancement in surface fluorination, Table 5.1 and Figure 5.3. The degree of overlap between the VUV emission lines and the absorption characteristics of both the polymer substrate and XeF_2 gas can help to explain the observed variations in surface modification, Figure 5.4. In all cases, the transmitted VUV radiation is capable of σ-σ^* alkyl chain excitation (i.e. $\lambda < 160$ nm[32]) to produce free radical centres in the near-surface region of the polymer;[33] this activated surface can subsequently react with incident XeF_2 molecules. The greater intensity of the noble gas VUV emission lines[27] will lead to more reactive sites, and thereby a greater level of fluorination.

Gas	M I emission lines / nm	M II emission lines / nm
O_2	130	-
N_2	149	-
	174	-
Ar	104.8	-
	106.7	-
Kr	116.5	-
	123.6	-
Xe	131.2	110
	147.0	124.5

Table 5.2: Strongest vacuum UV emission lines transmitted through the LiF window (cut-off at 104 nm).[36]

The absorption spectrum of XeF_2 in the VUV region is well documented;[34,35,36,37] it comprises a broad feature due to intravalence excitations i.e. $10\sigma_g$ - $7\sigma_u$ (maximum absorption at around 158 nm), and several progressions of sharp Rydberg transitions towards shorter wavelengths i.e. $5\pi_{u\,3/2}$ - $6sR$ at 145 - 141 nm, $5\pi_{u\,1/2}$ - $6sR$ at 136 - 132 nm, $5\pi_{u\,3/2}$ - $5d_\sigma R$ at 124 - 120 nm, $5\pi_{u\,1/2}$ - $5d_\sigma R$ at 117 - 114 nm, $5\pi_{u\,3/2}$ - $7sR$ at 116 - 112 nm, $10\sigma_g$ - $6p_\sigma R$ at 115 - 112 nm, $5\pi_{u\,3/2}$- $6dR$ at 110 - 108 nm, and $5\pi_{u\,3/2}$ - $8sR$ at 108 - 106 nm.[36] Formation of atomic fluorine via photo-excitation and dissociation of XeF_2 in the 180 - 105 nm VUV range can be summarised as follows:[36]

$$XeF_2 \text{ — } h\upsilon \longrightarrow XeF + F$$

$$XeF \longrightarrow Xe + F \text{ (fast)}$$

The XeF fragment dissociates quickly, since it is very weakly bound.[36] The Xe + F_2 product is not formed because the two F atoms are too far apart (~400 pm) in ground state.[36] The noble gas M(I) VUV emission lines, Ar (106.7 nm), Kr (116.5 nm), and Xe (147.0 nm) overlap with the $5\pi_{u\,3/2}$ - $8sR$, $5\pi_{u\,1/2}$ - $5d_\sigma R$, and 10s - $7\sigma_u$(broad band)

absorption features of XeF_2 respectively. The relative absorption cross sections of XeF_2 in these regions[35] and the relative intensities of the noble gas VUV emission lines[28] may explain the observed fluorination ranking of Kr > Xe > Ar VUV exposures. The minor ion-pair dissociation channel:

$$XeF_2 \text{ — } h\upsilon \longrightarrow XeF^+ + F^-$$

commences at excitation wavelengths below 129 nm,[36] and therefore overlaps with the onset of photoionisation of the polymer backbone (λ < 120 nm, where the photoabsorption cross-section increases by 100-fold).[32] Hence, ionic reactions between F^- and positively charged sites at the polymer surface can also occur for the noble gas VUV radiation sources. The slightly greater level of fluorination obtained for VUV exposure from a N_2 discharge compared to an O_2 plasma source might also be due to how well the VUV lines coincide with XeF_2 absorption regions: the N(I) line at 149 nm overlaps with the tail of the 10s - $7\sigma_u$ broad valence band for XeF_2, whereas, the O(I) line does not overlap with any of the XeF_2 absorption features and can therefore only give rise to indirect reaction via photo-activation of the polymer surface.

Extended Huckel molecular orbital calculations predict highly favourable energetics for the reaction of atomic fluorine with unsaturated >C=C< bonds compared to saturated bonds.[38] Clearly, fluorine addition across a >C=C< double bond will produce a greater rise in F:C ratio compared to fluorine substitution of a C-H bond. This explains the greater susceptibility of polystyrene compared to polyethylene towards fluorination. Furthermore, π-π^* photo-excitation of the pendant phenyl rings in polystyrene by the weak UV component of the electrical discharges (at λ < 280 nm)[33] will lead to a greater concentration of reactive free radical sites.

Some potential advantages of VUV assisted XeF_2 fluorination surface modification over other fluorination techniques include the capability of operating at atmospheric pressure (by using a weakly absorbing carrier gas for XeF_2), as well as circumventing the need for solvents or F_2 gas. Also, VUV-assisted XeF_2 fluorination could be used in conjunction with a mask to perform photolithography.

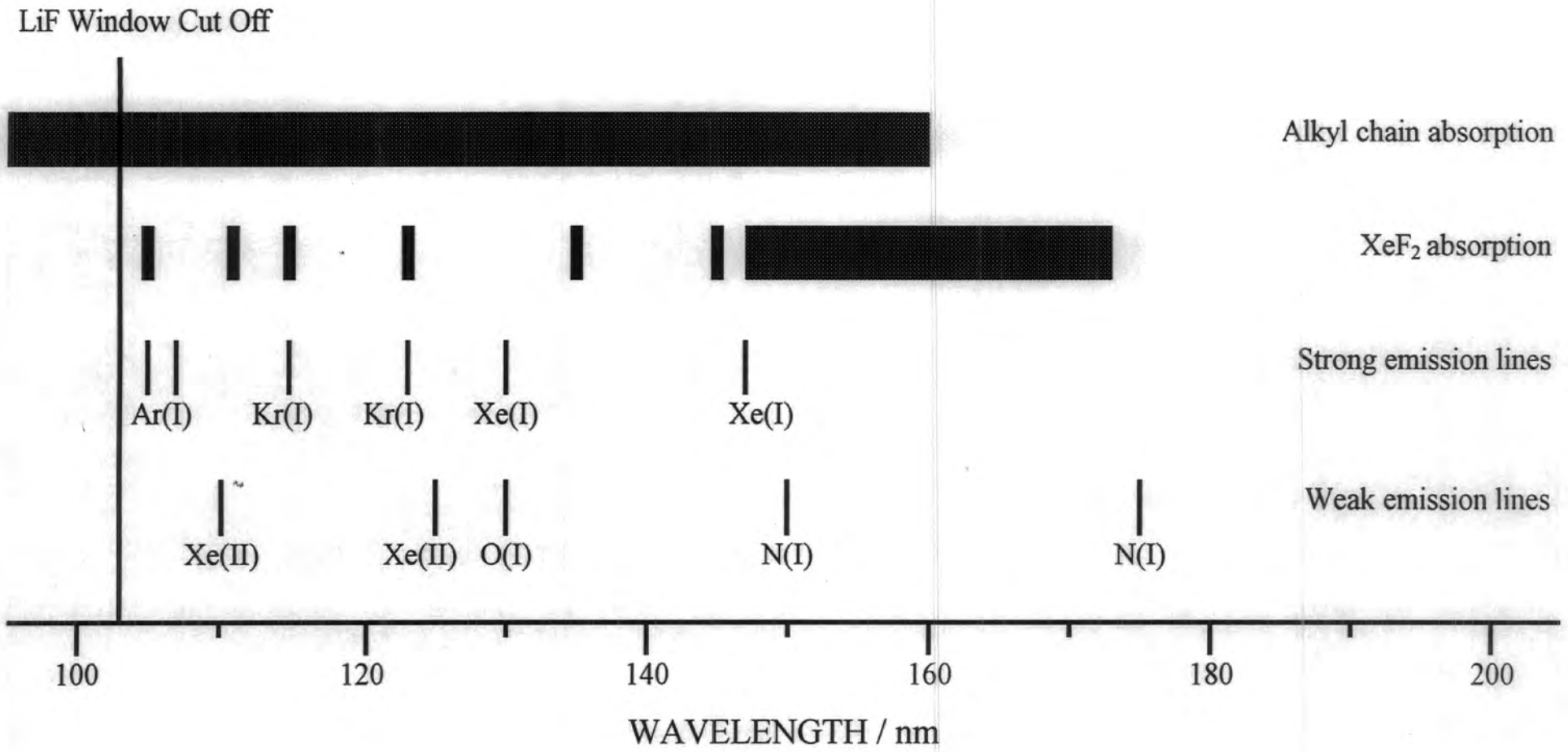

Figure 5.4: Summary of characteristic VUV emission lines and absorption features.

CONCLUSIONS

This work has shown that vacuum ultraviolet irradiation can be used to enhance the XeF_2 fluorination of polymer surfaces. The extent of reaction is governed by the overlap of the incident VUV emission lines with both the absorption characteristics of the polymer backbone and the XeF_2 gas. Surface modification is found to be greatest for VUV lines emitted by noble gas plasmas. Unsaturated >C=C< bonds contained within the polymer structure are more susceptible towards fluorination compared to saturated C-H bonds.

REFERENCES

[1] F. Arefi, P.M. Rahamati, V. Andre, and J. Amouroux, J. Appl. Polym. Sci. Appl. Polym. Symp. **46**, 33 (1990).

[2] F. Arefi, V. Andre, P.M. Rahamati and J. Amouroux, Pure Appl. Chem. **64**, 715 (1992).

[3] D.T. Clark, W.J. Feast, W.K.R. Musgrove and I. Ritchie, J. Polm. Sci. Polym. Chem. **13**, 857 (1975).

[4] W.W. Schmiegel, *Chemistry of Organic Fluorine Compounds*, eds M. Hudlicky and A.E. Pavlath, (ACS, Washington, 1995) Chapter 7.

[5] D.S. Everhart and C.N. Rielley, Anal. Chem. **53**, 665 (1981).

[6] R.H. Popat, I. Sutherland and E-S. Shang, J. Mater. Chem. **5**, 713 (1995).

[7] R. d'Agostino, F. Cramarossa and S. DeBenedictis, Plasma Chemistry and Plasma Processing, **2**, 213 (1982).

[8] J. Hopkins and J.P.S. Badyal, J. Phys. Chem. **99**, 4261 (1995).

[9] A. Hynes, M.J. Shenton and J.P.S. Badyal, Macromolecules, **29**, 18 (1996).

[10] D.T. Clark and D. Shuttleworth, J. Polym. Sci. Polym. Chem. **18**, 27 (1980).

[11] L. Holland, H. Beiderman and S.M. Ojha, Thin Solid Films, **35**, L19 (1976).

[12] M.E. Ryan, J.L.C. Fonseca, S. Tasker and J.P.S. Badyal, J. Phys. Chem. **99**, 4261 (1995).

[13] J. Hopkins, S.H. Wheale and J.P.S. Badyal J. Phys. Chem. **100**, 14062 (1996).

[14] G. Schonhense and U. Heinzmann, J. Phys. E. Sci. Instrum. **16**, 74 (1983).

[15] H. Okabe, Journal of the Optical Society of America, **54**, 478 (1964).

[16] J.F. Evans, J.H. Gibson, J.F. Moulder, J.S. Hammond and H. Goretzki, Fresenius Z. Anal. Chemie, **319**, 841 (1984).

[17] G. Beamson and D.Briggs, *High Resolution XPS of Organic Polymers. The Scienta ESCA300 Database* (John Wiley and Sons, Chichester 1992).

[18] D.T. Clark, D.B. Adams, A. Dilks, J. Peeling and H.R. Thomas, J. Electron. Spec. **18**, 51 (1976).

[19] M. Strobel and C.S. Lyons, Proceeedings of the ACS Division of Polymeric Materials: Science and Engineering, Spring Meeting, Denver, Colorado, **56**, 232 (1987).

[20] J.C. Creasey, P.A. Hatherly, I.R. Lambert and R.P. Tuckett, Chem. Phys. Lett. **188**, 223 (1992).

[21] L.C. Lee, X. Wong and M. Suto, J. Chem. Phys. **85**, 6294 (1996).

[22] F.A. Houle, J. Chem. Phys. **79**, 4237 (1983).

[23] U. Streller, B. Li, A. Krabbe and N. Schwentner, Appl. Surf. Sci. **96-98**, 448 (1996).

[24] B. Li, U. Streller, H-P. Krause, I. Twesten and N. Schwentner, J. Appl. Phys. **77**, 350 (1995).

[25] U. Streller, A. Krabbe and N. Schwentner, Appl. Surf. Sci. **106**, 341-346 (1996).

[26] F.A. Houle, J. Chem. Phys. **80**, 4851 (1984).

[27] J.A.R. Samson, *Techniques of Vacuum Ultraviolet Spectrscopy*. (John Wiley, London 1967) Chapter 5.

[28] D.T. Clark and A. Dilks, J. Polym. Sci. **18**, 1233 (1980).

[29] A.G. Shard and J.P.S. Badyal, Polym. Commun. **32**, 217 (1991).

[30] A.F. Whitaker and B.Z. Jang, SAMPE Journal, **30**, 30 (1994).

[31] A. Hollander, J.E. Klemberg-Saphieha and M.R. Wertheimer, J. Polym. Sci. Polym. Chem, **33**, 2013 (1995).

[32] R.H. Patridge. J. Chem. Phys. **45**, 1688 (1966).

[33] J.F. McKellar and N.S. Allen, *Photochemistry of Man-made Polymers*, (Applied Science, London 1979)

[34] F.J. Comes, R. Haensel, U. Nielson and W.H.E. Schwarz, J. Chem. Phys. **58**, 516 (1973).

[35] U. Nielson and W.H.E. Schwarz, Chem. Phys. **13**, 195 (1976).

[36] M. Kono and K. Shobatake, J. Chem. Phys. **102**, 5966 (1995).

[37] G. Black, R.L. Sharpless, D.C. Lorents, D.L. Hustis, R.A. Gutcheck, T.D. Bonifield, D.A. Helms and G.K. Walter, J. Chem. Phys. **75**, 4840 (1981).

[38] S.R. Cain, F.D. Egitto and F. Emmi, J. Vac. Sci. Technol. **A5**, 1578 (1987).

CHAPTER 6

SURFACE OXIDATION OF DIFFERENT TYPES OF RUBBER

6.1 INTRODUCTION

Numerous studies have been devoted to the oxidation of polymer surfaces.[1-13] However, little work has been undertaken on the plasma surface modification of the polymers classed as rubbers. The starting material for rubber is a macromolecular substrate which is amorphous at room temperature, has a glass transition considerably below ambient temperature and can be crosslinked to form network structures.[14] These crosslinked polymer networks are given the name "rubber" as they exhibit elastic behaviour i.e. can be stretched easily but return to their original shape and length on removal of the tension.[14]

Rubbers are materials without which modern technology would be unthinkable; it is one of the main components used in tyres, shoe soling, cable insulation, food packaging, etc.[14,15] The annual consumption of rubber amounts to 13 million tonnes, about one third of which is natural rubber and the other two thirds is produced synthetically.[14] In order to achieve the range and level of properties required of the rubber other substances need to be added, e.g. fillers, antioxidants and reinforcers. The compound composition and production processes also have an effect on the properties of the rubber.

It is important that the susceptibility of these polymers to weathering is known as half the annual tonnage of rubbers is employed outdoors.[14] The main source of rubber degradation is attack by oxygen (especially ozone) in the presence of sunlight.[14,15] Artifical ageing processes are often used to simulate outdoor exposure e.g. ultraviolet radiation and ozone treatment.

This chapter compares the dielectric barrier discharge (also known as the silent discharge), the low pressure glow discharge and the ozone treatment of four of the main synthetic rubbers used today; ethylene propylene diene terapolymer (EPDM), butadiene acrylonitrile (NBR), styrene butadiene rubber (SBR) and chloroprene (CR). Both the industrial and additive-free (pure) forms were treated in order to evaluate the influence of the commercial additives.

EPDM

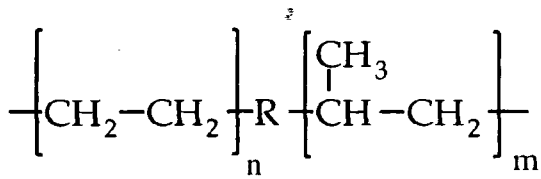

where m = 60, n = 30 and R = Diene

NBR

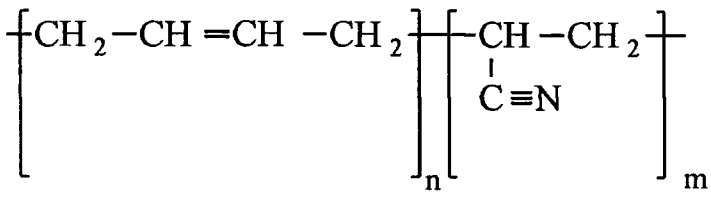

where m = 66 and n = 33

CR (Trans)

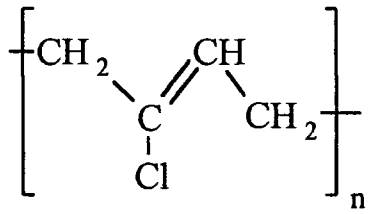

SBR

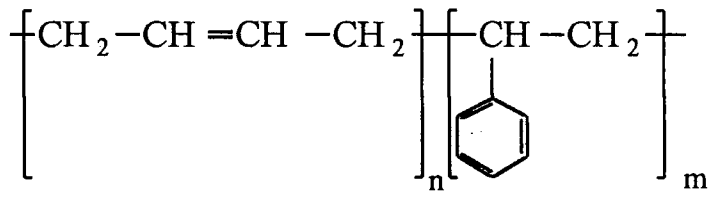

where m = 45 and n =55

6.2 EXPERIMENTAL SECTION

The industrial samples (supplied by the Danish Institute of Technology) were cut into small strips (0.5 x 2 cm), ultrasonically cleaned in a 50 : 50 mixture of toluene : hexane solvents for 30 s and left to dry overnight in air. Also additive-free poly(acrylonitrile-co-butadiene) 30-32 wt % acrylonitrile, poly(styrene-co-butadiene) 45 wt % styrene, poly(chloroprene) 10 % cis and poly(ethylene-co-propylene) 60 % ethylene were spun onto glass slides from a 2 % w/v toluene solution (all purchased from Aldrich). The additive free polymers were chosen to resemble as closely as possible the industrial monomer structures. Complete coverage of the substrate was checked using X-ray photoelectron spectroscopy to detect for the absence of the glass slide Si(2p) signal.

Low pressure glow discharge treatments were carried out in a electrodeless cylindrical reactor enclosed in a Faraday cage, see Figure 4.1. This was fitted with a gas

inlet, a thermocouple pressure gauge, and a two stage rotary pump attached to a liquid nitrogen trap. An impedance matching network was used to inductively couple a copper coil wound round the reactor to a 13.56 MHz radio frequency generator. All the joints were grease free. Before each experiment the reactor was scrubbed with detergent, rinsed with isopropyl alcohol, dried and then cleaned further using a 50 W air plasma for 30 min. A rubber sample was then inserted into the reactor and the system evacuated down to a base pressure of 4×10^{-3} mbar. Oxygen (99 9 % purity, BOC) was released into the chamber at a pressure of 0 2 mbar and left to purge for 10 mins. The glow discharge was then ignited at 10 W power for 30 s. After treatment, oxygen was allowed to continue to pass through the reactor for a further 10 mins, after which the whole system was let up to atmosphere.

Dielectric barrier discharge treatment (30 s) of each sample in air was carried out using a home-built parallel-plate dielectric barrier cell operating at 3 Hz, 11 kV, with an electrode gap of 3 mm.[1] Prior to each experiment, the electrodes were chemically polished and degreased using isopropyl alcohol.

For the ozone treatment of the samples, ozone was produced endothermically in a controlled manner from oxygen using UV radiation (Hampden ozone cabinet, model 803). An electrochemical cell was used to detect the quantity of ozone in the chamber. The additive-free and industrial samples were placed in the chamber simultaneously and the ozone concentration was increase steadily to 200 pphm (parts per hundred million) on ignition of the UV lamp.

A Kratos ES300 electron spectrometer equipped with a Mg Kα X-ray source (1253.6 eV) and a concentric hemispherical analyser was used to analyse the rubber surfaces by X-ray photoelectron spectroscopy (XPS). The fixed retarding ratio mode was used (22:1) and the XPS spectra were acquired on an interfaced PC computer. Instrumentally governed sensitivity factors were taken as C(1s) : O(1s) : S(2p) : N(1s) : Cl(2p) equals 1 : 0.55 : 0.54 : 0.74 : 0.42 respectively.

6.3 RESULTS

Wide-scan XPS spectra of the all the rubber samples showed that the major element present at the surface was carbon (hydrogen cannot be detected by XPS). The industrial samples and the pure NBR and SBR all contained oxygen even before treatment, Table 6.1. Both forms of NBR contained a small quantity of nitrogen, however, the industrial form contained less than expected from the monomer structure. The pure CR contained carbon and chlorine in proportions consistent with monomer structure (0.25), however, the industrial CR contained less chlorine. For the industrial SBR sulfur was present. The C(1s) XPS spectra for the pure and industrial forms are displayed in Figures 6.1 and 6.2 respectively; π-π^* shake-up for the untreated pure samples of NBR and CR was visible at 291.7 eV, Figures 6.1(b) and (c). This shake-up was not present for the pure SBR, however, an additional peak at 289.0 eV was observed, Figure 6.1(d).

During each of the three treatments all the rubber samples became oxidised and the O:C ratios for the samples were calculated, Table 6.1. Dielectric barrier discharge treatment gave the greatest level of oxidation for the additive-free polymers, Figure 6.3. However, the low pressure glow discharge treatment produced the largest O:C ratio for the industrial rubber samples, Figure 6.4.

In the case of the dielectric barrier discharge treated pure rubber samples, Figure 6.5, C(1s) XPS spectra were fitted with Gaussian peaks of equal full-width-half-maximum (FWHM),[16] using a Marquardt minimisation computer program. Energies distinctive of different types of oxidised moieties were referenced to the hydrocarbon peak (-$\underline{C}_xH_y$-) at 285.0 eV:[17] carbon adjacent to a carboxylate group ($\underline{C}$-CO_2) at 285.7 eV, carbon singly bonded to one oxygen atom ($\underline{C}$-O-) at 286.6 eV, carbon singly bonded to two oxygen atoms or carbon doubly bonded to one oxygen atom (-O-$\underline{C}$-O- / $\underline{C}$=O) at 287.9 eV, carboxylate groups (-O-$\underline{C}$=O) at 289.0 eV and carbonate groups (-O-$\underline{C}$O-O-) at 290.4 eV, (with cyano group at 286.6 eV for NBR and carbon bonded to chlorine C-Cl at 286.1 eV for CR). The percentage of each functionality was calculated, Table 6.2. The major group present for EPDM was C-O, for NBR, CR and SBR it was the C=O and O-C=O groups.

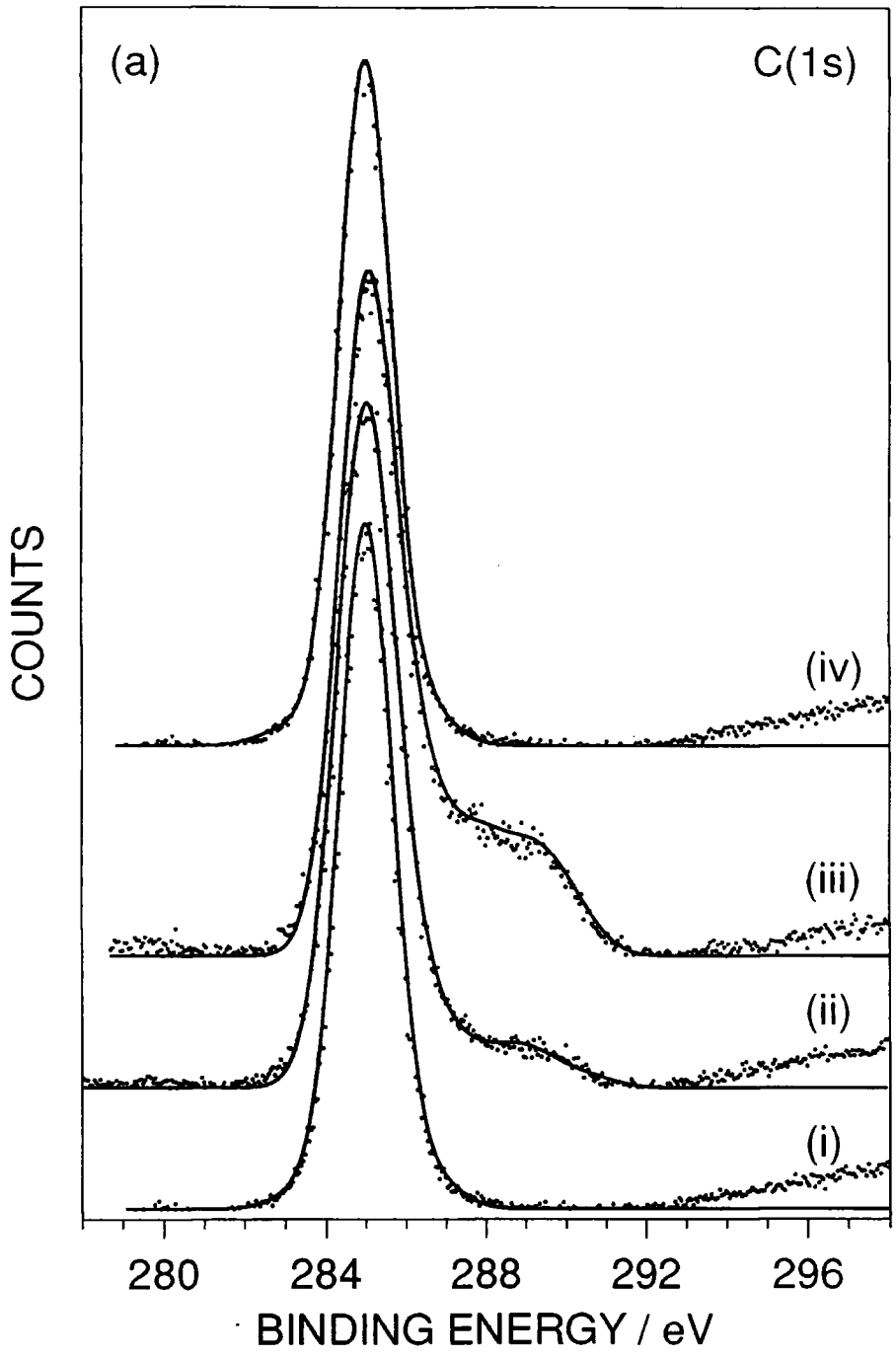

Figure 6.1(a): XPS C(1s) spectra for the following treatments of additive free EPDM: (i) clean: (ii) low temperature glow discharge 30 s; (iii) dielectric barrier discharge 30 s; and (iv) ozone treatment 4 hrs.

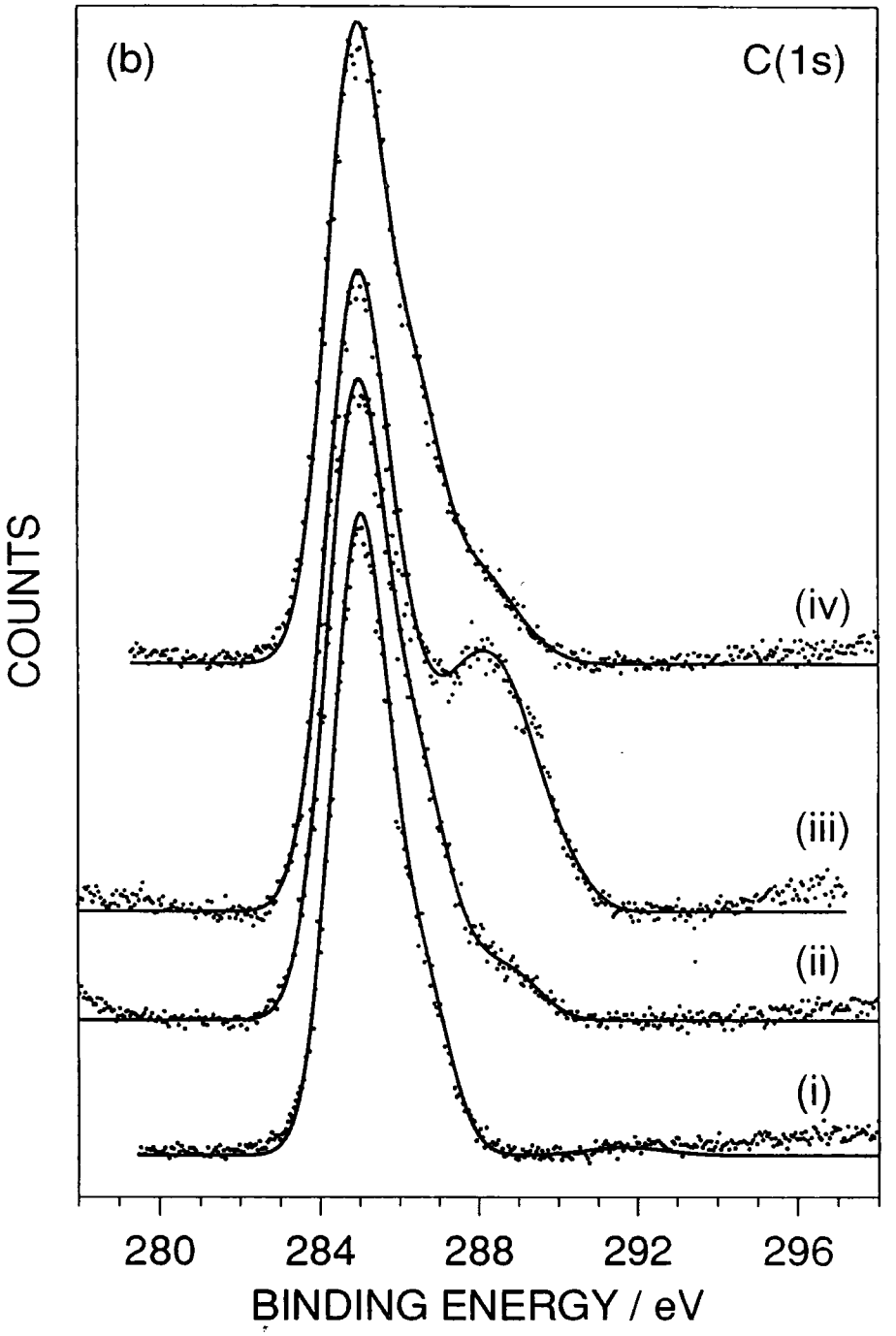

Figure 6.1(b): XPS C(1s) spectra for the following treatments of additive free NBR: (i) clean: (ii) low temperature glow discharge 30 s; (iii) dielectric barrier discharge 30 s; and (iv) ozone treatment 4 hrs.

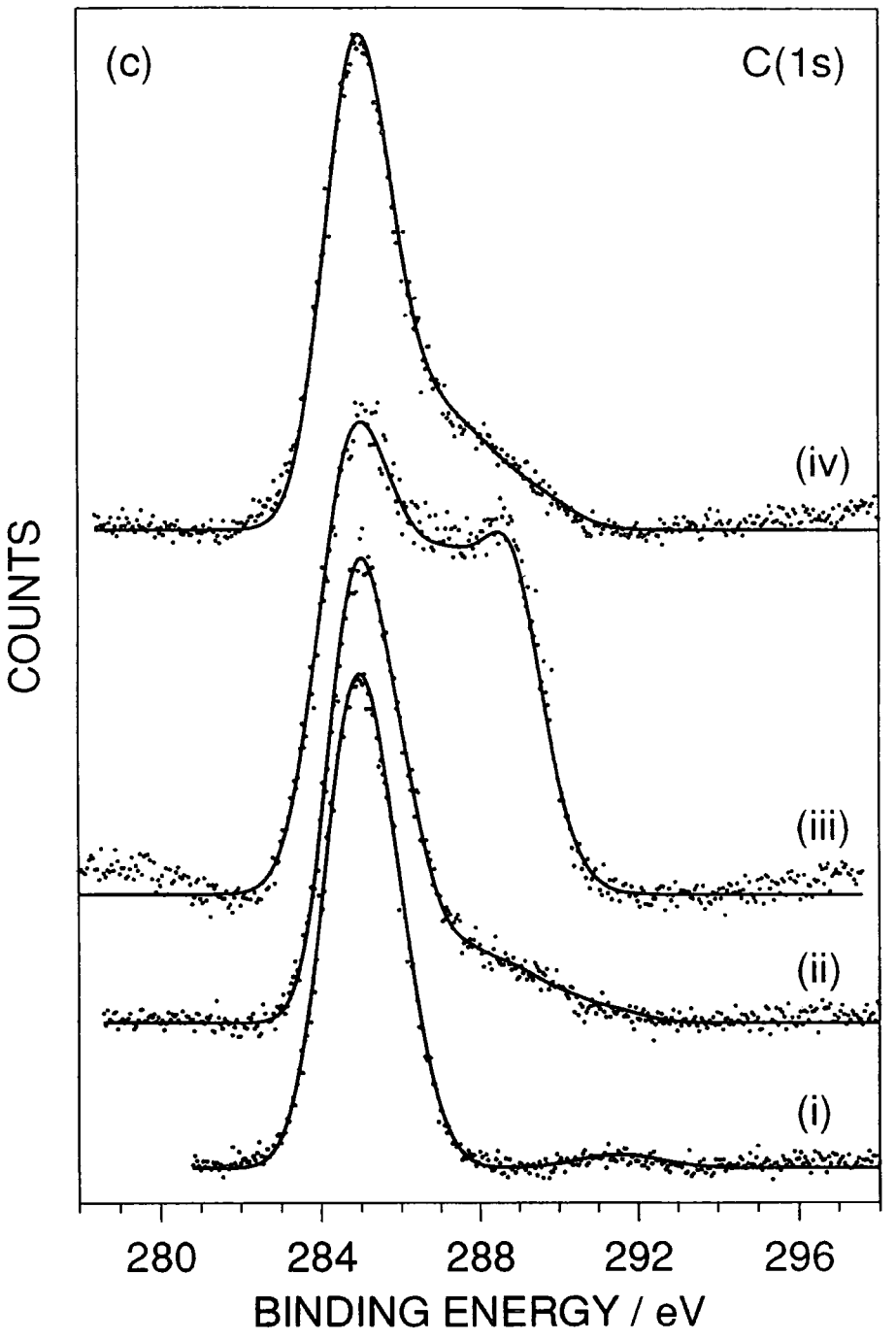

Figure 6.1(c): XPS C(1s) spectra for the following treatments of additive free CR: (i) clean: (ii) low temperature glow discharge 30 s; (iii) dielectric barrier discharge 30 s; and (iv) ozone treatment 4 hrs.

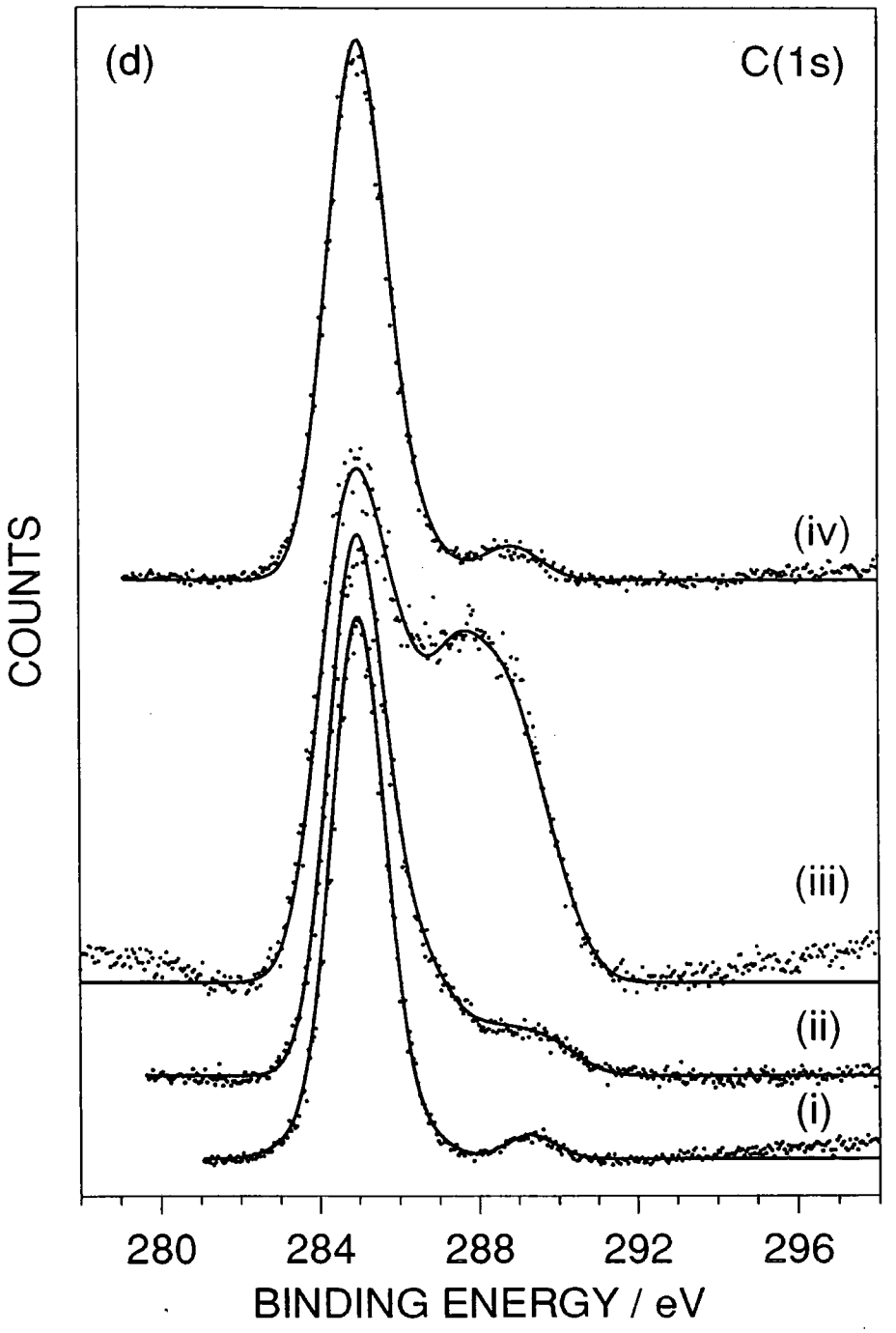

Figure 6.1(d): XPS C(1s) spectra for the following treatments of additive free SBR: (i) clean: (ii) low temperature glow discharge 30 s; (iii) dielectric barrier discharge 30 s; and (iv) ozone treatment 4 hrs.

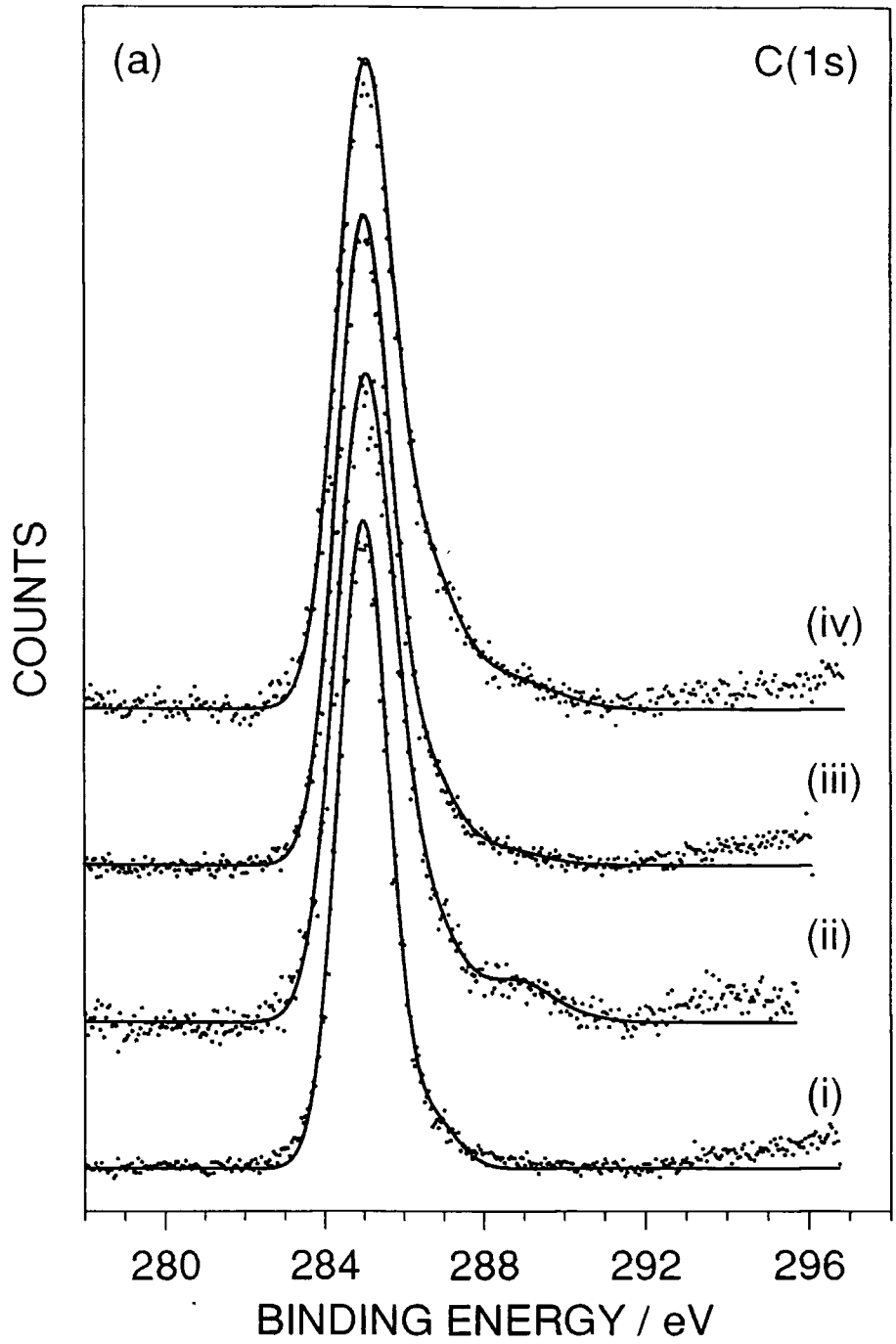

Figure 6.2(a): XPS C(1s) spectra for the following treatments of industrial EPDM: (i) clean: (ii) low temperature glow discharge 30 s; (iii) dielectric barrier discharge 30 s; and (iv) ozone treatment 4 hrs.

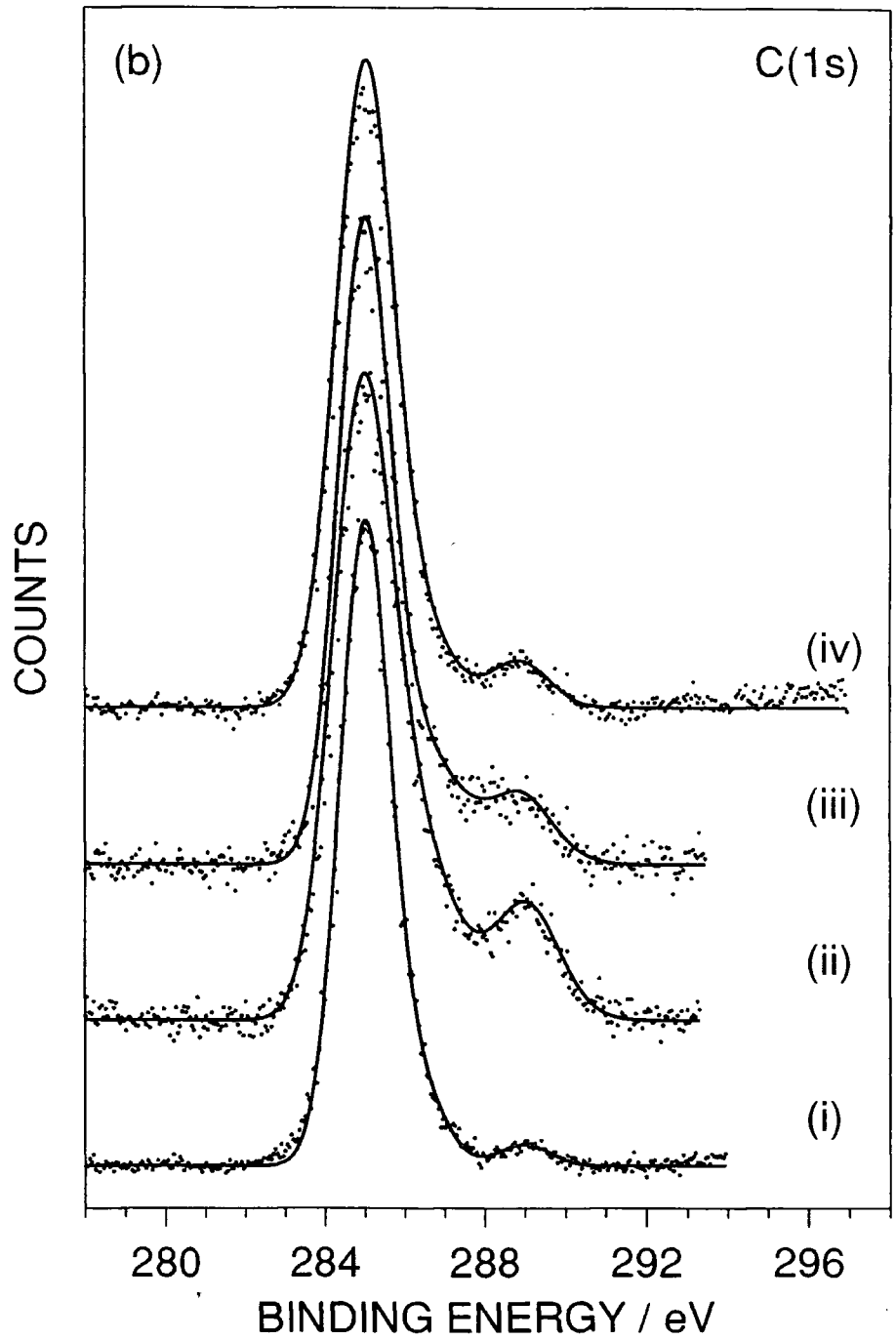

Figure 6.2(b): XPS C(1s) spectra for the following treatments of industrial NBR: (i) clean: (ii) low temperature glow discharge 30 s; (iii) dielectric barrier discharge 30 s; and (iv) ozone treatment 4 hrs.

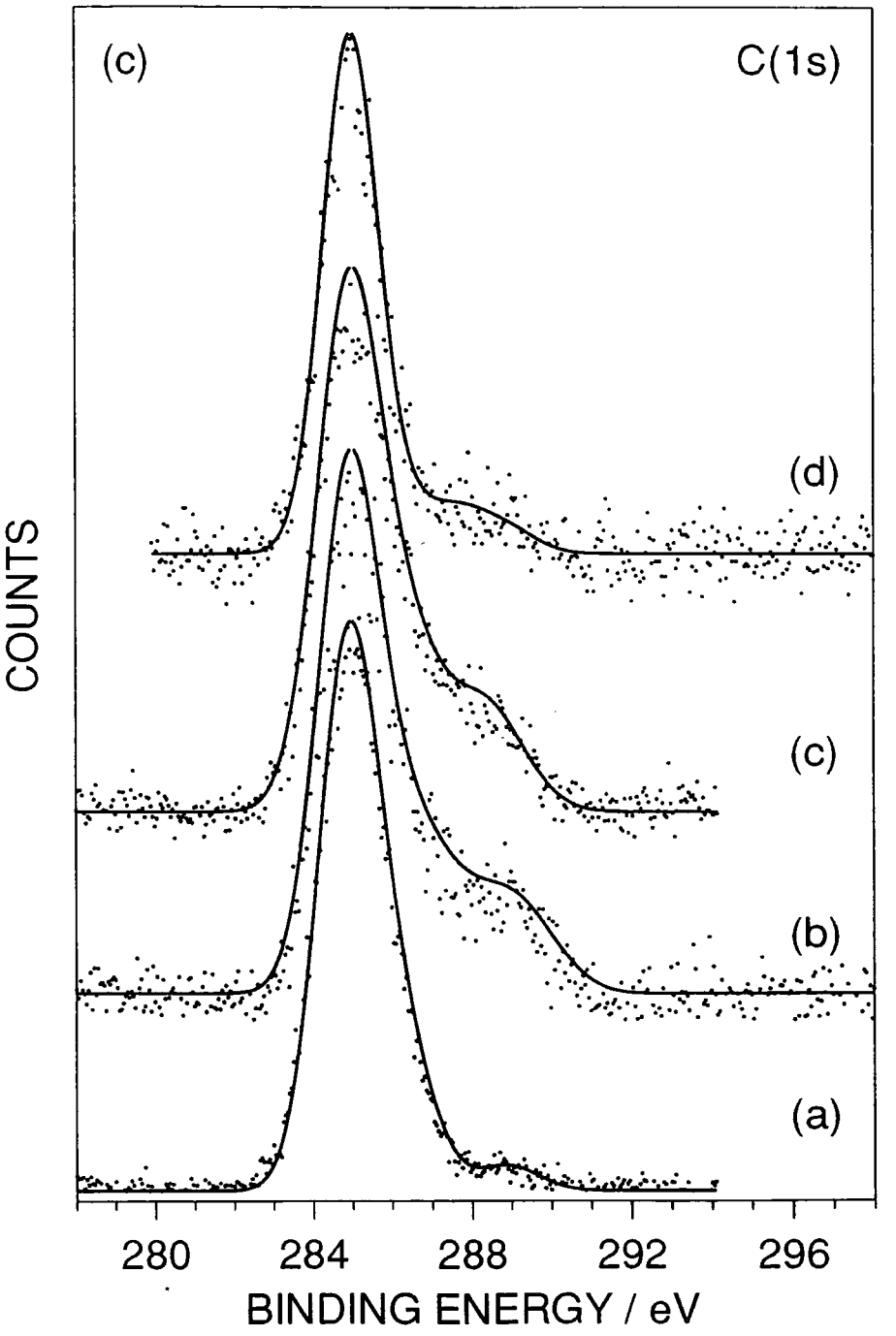

Figure 6.2(c): XPS C(1s) spectra for the following treatments of industrial CR: (i) clean: (ii) low temperature glow discharge 30 s; (iii) dielectric barrier discharge 30 s; and (iv) ozone treatment 4 hrs.

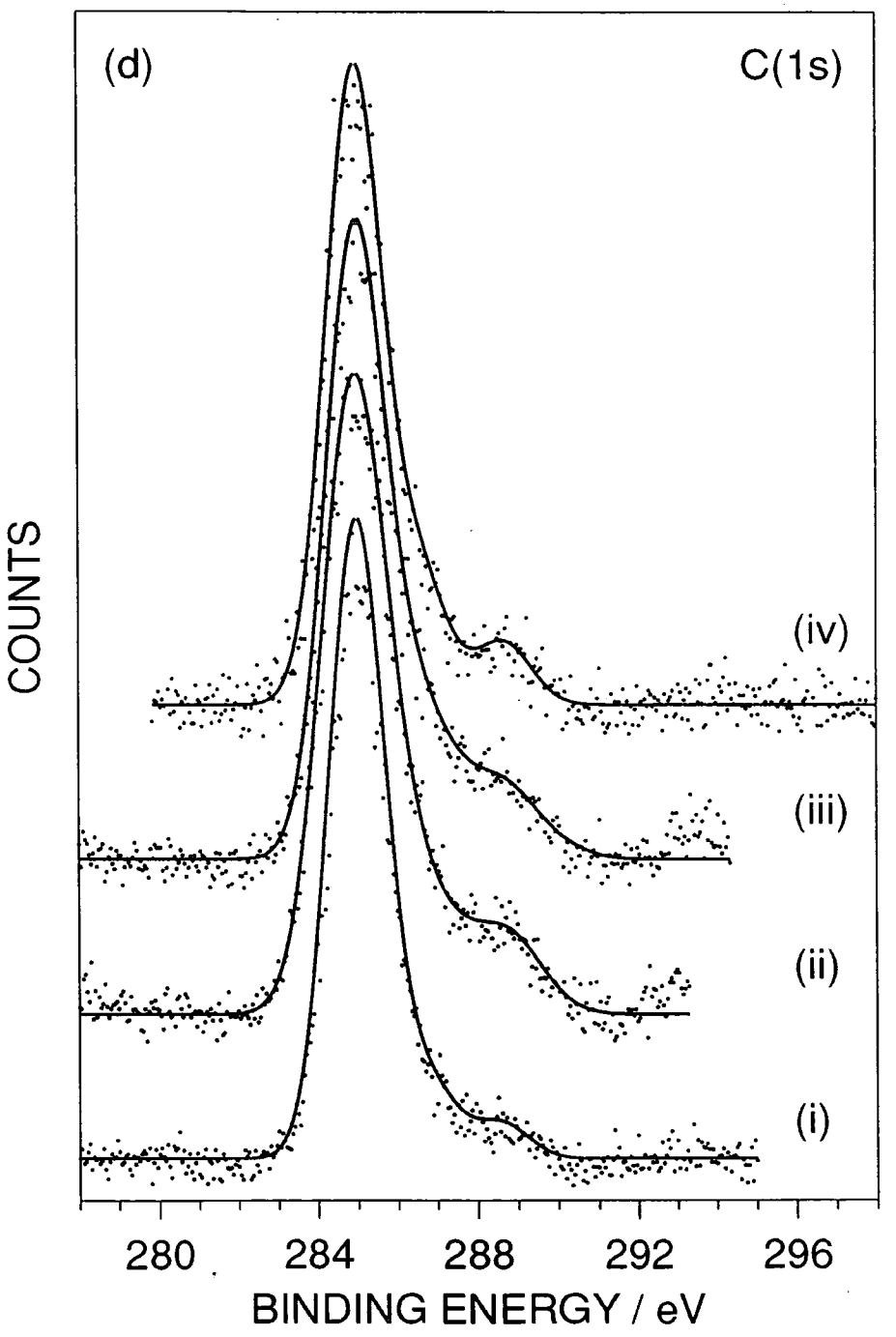

Figure 6.2(d): XPS C(1s) spectra for the following treatments of industrial SBR: (i) clean: (ii) low temperature glow discharge 30 s; (iii) dielectric barrier discharge 30 s; and (iv) ozone treatment 4 hrs.

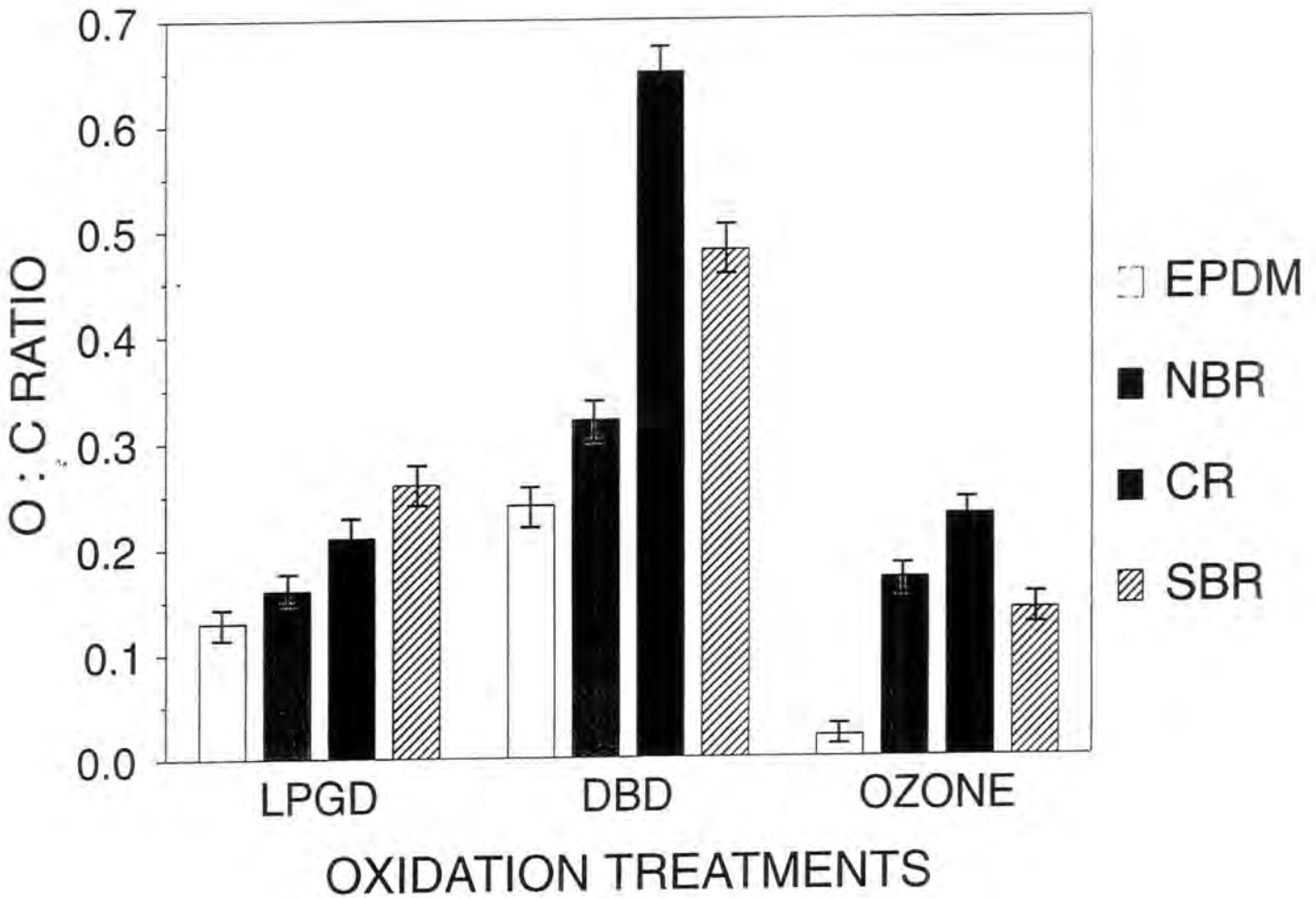

Figure 6.3: O:C ratio for the low pressure glow discharge (LPGD), the dielectric barrier discharge (DBD) and the ozone treatment of the four pure rubber substrates.

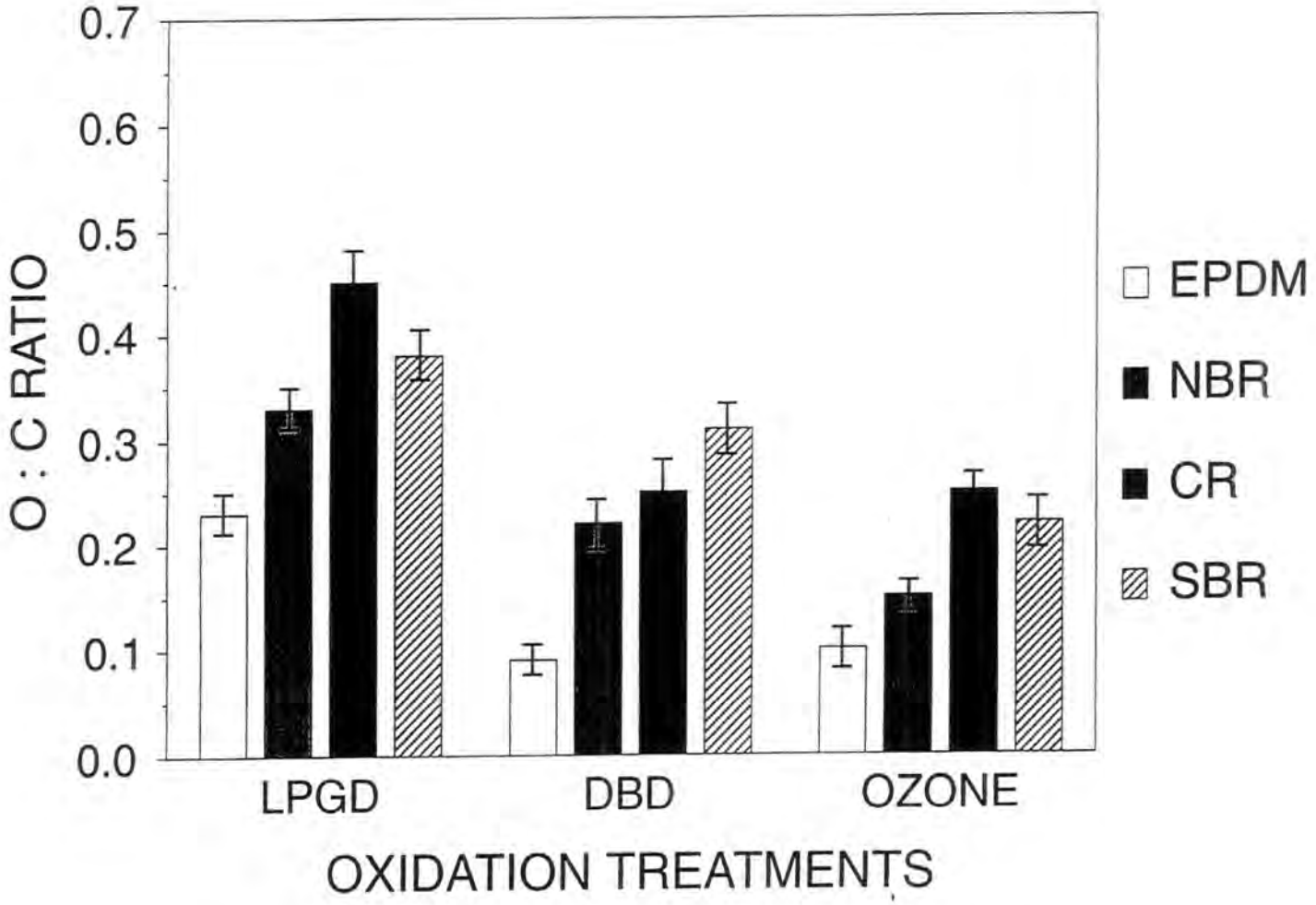

Figure 6.4: O:C ratio for the low pressure glow discharge (LPGD), the dielectric barrier discharge (DBD) and the ozone treatment of the four industrial rubber substrates.

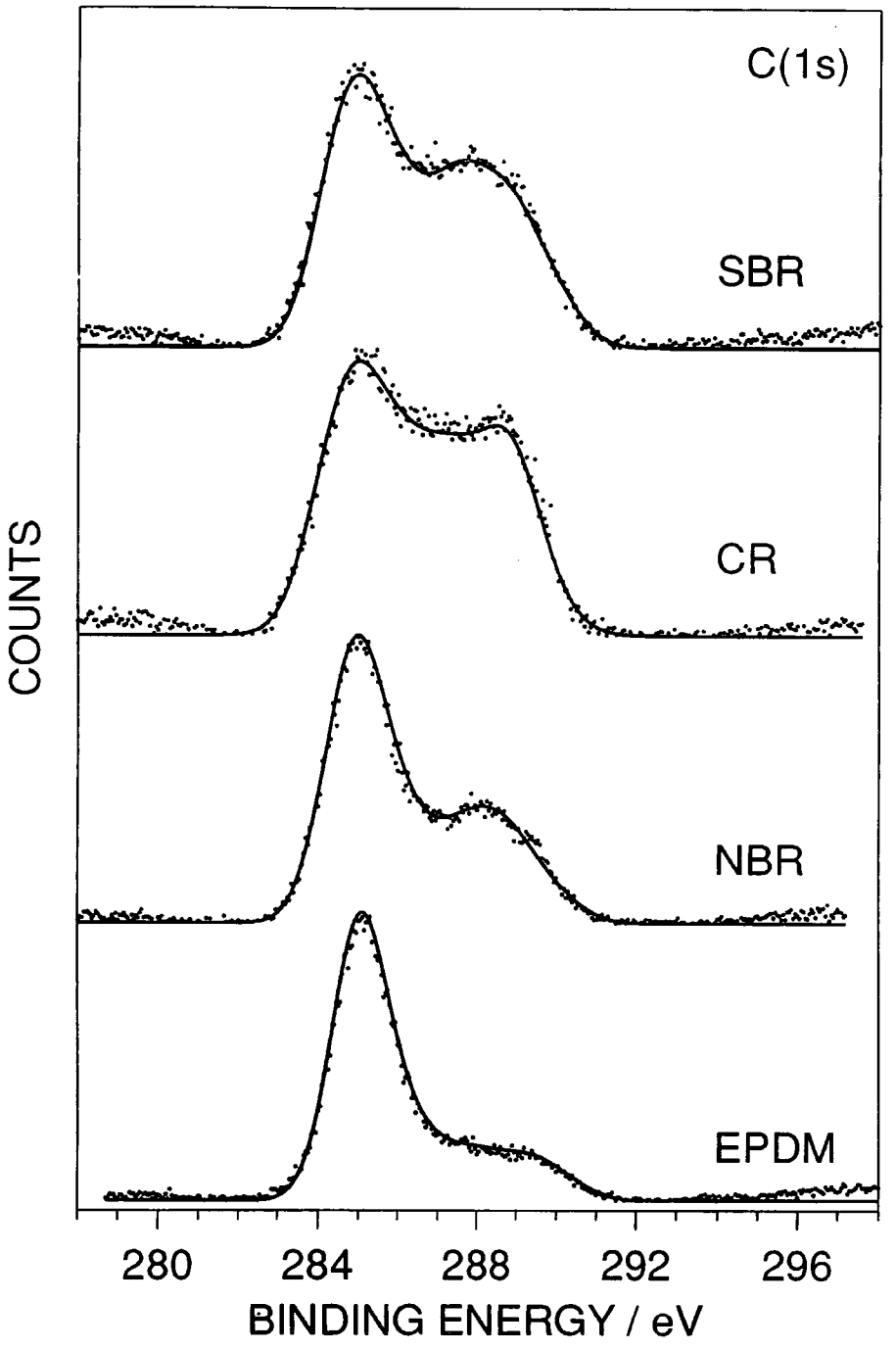

Figure 6.5: XPS C(1s) of the dielectric barrier discharge treated pure rubber substrates.

TREATMENT	EPDM		NBR		CR		SBR	
	PURE O : C	INDUST O : C [S : C]	PURE O : C [N : C]	INDUST O : C [N : C]	PURE O : C [Cl : C]	INDUST O : C [Cl : C]	PURE O : C	INDUST O : C [S : C]
CLEAN	0	0.03 [0.01]	0.02 [0.08]	0.06 [0.01]	0 [0.27]	0.18 [0.01]	0.09	0.06 [0.02]
LOW PRESSURE 30 s	0.13	0.23 [0.07]	0.16 [0.08]	0.33 [0.02]	0.21 [0.26]	0.45 [0.16]	0.26	0.38 [0.03]
SILENT DISCHARGE 30 s	0.24	0.09 [0.03]	0.32 [0.07]	0.22 [0.02]	0.65 [0.27]	0.25 [0.17]	0.48	0.31 [0.03]
OZONE 4 hrs	0.02	0.10 [0.01]	0.17 [0.08]	0.15 [0.02]	0.23 [0.25]	0.25 [0.16]	0.14	0.22 [0.02]

Table 6.1: Summary of oxidation treatments for the industrial and additive free polymers (error = $\pm$ 0.03)

(where PURE = additive-free rubbers and INDUST = industrial rubbers).

POLYMER	$\underline{C}_xH_y$	$\underline{C}$-CO_2	$\underline{C}$-Cl	$\underline{C}$-O (and cyano for NBR)	$\underline{C}$=O / O-$\underline{C}$-O	O-$\underline{C}$=O	O-$\underline{C}$O-O	O : C ($\pm$ 0.02)
EPDM	59.6	8.1	0	12.0	8.3	8.0	4.1	0.24
NBR	42.0	13.9	0	11.7	14.3	13.8	4.3	0.32
CR	22.9	14.4	16.8	9.5	16.3	15.2	4.9	0.65
SBR	31.7	16.8	0	14.0	16.3	16.5	4.8	0.48

Table 6.2: Summary of DBD oxidation treatment for the additive free polymers (error = $\pm$ 2 %).

6.4 DISCUSSION

Electrical discharges contain many species which can react with a polymer surface. The relative concentrations and energies of these species vary in the type of discharge used and influence the mode of surface modification. The two main types of electrical discharges often used to oxidise a polymer surface are the low temperature glow discharge oxygen plasma and the air dielectric barrier discharge.

A low pressure non-equilibrium oxygen plasma consists of a range of energetic species e.g. molecular, atomic, electronically excited oxygen moieties, electrons, ions and electromagnetic radiation.[18] Vacuum ultraviolet (VUV) and atomic atoms are thought to be the prominent components which cause oxidation of polymer surfaces.[19]

The O atoms are produced by collision of ions, electrons and photons with O_2 molecules.

$$O_2 \longrightarrow O\bullet + O\bullet$$

The atomic oxygen can react with polymers by hydrogen abstraction and / or addition across carbon-carbon double bond.[13] Extended Huckel molecular orbital calculations predict highly favourable energetics for the reaction of atomic oxygen with unsaturated >C=C< bonds (including phenyl rings) compared to saturated bonds.[13] Clearly, oxygen addition across a >C=C< double bond will produce a greater rise in O:C ratio compared to oxygen substitution of a C-H bond.

$$RH + O\bullet \longrightarrow R\bullet + OH$$

$$RC{=}CR + O\bullet \longrightarrow RCO\text{-}(\bullet)CR$$

Free radicals are also produced at the polymer surface due to the VUV component of the plasma cleaving saturated bonds and exciting unsaturated bonds. The main atomic emission line in an oxygen plasma is at 130 nm.[7]

$$RH + h\upsilon \longrightarrow R\bullet + H\bullet$$

Polymers containing phenyl rings undergo greater oxidation due to the π-π^* photo-excitation of pendant phenyl rings by the weak UV component of the electrical discharges at $\lambda < 280$ nm.[20] This leads to the formation of reactive free radical sites. The atomic oxygen then reacts with these free radicals. This reaction of atomic oxygen with the free radical sites created by the VUV radiation is the most likely mechanism of oxidation.[21]

$$R\bullet + O\bullet \longrightarrow RO$$

The dielectric barrier discharge is a non-equilibrium plasma which operates at atmospheric pressure and produces uniform electrical breakdown.[22] The parallel plate dielectric barrier discharge produces bright filamentary streamers of electrons and positive ions which extend between the two planar electrodes. Electronic collisions generate electrons, excited neutrals, ions and photons. Ozone is the main constituent of an air discharge and is produced in a two step process (lifetime is in seconds, 100 x more concentrated than electrons, 10 x more than excited molecular species).[23]

$$e + O_2 \longrightarrow 2O\bullet + e$$
$$O + O_2 + M \longrightarrow O_3 + M$$

where M = $O\bullet$, O_2, O_3

Saturated polymers react with ozone via a peroxy radical mechanism, Scheme 6.1.[6,24]

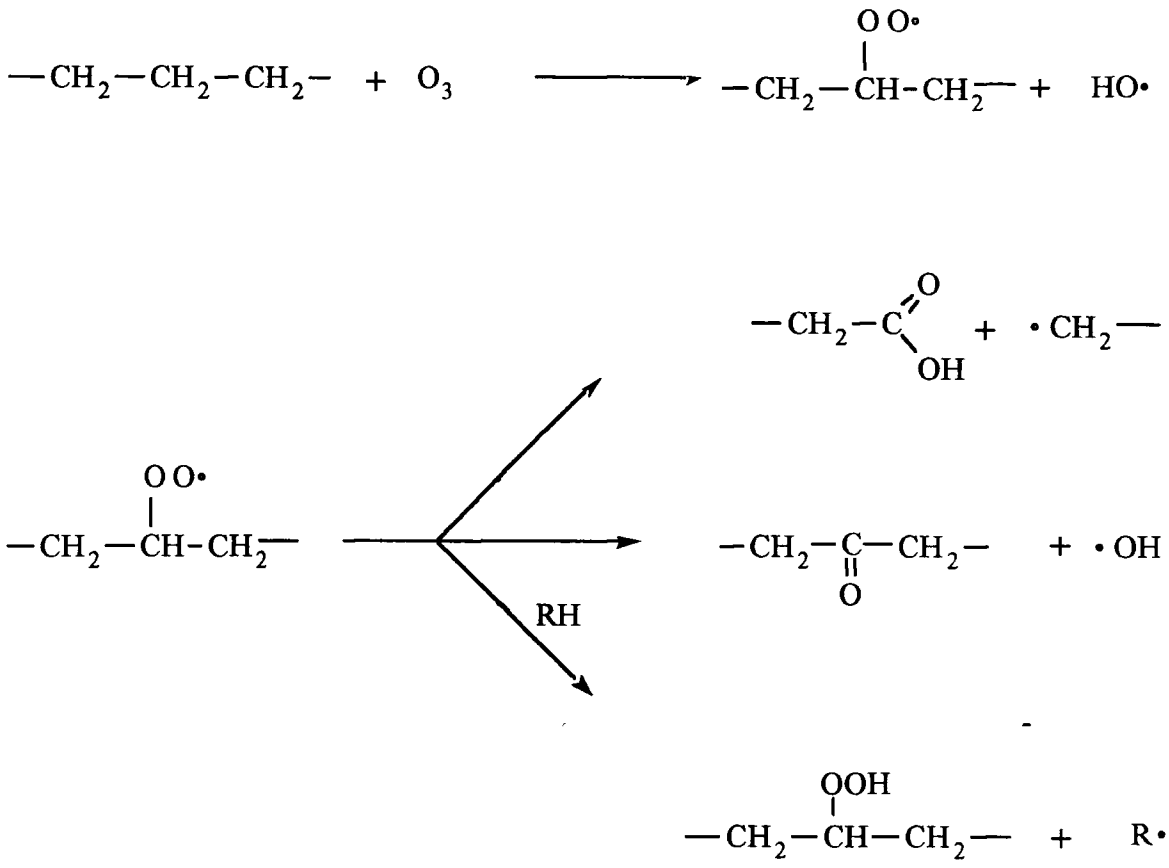

Scheme 6.1: Ozone attack at saturated hydrocarbon sites.

Unsaturated polymers are prone to oxidative degradation by ozone due to their inherent reactivity.[25] They react via a Criegee addition mechanism to yield ozonides.[6,24,26,27] O_3 reacts with the >C=C< to give an unstable primary ozonide (molozonide) which rearranges to an ozonide and further decomposes to carboxylic acid and carbonyl groups, Scheme 6.2.[6,24,25,26]

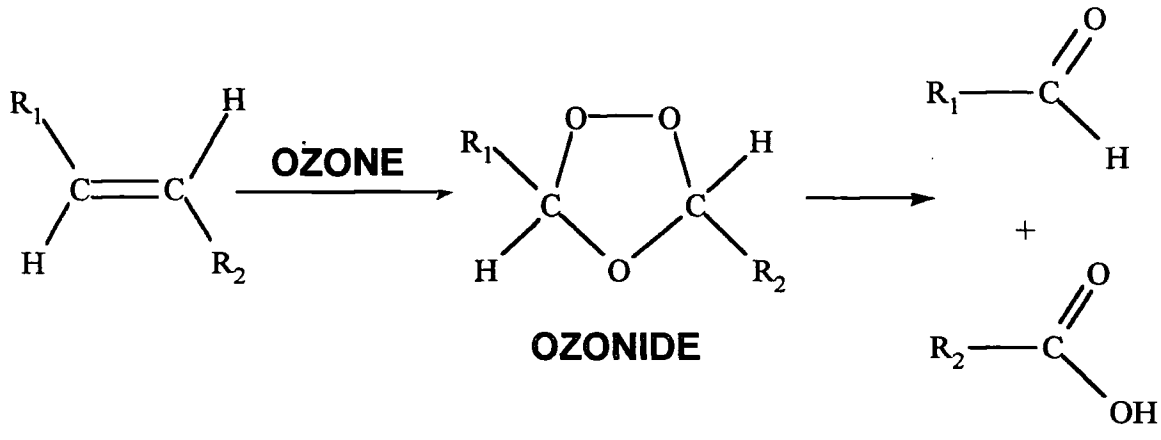

Scheme 6.2: Ozone attack at unsaturated hydrocarbon functionalities.[24]

Ozone is a useful reagent for cleaving double bonds;[26] however, despite the unsaturation in phenyl rings they are relatively inert to ozone treatment in comparison to unsaturated >C=C< bonds. This is due to the stability of the phenyl ring resonance structure i.e. it resists oxidation. Ozone therefore oxidises double bonds to a greater extent than aromatics, with saturated polymers being the least oxidised,[6] Table 6.3.

POLYMER	OZONATION RATE CONSTANT[6] ($l/mole^{-1}s^{-1}$)
Polyethylene	0.012
Copolymer of Ethylene and Propylene	0.06
Polypropylene	0.08
Polystyrene	0.12
Polybutadiene	8×10^4
Polyisoprene	10^5

Table 6.3: Rate constants for the reaction of ozone with various polymers.[6]

In this work it has been found that the relative concentrations of saturated carbons, unsaturated carbons (i.e. >C=C<) and phenyl rings in the pure polymers has a different effect on their oxidation susceptibility during the three treatments. The low pressure glow discharge caused the greatest oxidation of the unsaturated (phenyl rings and >C=C<) polymers due to the reaction of O atoms with any unsaturated moieties being more favourable than the reaction with saturated bonds.[13] The O:C ratio order followed that for concentration of >C=C< i.e. SBR > CR >NBR > EPDM, Figure 3. However, for ozone treatment the O:C ratio follows the order CR > NBR $\geq$ SBR > EPDM. This is consistent with ozone oxidising polymers containing double bonds to a greater extent

than those containing phenyl rings, and much greater than those with saturated polymers.[6] For the dielectric barrier discharge treatment a combination of the two orders is observed i.e. CR > SBR > NBR > EPDM. This is due to the combination of electron/photon excitation and ozone chemistry in an air dielectric barrier. Even though ozone is the main reactive component of a dielectric barrier discharge the photon component has to be taken into consideration. The radiation interacts with the polymer surface and alters the susceptibility of phenyl rings to oxidation i.e. the order of oxidation is different to that for pure ozone.

The dielectric barrier causes the greatest oxidation of the polymers and ozone the least. This indicates that polymers are highly susceptible to ozonation in the presence of radiation. As the O:C ratio increases for the polymers in the order CR > SBR > NBR > EPDM the oxidised shoulder visible for the silent discharge treated pure rubbers becomes more predominant Figure 6.5, i.e. the concentration of O=C-O and C=O groups increases, Table 6.2. This is consistent with production of carboxylic acid (O=C-O) and carbonyl (C=O) groups formed in the ozone attack of double bonds, Scheme 6.2.

For the industrial rubbers different oxidation series were found. This is due to impurities such as fillers added during the industrial processing.[14,15,28] The main impurity in all four samples is carbon black, other impurities include zinc oxide and hydrocarbon species, Table 6.4. Carbon black is used to improve abrasion and tear resistance, tensile strength and stiffness of the rubber.[14] For the low pressure glow discharge treatment the concentration of pure polymer contained in the rubber alters the oxidation order, i.e. there is more polymer contained in CR than SBR so its relative susceptibility to oxidation increases. In the dielectric barrier discharge case the high concentration of carbon black causes the silent discharge to arc, thus reducing its oxidising capabilities. It can therefore be seen that the additives in the rubber alter their susceptibility to oxidation.

6.5 CONCLUSIONS

The ozone, the low pressure glow discharge and the dielectric barrier discharge treatments all caused oxidation of the rubber surfaces. In the additive-free rubbers the dielectric barrier discharge caused the greatest oxidation. This is due to the combination of ozone and radiation interacting with the polymer surface. The relative concentrations

of saturated carbons, unsaturated carbons and phenyl rings in the polymers affected the oxidation susceptibility differently during each of the three treatments. For the industrial samples the amount of oxidation is altered by the additional impurities contained in the polymers.

	EPDM	SBR	CR	NBR
Polymer	41.5 %	58.8 %	71.7 %	58.8 %
Carbon Black	33.9 %*	29.4 %#	22.0 %*	29.0 %#
Zinc Oxide	2.1 %	2.8 %	3.0 %	2.9 %
Stearic Oxide	0.4 %	1.2 %	-	1.2 %
Mineral Oil (C_xH_y)	20.1 %	-	-	5.9 %
Sulphur Compounds	0.4 %	0.9 %	-	1.0 %
Magnesium Oxide	-	-	2.0 %	-
Others	1.6 %	6.9 %	0.4 %	1.2 %

Table 6.4: Relative % amounts of the components in the four rubbers (* N550, # N774).

6.6 REFERENCES

[1] O.D. Greenwood, S.Tasker and J.P.S. Badyal, J. Polym. Sci; Polym Chem. **32**, 2379 (1994).

[2] O.D. Greenwood, R.D. Boyd, J. Hopkins and J.P.S. Badyal, J. Adhesion Sci. Technol. **9**, 311 (1995).

[3] O.D. Greenwood, J. Hopkins and J.P.S .Badyal, Macromolecules **30**, 1091 (1997).

[4] G.N. Taylor and T.M. Wolf, Polym. Eng. Sci. **20**, 1087 (1980).

[5] A.F. Whitaker and B.Z. Jang, J. Polym. Appl. Sci. **48**, 1341 (1993).

[6] S.D. Rasumovskii, A.A. Kefeli and G.E. Zaikov, Eur. Polym. J. 7, 275 (1971).

[7] A.F. Whitaker and B.Z. Jang, SAMPE Journal **30**, 30 (1994).

[8] M. Morra, E. Occhiello, L. Gila and F. Barbassi, J. Adhesion **33**, 77 (1990).

[9] A.G. Shard and J.P.S. Badyal, J. Phys. Chem. **95**, 9436 (1991).

[10] R. Hansen, J.V. Pascale, T. DeBenedictis and P.M. Rentzepis, J. Polym. Sci; Polym Chem. **3**, 2205 (1965).

[11] M.A. Golub and R.D. Cormia, Polymer **30**, 1576 (1989).

[12] R. Foerch, N.S. McIntyre and D.H. Hunter, J. Polym. Sci; Polym. Chem. **28**, 193 (1990).

[13] S.R. Cain, F.D. Egitto and F. Emmi, J. Vac. Sci. Technol. **A5**, 1578 (1987).

[14] W. Hofmann, *Rubber Technology Handbook* (Hanser Publications, Munich, 1989).

[15] F.W. Barlow, *Rubber Compounding* (Marcel Dekker, New York, 1993).

[16] J.F. Evans, J.H. Gibson, J.F. Moulder, J.S. Hammond and H. Goretzki, Fresenius Z. Anal. Chemie, **319**, 841 (1984).

[17] G. Beamson and D.Briggs, *High Resolution XPS of Organic Polymers. The Scienta ESCA300 Database* (John Wiley and Sons, Chichester 1992).

[18] *Techniques and Applications of Plasma Chemistry*, edited by J. R. Hollahan and A.T. Bell (Wiley, New York, 1974).

[19] F.K. McTaggart, *Plasma Chemistry in Electrical Discharges* (Elsevier, Amsterdam, 1967).

[20] J.F. McKellar and N.S. Allen, *Photochemistry of Man-made Polymers*, (Applied Science, London 1979).

[21] J. Hopkins, S.H. Wheale and J.P.S. Badyal, J. Phys .Chem. **100**, 14062 (1996).

[22] B. Eliasson and U. Kogelschatz, IEÉE Trans. Plasma Sci. **19**, 309, (1991).

[23] B. Eliasson, M. Hirth and U. Kogelschatz, J. Phys. D: Appl. Phys. **20**, 2047 (1983).

[24] B. Ranby and J.F. Rabek, *Photodegradation, Photo-oxidation and Photostabilization of Polymers* (Wiley, Bristol, 1975).

[25] A. Davis and D. Sims, *Weathering of Polymers* (Elsevier, London, 1986).

[26] J. McMurry, *Organic Chemistry* (Brooks/Cole, California, 1988).

[27] J. March, *Advanced Organic Chemistry* (Wiley, New York, 1992).

[28] J.W. Hoover, M.E. Wheeler, J.V. Fusco and H.L. Kaufman, U.S Pat. 5650454 (1995).

CHAPTER 7

CONCLUSIONS

7.1 CONCLUSIONS

This thesis has investigated the physicochemical processes occurring at the plasma - polymer interface. A new mass spectrometric technique has been developed to overcome the major stumbling blocks previously encountered with insitu diagnostic techniques. Primary reaction products formed at the electrical discharge - polyethylene interface permeate through the polymer to be detected and analysed by a quadrupole mass spectrometer. The processes occurring at the interface are found to be dependent upon the feed gas used. Also, two new highly effective approaches for fluorinating polymer surfaces have been examined, as well as the oxidation of various rubber substrates.

In the case of nitrogen plasma treatment of polyethylene the importance of vacuum ultraviolet (VUV) initiated reactions (i.e. chain scission leading to hydrocarbon fragments) has been confirmed. An overall improvement in gas barrier performance of the polyethylene substrate has been observed, and attributed to the VUV induced crosslinking in the polymer subsurface restricting polymer chain mobility. For oxygen plasma treatment oxidised products were observed, with the clean polymer surface giving the greatest oxidation rate. A corresponding consumption of oxygen was also seen. Hydrocarbons were again produced due to VUV initiated chain scission. However, their intensity was greater than for nitrogen glow discharge treatment due to the weakening of adjacent carbon-carbon bonds by oxygenated centres. This effect was confirmed when on pulsing oxygen into a stream of nitrogen during plasma treatment an increase in hydrocarbon intensity was detected. The reaction product intensities formed during air electrical discharge treatment of polyethylene were found to be a combination of those for the nitrogen and oxygen plasma treatments.

During hydrogen glow discharge treatment of polyethylene the intensity of the hydrocarbon fragments was found to be much less than for the nitrogen plasma treatment. This is due to the hydrogen atoms produced in the plasma reacting with the polymer free radicals. This terminates the chain scission and thus impedes hydrocarbon formation. Additional pulsing experiments where the intensity of the hydrocarbons dropped on pulsing hydrogen / deuterium into a nitrogen plasma confirmed these deductions.

It was also found that absorbed water within the polymer bulk leads to oxidation of the polymer surface, even when the feed gas is oxygen free. It is therefore imperative that polymer substrates are annealed prior to plasma treatment.

Xenon difluoride (XeF_2) glow discharge treatment of polymer substrates gives even greater fluorination than the commonly used carbon tetrafluoride (CF_4) plasma treatment. This might be due to the stoichiometrically higher concentration of fluorine atoms in XeF_2. XeF_2 also offers the advantage of being easily transported and not producing any additional reactive intermediates other than fluorine atoms. The susceptibility of various polymers to XeF_2 plasma fluorination can be accounted for in terms of a structure-behaviour relationship based on extended Huckel molecular orbital calculations. Hydrogen substitution by fluorine occurs for saturated polymers, with further fluorination via addition occurring for polymers containing carbon-carbon double bonds.

Another method for fluorinating polymer surfaces is based on VUV-assisted XeF_2 fluorination. The VUV radiation is produced using a glow discharge and passes through a LiF window (cut-off wavelength 104 nm) into the fluorination chamber. Here it is capable of interacting with the polymer surface to produce reactive free radical sites. However, unlike CF_4, XeF_2 can also absorb VUV radiation of wavelengths greater than 104 nm to produce fluorine atoms The extent of polymer surface fluorination is governed by the overlap of the incident VUV emission lines with both the absorption characteristics of the polymer backbone and the XeF_2 gas. As with the XeF_2 plasma fluorination, unsaturated >C=C< bonds contained within the polymer structure are more susceptible towards fluorination compared to saturated C-H bonds. Surface modification is found to be greatest for VUV lines emitted by noble gas plasmas.

Low pressure glow discharge, dielectric barrier discharge and ozone treatments all caused oxidation of the synthetic rubbers. Dielectric barrier discharge gave the greatest oxidation of the additive free samples, due a combination of ozone attack and vacuum ultraviolet radiation. The relative concentrations of unsaturated carbons, phenyl rings and saturated carbons in the rubber influences their oxidation susceptibility differently during each of the three treatments. The additives added to rubber to improve their properties alter their degree of oxidation.

To conclude, this thesis presents alternative methods for fluorinating polymer surfaces, a new technique which has enabled the deduction of the processes occurring at

the plasma - polymer interface and a study of the oxidation of synthetic rubber substrates.

CHAPTER 8

APPENDIX A: FIGURES FOR NOBLE GAS AND CF_4 TREATMENT

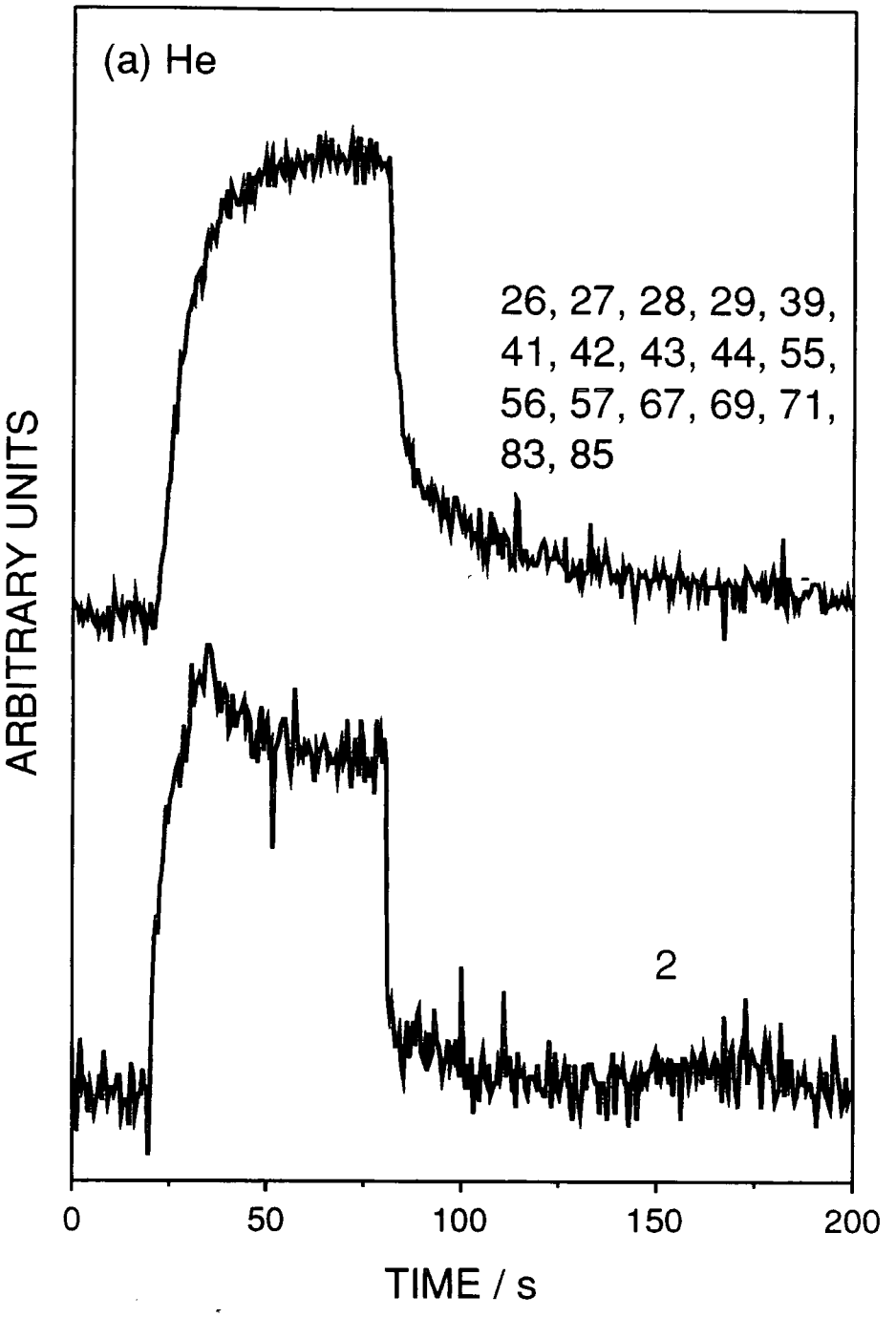

Figure 8.1(a): Mass profiles obtained using a 20/60/120 s, off/on/off sequence for the He electrical discharge (all profiles typical for the relevant masses).

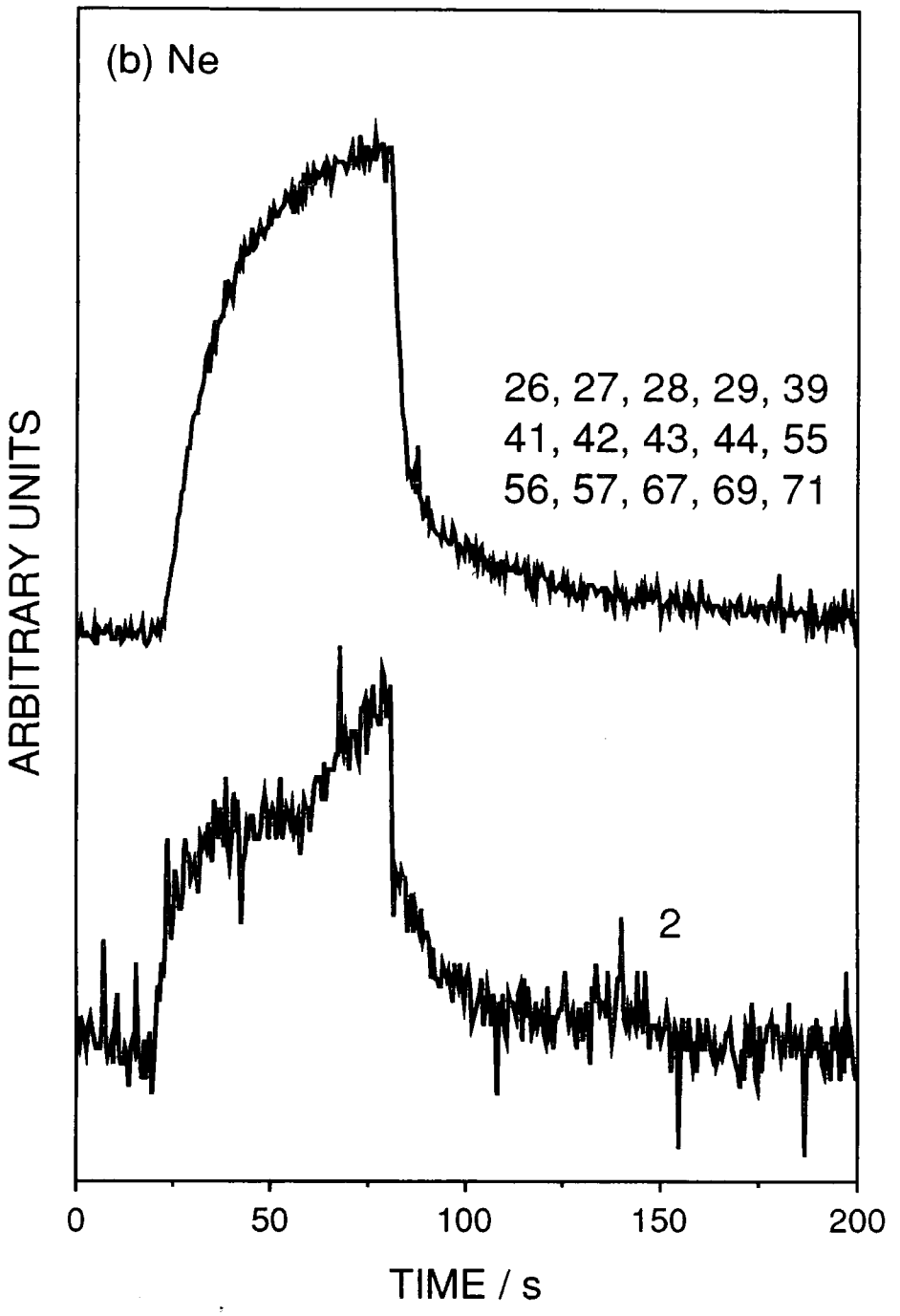

Figure 8.1(b): Mass profiles obtained using a 20/60/120 s, off/on/off sequence for the Ne electrical discharge (all profiles typical for the relevant masses).

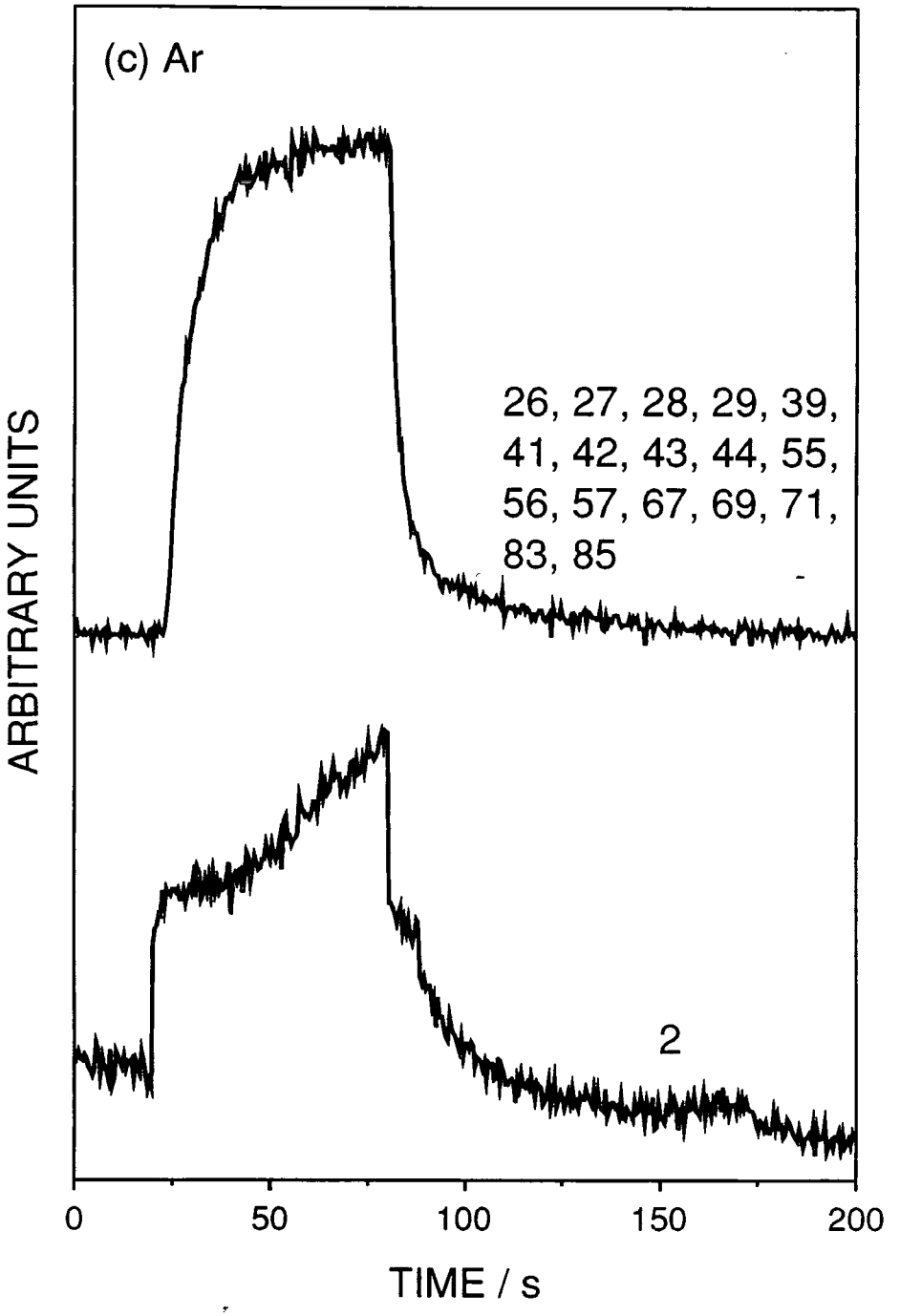

Figure 8.1(c): Mass profiles obtained using a 20/60/120 s, off/on/off sequence for the Ar electrical discharge (all profiles typical for the relevant masses).

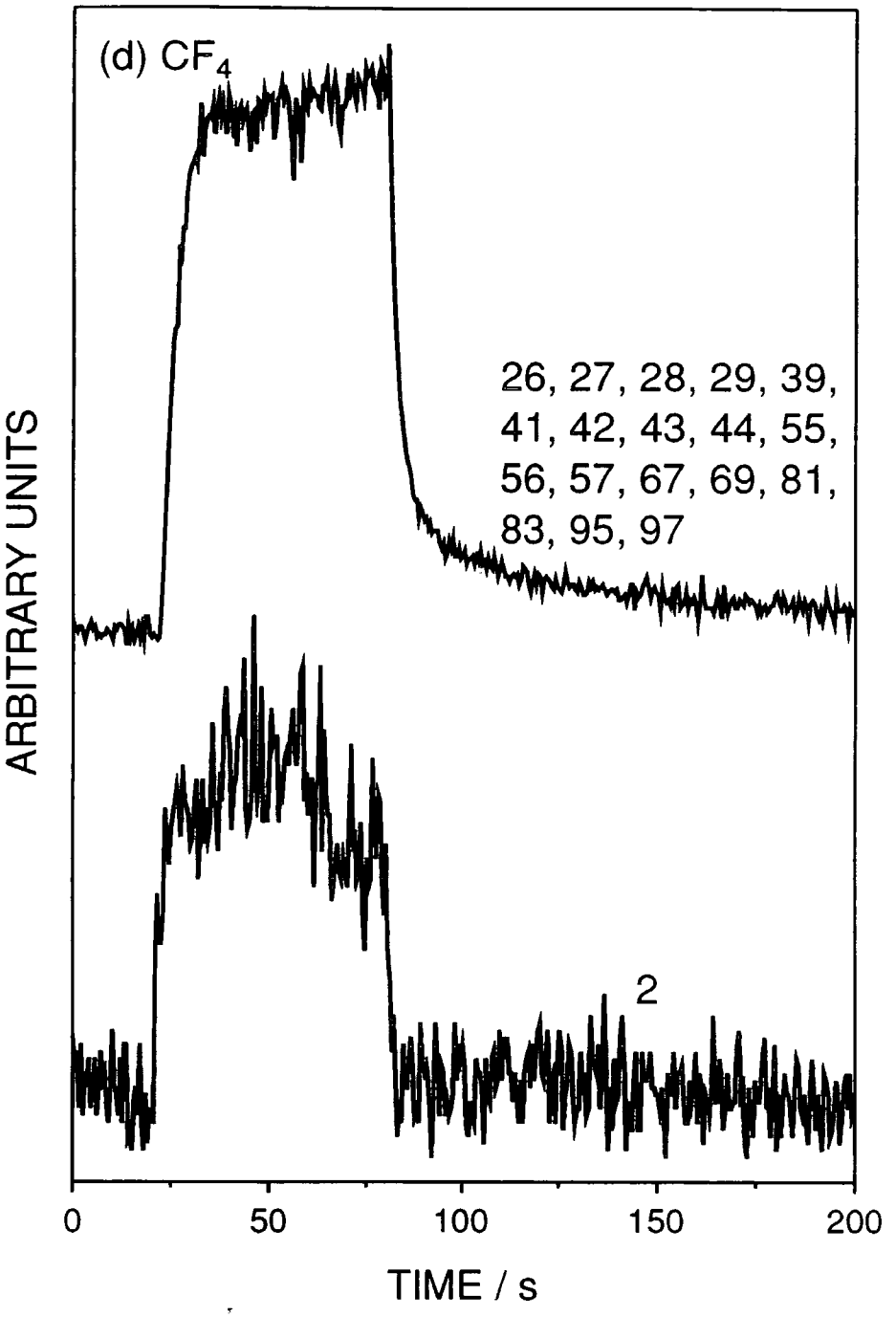

Figure 8.1(d): Mass profiles obtained using a 20/60/120 s, off/on/off sequence for the CF_4 electrical discharge (all profiles typical for the relevant masses).

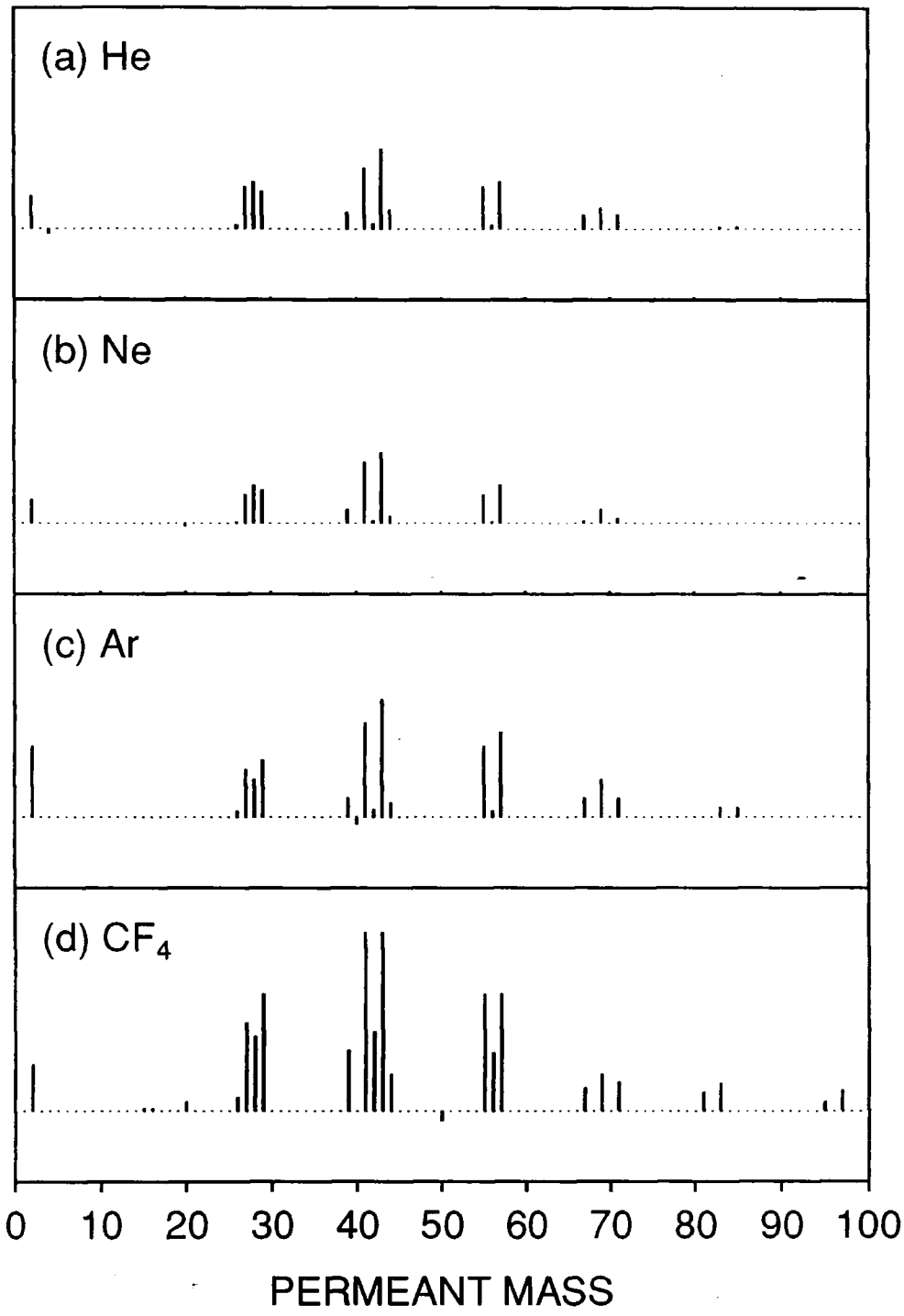

Figure 8.2: Maximum variation in mass signal intensities during plasma treatment: (a) He; (b) Ne; (c) Ar; and (d) CF_4.

APPENDIX B: COLLOQUIA, SEMINARS, PRESENTATIONS AND LECTURE COURSES

UNIVERSITY OF DURHAM

BOARD OF STUDIES IN CHEMISTRY

COLLOQUIA AND SEMINARS FROM INVITED SPEAKERS

1994

October 19	Prof. N. Bartlett, University of California Some Aspects of Ag(III) and Ag(III) Chemistry
October 26	Dr. G. Rumble, Imperial College Real or Imaginary 3rd Order Non-Linear Optical Materials
December 7	Prof. D. Briggs, ICI and University of Durham Surface Mass Spectrometry

1995

March 1	Dr. M. Rosseinsky, Oxford University Fullerene Intercalation Chemistry
April 26	Dr. M. Schroder, University of Edinburgh Redox Active Macrocyclic Complexes
May 3	Prof. E. W. Randall, Queen Mary & Westfield College New Perspectives in NMR Imaging
October 4	Prof. D. Tuck, University of Windsor, Ontario Electron Transfer Processes in Main Group Chemistry
October 11	Prof. P. Lugar, University of Berlin Low Temperature Crystallography

November 17	Prof. D. Bergbreiter, Texas A&M Design of Smart Catalysts, Substrates and Surfaces
November 22	Prof. I. Soutar, Lancaster University A Water of Glass? Luminescence Studies of Water Soluble Polymers
December 8	Prof. M. Reetz, Mullheim Size Selective Synthesis of Metal Clusters

1996

January 10	Dr. B. Henderson, Waikato University Electrospray Mass Spectrometry - A New Technique
January 17	Prof. J. W. Emsley, Southampton University Liquid Crystals: More than Meets the Eye
January 31	Dr. G. Penfold Soft Soap and Surfaces
February 14	Prof. R. Nolte Design Strategies for Supramolecular Architectures
March 6	Dr. R. Whitby, University of Southampton New Approaches to Chiral Catalysts
March 12	Prof. V. Balzani, University of Bologna Supramolecular Photochemistry
October 22	Prof. B. J. Tighe, Aston University Polymers for Biomedical Application

October 23	Prof. H. Ringsdorf, Johannes Gutenberg-Universitat Function Based on Organisation
November 6	Dr. K. Reid, Nottingham University Probing Dynamic Processes with Photoelectrons
November 18	Prof. Olah Crossing Conventional Lines in my Chemistry of the Elements
November 20	Prof. J. Earnshaw, Belfast University Surface Light Scattering: Ripples and Relaxation
December 4	Prof. K. Muller-Dethlefs, York University Very High Resolution ZEKE Spectroscopy

1997

February 6	Prof. P. Bartlet, Southampton University Integrated Chemical Systems
February 19	Brian E. Hayden Dynamics of Dissociation at Surfaces
March 3	Dr. M. Owen and Dr. D. Gravier, Dow Corning Siloxanes at Surfaces
March 6	Prof. K. Toth Advances in Scanning Electrochemical Microscopy

EXAMINED LECTURE COURSES

October - December 1994	Polymer Physical Chemistry (Dr. R. W. Richards)
October 1994 - January 1995	General Laboratory Techniques (Dr. D. P. Hampshire) Electron Microscopy (Dr. K. Durose) Spectroscopy (Dr. D. P. Halliday)

COURSES ATTENDED

September 1996	Neutron Reflectivity Training Course, Rutherford Appleton Laboratories.